UNIVERSITY OF TURKISH AERONAUTICAL ASSOCIATION
INSTITUTE OF SCIENCE AND TECHNOLOGY

INVESTIGATION OF REACTIVE POWER COMPENSATION IN A
POWER DISTRIBUTION NETWORK

MASTER THESIS

Ietiqal Mahmood ALWAN

ELECTRICAL AND ELECTRONIC ENGINEERING DEPARTMENT

MASTER SCIENCE PROGRAM

OCTOBER 2017

UNIVERSITY OF TURKISH AERONAUTICAL ASSOCIATION
INSTITUTE OF SCIENCE AND TECHNOLOGY

INVESTIGATION OF REACTIVE POWER COMPENSATION IN A
POWER DISTRIBUTION NETWORK

MASTER THESIS

Ietiqal Mahmood ALWAN

1406030034

ELECTRICAL AND ELECTRONIC ENGINEERING DEPARTMENT

MASTER SCIENCE PROGRAM

Supervisor: Prof. Dr. Doğan ÇALIKOĞLU

Ietiqal Mahmood ALWAN, having student number 1406030034 and enrolled in the Master Program at the Institute of Science and Technology at the University of Turkish Aeronautical Association, after meeting all of the required conditions contained in the related regulations, has successfully accomplished, in front of the jury, the presentation of the thesis prepared with the title of: "Investigation of Reactive Power Compensation in a Power Distribution Network".

Supervisor : **Prof. Dr. Doğan ÇALIKOĞLU**

                University of Turkish Aeronautical Association

Jury Members : **Prof. Dr. Doğan ÇALIKOĞLU**

                University of Turkish Aeronautical Association

      : **Assoc. Prof. Dr. Ahmet KARAARSLAN**

           Ankara Yıldırım Beyazıt University

      : **Assist. Prof. Dr. Ibrahim MAHARIQ**

           University of Turkish Aeronautical Association

Thesis Defense Date: 16.10.2017

UNIVERSITY OF TURKISH AERONAUTICAL ASSOCIATION
INSTITUTE OF SCIENCE AND TECHNOLOGY

I hereby declare that all the information in this study I presented as my Master's Thesis, Called: Investigation of Reactive Power Compensation in a Power Distribution Network: has been presented in accordance with the academic rules and ethical conduct. I also declare and certify with my honor that I have fully cited and referenced all the sources I made use of in this present study.

16.10.2017

Ietiqal Mahmood ALWAN

ACKNOWLEDGEMENTS

October, 2017   Ietiqal Mahmood ALWAN

TABLE OF CONTENTS

LIST OF TABLES

LIST OF FIGURES

LIST OF ABBRIVIATION

AC	:	Alternating Current
AI	:	Artificial Intelligent
ANN	:	Artificial Neural Network
DC	:	Direct Current
DE	:	Differential Evolution
FACTS	:	Flexible Alternating Current Transmission System
FBSM	:	Forward Backward Sweep Method
FC	:	Fixed Capacitance
FC-TCR	:	Fixed Capacitance-Thyristor Controlled Reactor
GA	:	Genetic Algorithm
GSA	:	Gravitational Search Algorithm
GWO	:	Grey Wolf Optimization
HVDC	:	High Voltage DC
IPFC	:	Interline Power Flow Controller
MATLAB	:	Matrices Laboratory
P F	:	Power Factor
PCC	:	Point of Common Coupling
PFC	:	Power Factor Correction
PSO	:	Particle Swarm Optimization
RMS	:	Root Mean Square
SMIB	:	Single Machine Infinite Bus
SMPS	:	Switch Mode Power Supply
SPST	:	Static Phase Shifting Transformer
SSR	:	Sub Synchronous Resonance
SSSC	:	Static Synchronous Series Compensator
STATCOM	:	STATic COMpensator
SVC	:	Static VAR Compensator
TCPST	:	Thyristors Controlled Phase Shifting Transformer
TCR	:	Thyristor Controlled Reactor
TCSC	:	Thyristors Controlled Series Compensator
TCT	:	Thyristor Controlled Transformer
TDD	:	Total Demand Distortion
THD	:	Total Harmonic Distortion
TIF	:	Telephone Influence Factor
TSC	:	Thyristors Switched Capacitor
TSC-TCR	:	Thyristor Switched Capacitor- Thyristor Controlled Reactor
TSR	:	Thyristors Switched Reactor
UPFC	:	Unified Power Flow Controller
VAR	:	Volt Amper Reactive
VSC	:	Voltage Source Converter
XLPE	:	Cross Linked Poly Ethylene

ABSTRACT

INVESTIGATION OF REACTIVE POWER COMPENSATION IN A POWER DISTRIBUTION NETWORK

ALWAN, Ietiqal

Master, Department of Electrical and Electronic Engineering

Supervisor: Prof. Dr. Doğan ÇALIKOĞLU

October 2017, 114 Pages

Power quality is one of the most important issues in the distribution network for electricity consumers for all types of usage. The unbalanced operation of three-phase power systems causes zero and negative sequence current components to increase, which causes the transformers to go to saturation, instability problems in generators or ripple in rectifiers, excessive losses of power in neutral lines , and excessive heating of machines, all of which are undesirable effects. The difference in loads of different phases leads to unbalanced operating conditions. Therefore, the management of these loads is important for the efficient operation of a power system. The compensation of reactive power is utilized to enhance power transfer capability and to achieve a balanced operation of the system from an unbalanced state only if the unbalanced state is due to the existence of reactive power.

In this study, The Static VAR Compensator (SVC) {Fixed Capacitor-Thyristor Controlled Reactor (FC-TCR) type} is considered to achieve a balanced operation of the system from an unbalanced state and to enhance the operational efficiency of a distribution network. The SVC is a versatile controller that absorbs or injects reactive power automatically so as to maintain the voltage at a specified value at the connection point. The operation of a reactive power compensator, which uses switching elements, causes harmonics to be introduced into the power system. The elimination, or at least the minimization, of these harmonics is very important. The proposed model has been simulated for a feeder in the Baghdad distribution network,

namely the New Jadrea-Arkheta 33 KV feeder of length 7.25 km. The software of the proposed model has been written using the MATLAB program. The efficiency and reliability of this software is demonstrated by the obtained results using the parameters of SVCs.

Keywords: Power Factor, Power System, Reactive Power Compensation, Thyristor Controlled Reactor.

ÖZET

GÜÇ DAĞITIM AĞINDA REAKTİF GÜÇ KOMPANZASYONUNUN İNCELENMESİ

ALWAN, Ietiqal

Yüksek Lisans, Elektrik ve Elektronik Mühendisliği

Tez Danışmanı: Prof. Dr. Doğan ÇALIKOĞLU

Ekim 2017, 114 sayfa

Güç kalitesi, dağıtım şebekesinde elektrik tüketicilerinin her türlü kullanımı için en önemli konulardan biridir.Üç fazlı güç sistemlerinin dengesiz çalışması,sıfır ve negatif dizi akım bileşenlerinin artırmasına; transformatörlerin doyuma gitmesine, jeneratörde kararsızlık problemlerine veya doğrultucularda dalgalanmalara,nötr hatlarda aşırı güç kaybına ve makinelerin aşırı ısınmasına neden olur,bunların hepsi istenmeyen etkilerdir. Farklı fazların yüklerindeki değişim dengesiz çalışma koşullarına yol açar.Bu nedenle,bu yüklerin yönetimi bir güç sisteminin verimli çalışması için önemlidir. Reaktif güç kompanzasyonu dengesiz durumun reaktif güç varlığından kaynaklanması durumunda güç aktarım yeteneğini arttırmak ve dengesiz durumdan sistemin dengeli bir şekilde çalışması için kullanılır.

Bu çalışmada, dengesiz işletim sistemlerinden dengeli bir işletim sistemi elde etmek ve bir dağıtım şebekesinin çalışma verimliliğini artırmak için Statik VAR kompansatör (SVK) (Sabit Kapasitör-Tristör Kontrollü Reaktör (SK-TKR) tipi) kullanıılmıştır. SVK, voltajı bağlantı noktasında belirli bir değere ayarlamak için otomatik olarak reaktif gücü emen veya enjekte eden çok yönlü bir denetleyicidir. Anahtarlama elemanları kullanan reaktif güç kompansatörün çalışması harmoniklerin güç sistemine aktarılmasına neden olur.Bu harmoniklerin eliminasyonu veya en azından küçültülmesi çok önemlidir.Önerilen model Bağdat dağıtım şebekesinde bir besleyiciye uygulanmıştır.Yeni Jadrea-Arkheta 33 KV besleyici, uzunluğu 7.25 km'dir.Önerilen model MATLAB programı alt yapısı

kullanılarak yazılmıştır.Bu yazılımın etkinliği ve güvenilirliği SVK parametreleri kullanılarak elde edilen sonuçlar ile gösterilmiştir.

Anahtar Kelimeler: Güç Faktörü, Güç Sistemi, Reaktif Güç Kompanzasyonu, Tristör Kontrollü Reaktör.

CHAPTER ONE

INTRODUCTION

1.1 Presentation of the Work

In this thesis a 33 kV distribution network is investigated to improve its performance by providing compensation for its reactive power. A Static VAR Compensator (SVC) device is used to accomplish this compensation. The parameters of the Static VAR Compensator (SVC) device that meets all the requirements of the objective function to enhance operational efficiency for the system is found.

A part of Baghdad's 33 kV distribution network (Al-Rusafa on the east side of Baghdad) was selected as a case for study. A feeder from the Baghdad distribution network, namely the New Jadrea-Arkheta 33 kV feeder, was considered during this work. As shown in Figure 1.1, the Arkheta substation is supplied by a main feeder from the New Jadrea station with a length of 7.25 km. New Jadrea station is equipped with three power transformers of 132/33/11 kV. Each transformer has a power rating of 63 MVA and five 33 kV feeders are outgoing from each. Arkheta substation contains two distribution transformers of 33/11 kV with a power rating of 31.5 MVA. Seven feeders of 11 kV are outgoing from each transformer of the Arkheta substation feeding a large area of mixed residential, industrial and commercial loads.

A feeder of 33 kV outgoing from transformer No. 1 from New Jadrea station is considered in this work. A single core, 1*400 mm 33 kV underground cable with cross-linked polyethylene (XLPE) insulation is used in the New Jadrea-Arkheta feeder for each phase.

The parameter of the considered line between the load bus (Arkheta) and the source bus (New Jadrea) is taken as X=2.158 Ω per phase and R=1.13295 Ω per phase.

Simulation results were verified by using the Forward Backward Sweep power flow method. All the simulations are performed using the MATLAB R2014a software.
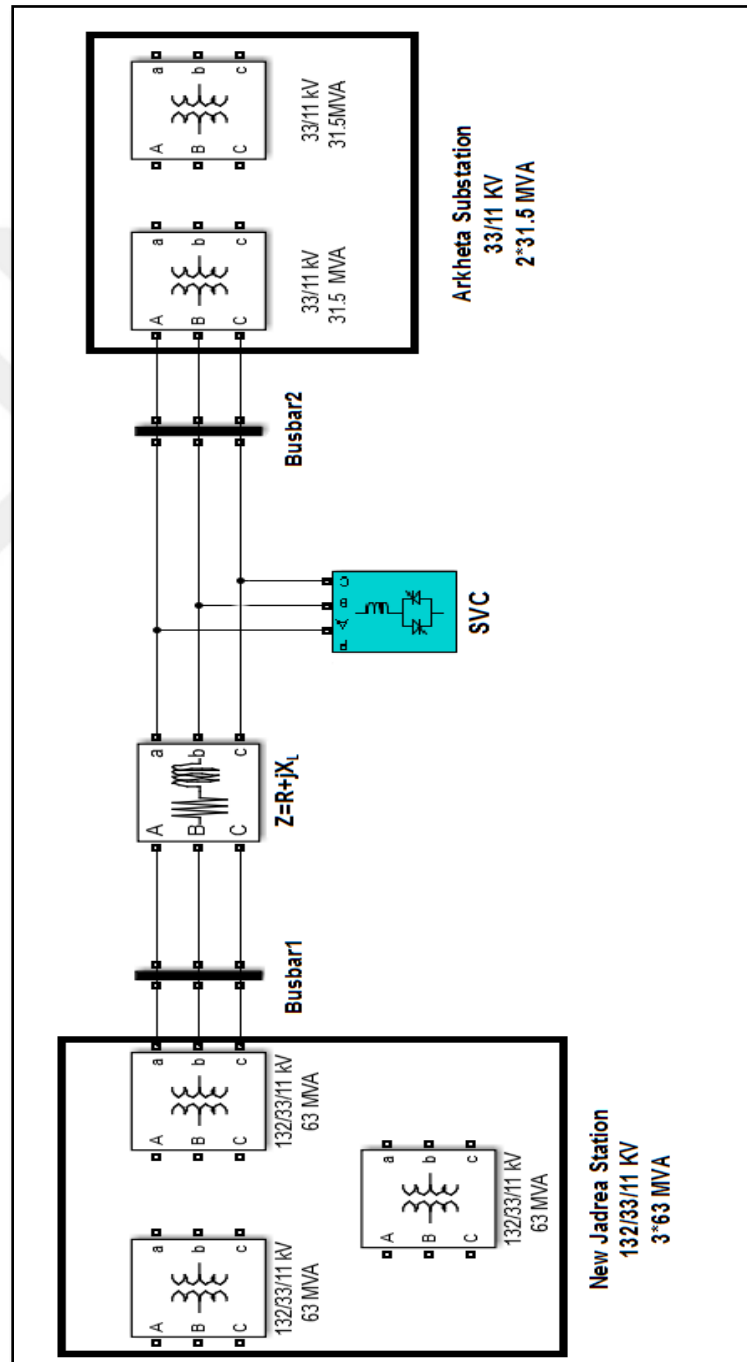
Figure 1.1: Schematic diagram of New Jadrea-Arkheta 33 KV feeder with SVC.

Active power consumption is accompanied by the consumption of a specific amount of reactive power due to the existence of inductive elements in the circuit. In an ideal alternating current power system, the frequency and voltage should be constant and free from harmonics at every supply point, unity power factor, and the 3-phase AC system should work as a balanced system. In particular, these parameters depend on the size and characteristics of the consumer's load.

Increasing the consumption of reactive power leads to lower values of the power factor, which in turn increases losses in the distribution system, voltage drops, instability of the power system and power quality problems such as a reduction of the effective capacity of generating units and system components. Most alternating current systems are 3-phase and they are designed for balanced working conditions. Any unbalanced functioning, such as unbalanced consumption of reactive power, produces a rise to undesired current components in the wrong phase sequence, and such components have undesirable impacts, including:

1. Saturation of transformers;
2. Excessive heating of machines;
3. Instability problems in the generator or ripple in rectifiers;
4. Excessive losses of power in neutral lines; and
5. Interference and protection problems.

Thus, it is significant to manage the reactive power so that the alternating current electric power system works as close as possible to the ideal power system. Partial or complete reactive power compensation is continuously gaining increasing interest since generation, transmission and consumption networks are becoming larger and more complicated day after day [1].

During the past decades, many various types of conventional compensators have been used, including series capacitor compensators, synchronous condensers, shunt capacitor compensators, shunt reactors, and so on. Now, the advent of the Flexible Alternating Current Transmission System (FACTS) technologies plays an effective role in reducing all problems. Using FACTS devices in a network provides more options to power system operators by increasing operation flexibility in the electrical network. Generally, FACTS controllers are placed into networks in order to provide continuous and fast power flow control (reactive and active power) in distribution networks throughout one of the following aspects:

1. Change of impedances of transmission lines;

2. Control of voltages at critical buses;

3. Compensating for reactive power that is drawn from a source; and

4. Control of phase angles between transmission line terminals.

Without topological changing of the network and/or generation rescheduling, FACTS controllers can control the flow of power in the system during normal and abnormal conditions. They can also reduce power system losses and improve the steadiness and performance of electric power networks [2].

Among the Flexible Alternating Current Transmission controllers, SVC has been explored and deployed to reactive power compensation so as to achieve load balancing and power factor correction. For study in this thesis, SVC, which is a variable impedance element that connects in a shunt manner with a power system, was selected. It can generate or absorb the required reactive power for load compensating continuously and rapidly [3].

A Thyristor Controlled Reactor (TCR) operates at different conduction angles, so it can be utilized profitably to provide for the unbalanced demand of reactive power and varying load in the network. Such an operation can produce pollution of the power source by creating harmonics due to non-sinusoidal currents; therefore, it is necessary either to eliminate (minimize) the generation of harmonics in SVC internally or provide appropriate external filter that may be included with the SVC design, which will be costly and more complex [4].

1.2 Literature Review

At this stage, it is of interest to review some of the research work which has focused on the reactive power compensation field, most of which is directed towards improving the compensation methods and their conclusions.

D. Thukaram, et al. (2004) [5] used two types of SVCs: a Fixed Capacitor Thyristor Controlled Reactor (FC-TCR) and a Thyristor Switched Capacitor-Thyristor Controlled Reactor (TSC-TCR), which were taken into account for the analysis to minimize the influence of harmonics by utilizing Total Harmonic Distortion (THD) and Telephone Influence Factor (TIF). They concluded that the operation of the compensator (FC-TCR) under certain ranges can increase the

injection of harmonics into the system. They therefore suggested selecting the size of the capacitor and reactor based on overall requirements of meeting loads.

A. Rajapakse, et al. (2006) [6] presented an improvement of the Artificial Neural Network (ANN) controller for unbalanced fluctuation load compensation. Their proposed controller reduced and balanced reactive power that was delivered from the supply while keeping the injection of harmonics to the PCC low. Total Demand Distortion (TDD) was taken as a constraint in order to calculate the injections of harmonics. Using fuzzy logic systems, they obtained the optimum firing angles of TSC-TCR thyristors that met all the constraints.

Ismail K. Said, et al. (2009) [7] used a capacitor bank with a thyristor reactor (FC-TCR) Y, Δ connected respectively, which is controlled by an ANN to enhance power transfer capability and to achieve a balanced operation of the AC system from an unbalanced operation. Unbalanced cases were simulated using MATLAB with 33 kV systems. The proposed algorithm showed the ability to balance the three - phase current.

D. B. Kulkarni, et al. (2009) [8] proposed a new method to keep the harmonic injection to the point of common coupling (PCC) low while balancing source reactive power. The genetic algorithm (GA) based ANN training was used to determine the firing angles of the TSC-TCR to achieve optimum operation. They assumed 3-phase balance voltages at the load side in their calculations.

V. Lakshmi Devi, et al. (2011) [9] applied a static VAR compensator (SVC) type (TSC-TCR) to the (11/0.4) kV distribution transformer feeding loads consisting of laboratory equipment, single phase and three phase motors, and SMPS to increase the power factor and load balancing. During the operation of the TCR to meet the unbalanced reactive power demand, harmonics were generated because of the unbalance firing angles of the thyristor, so they proposed ANN with a fuzzy logic system in order to obtain the optimum combinations to fire delay angles that meet a minimum THD with acceptable reactive power delivered from the source (Q_s). The MATLAB software was used to prove their study.

Carl John O. Salaan, et al. (2011) [10] presented a real-time reactive power controller that depended on an artificial neural network (ANN). The objectives of the ANN were to switch the capacitor on and off during abnormal and normal situations. The network was trained with minimum mean square errors. For each load, the ANN

inputs were of real power and reactive power. A Zilog Microcontroller was used to implement the controller and the model in which it was tested was a radial distribution power system.

Javid Akhtar, et al, (2012) [11] used a fuzzy logic based supplementary controller for the SVC that was improved for power quality enhancement in the distribution, generation, and transmission side of the power system. In the generation side, the fuzzy logic based SVC controller was used to enhance transient stability and to dampen the rotor angle oscillations, while in the distribution side; it was used to minimize the injection of harmonics into the network because of the operation of (TSC-TCR) by the optimum firing angles that met all the constraints. A comparative study was made with other studies found that the proposed controller operated better and at a faster rate when dampening the oscillation of the system.

Dhruvang R Gayakwad, et al. (2014) [12] demonstrated a methodology to adjust the SVC firing angles of the FC-TCR type so that the reactive power delivered from the source was lower and maintained the source power factor near to unity. The PSIM software was used to simulate a three phase 440 V system with different Series R-L loads. The power factor and reactive power variation was examined before and after the compensation. With the help of a close loop control, they approved their methodology by increasing the firing angle of the delta connected TCR from [$90°$ to $180°$] and look up table that was made by a trial-and-error method for the specific load.

Mr. Sanjay Prajapati, et al., 2015 [13] proposed a combination of an artificial intelligence (AI) technique and SVC with a passive filter to minimize the injection of harmonics into the system due to SVC work ,TSC-TCR type, during fast changes in loads. Three cases where simulated in MATLAB (without SVC or filter, with SVC and filter, and with SVC and artificial intelligence (AI)). Comparisons of all the cases where made and defined such that an SVC with the artificial intelligence (AI) technique method was better in comparison to the others. THD was taken as the constraint.

Al-Attar Ali Mohamed, et al. (2015) [14] introduced a novel design of an SVC controller to meet the power system damping oscillation. They used a multi- layer ANN tuned with the GWO algorithm (Grey Wolf Optimization) to optimize the connections of all the weights and biases for the ANN. They executed the controller

on the 2-axis nonlinear Single Machine Infinite Bus (SMIB) system and then tested it with a three phases fault. They achieved all the possible input values of the ANN control by varying the reference generator voltage with a wide range of operating conditions of the SVC to address the imbalanced signal problem. A comparison was made with traditional PI controllers and the results showed that the proposed controller behavior meeting the power system dynamic damping was better than the PI traditional controller.

Mohammad Hasanuzzaman Shawon, et al. (2015) [15] Two different configurations of the FC-TCR type SVC were studied within their specifications. Various current and voltage properties were analyzed in addition to their harmonics. They proposed these two configurations of FC-TCR (changing the topology) in order to obtain lower THD, where this factor was taken as the constraint. This system was simulated in MATLAB.

Bilpab Bhattacharyya, et al. (2016) [16] applied gravitational search algorithm (GSA) based optimization techniques to obtain optimum allocation of FACTS devices (SVC and TCSC) to increase power system loadability. The effect of the SVC and TCSC devices on the power systems' transfer capacity of each single generator was investigated. This algorithm was tested on 30- and 57-bus test systems in addition to a comparative study being made between GSA and other optimization techniques (GA, DE, and PSO). The results showed the efficiency of the GSA algorithm in reducing active power losses, total operating costs and enhancing voltage profiles.

V. Suma Deepthi, et al. (2016) [17] proposed a PI controller with a fuzzy logic system to obtain optimum triggering delay angles $[0^{\circ}\text{-}90^{\circ}]$ of the SVC type TSC-TCR to balance the reactive power and to reduce harmonics injected into the network due to its operation with fast changing in loads. They simulated, in MATLAB, a 100 KVA distribution substation with a fluctuating load consisting of three - phase and single-phase electric motors, SMPS, and laboratory equipment. Results showed that the Total Harmonic distortion (THD) was taken as a constraint in the optimization to minimize the harmonics injected with acceptable reactive power delivered by the source.

This work is different from others such that:

1- For the source of the data that are used as an input reactive power load demand, most previous literatures depended on laboratory load data while this work depends on real Iraqi 33 KV distribution grid data with different loads.

2- Most researchers assumed three-phase balanced voltages at the load bus in their calculations. In this work, unbalanced three-phase voltages are used to maintain more realistic calculations.

3- We study the effect of the feeder length on the load balancing process by calculating the effect of voltage drop, whereas the previous literature ignored the length effect of the feeder.

1.3 Study Purpose

The Static VAR Compensator (SVC) model, Fixed Capacitor-Thyristor-Controlled Reactor (FC-TCR) type ,is considered for analysis of part of Baghdad's 33 kV distribution network (Al-Rusafa on the east side of Baghdad) in order to acquire the following:

1. Load balances, by balancing the reactive power delivered by the source;

2. Improvement of the power factor by minimizing the balanced reactive power that is drawn from the station;

3. Minimum current supplied by the source which leads to a reduction of the total power losses in the line; and

4. Load voltage improvement.

1.4 Thesis Organization

This dissertation consists of five sections divided as follows:

Chapter 1:

This chapter presents an introduction to the concept of reactive power compensation, a literature review and the purpose of this study. It ends with the arrangement of this dissertation.

Chapter 2:

This chapter presents reactive power compensation, its conventional types and control strategies. Its role in this work will be justified and explained and its contribution to the application here will be explored.

Chapter 3:

This chapter presents an introduction to the history of FACTs devices and their role in solving different issues in power systems as well as explanations, definitions, types, principles of operation, and their advantages. Harmonics is also summarized.

Chapter 4:

This chapter presents a theoretical analysis and the simulation results.

Chapter 5:

This chapter covers conclusions of this work and future study suggestions in the field of reactive power.

CHAPTER TWO

REACTIVE POWER COMPENSATION

2.1 Reactive Power Compensation

Voltages are significantly influenced by network topology changes and load variations in electric power systems. When a system is working under high load voltages, it may decrease extremely and even collapse. This may lead to under-voltage relay triggering and other controllers sensitive to voltage, hence a loads disconnection which inversely affects company revenue and consumers. On the other hand, over-voltages may arise because of the Ferranti impact, when the system is working under low loading. Capacitive over- compensation and over- excitation of synchronous machines can also occur. Over-voltage causes equipment damage due to magnetic saturation in transformers and insulation breakdown, resulting in the generation of harmonics. Therefore, the voltage magnitude throughout the system cannot deviate from its nominal level significantly if a reliable and efficient operation of the system is to be accomplished.

By adjusting the absorption, generation, and reactive power flow throughout the system regulation of voltage is achieved. Sinks and sources of reactive power; like synchronous condensers, shunt reactors, and shunt capacitors; are utilized for this objective. Using FACTS devices, alternating current system can be worked more flexibly and effectively. Among FACTS controllers, SVC is a versatile controller that absorbs or generates reactive power automatically to keep bus voltage at a specified magnitude in the point of connection [3].

Reactive power compensation is defined as the management of reactive power to enhance the performance of an AC system. Generally, the issue of reactive power compensation is viewed from two aspects: voltage support and load compensation [18].

2.1.1 Load Compensation

Reactive power compensation is generally required to enhance supply quality in AC power systems. In general, loads which have low value of power factor, which are unbalanced, which have DC components and contain harmonics require compensation. The compensating equipment is usually installed near to the load at consumer buildings. There are three main objectives in load compensation [1]:

1. Power factor correction (PFC);
2. Voltage regulation improvement; and
3. Load balancing.

2.1.1.1 Power Factor Correction (PFC)

A majority of load types are industrial with a lagging power factor; in other words, they consume reactive power. Therefore; load current has a tendency to exceed requirements in order to provide active power only, which increases voltage drop, active power losses, and decreases the effective capacity of other system components and generating units. For all these reasons, in many countries, suppliers of electricity fix a low power factor limit below which consumers should pay a penalty for their excess reactive power consumption [12].

Power factor correction (PFC) normally implies the practice of generating (some or all) reactive power closer to meeting load requirements instead of providing it from a distant power station. Therefore, shunt capacitors are applied at medium levels of voltage ((11-33) kV) by design engineers. One of the methods utilized for improving the power factor is the individual compensation method.

A number of advantages to be gained from the utilization of compensation to improve the power factor include [1, 19]**:**

1. Increases in apparent power capacity;
2. Reductions of line losses; and
3. Reductions of transformer losses.

$$PF = \cos\theta \tag{2.1}$$

From the power triangle we get:

$$\tan\theta = \frac{Q}{P} \tag{2.2}$$

$$\theta = \tan^{-1}\frac{Q}{P} \tag{2.3}$$

By substituting equation (2.3) in equation (2.1) we obtain:

$$PF = \cos\left(\tan^{-1}\frac{Q}{P}\right) \tag{2.4}$$

2.1.1.2 Voltage Regulation

One measure of service quality is the steadiness of the supply voltage at the point of consumption. A typical goal of the distribution system designer is to maintain the customer's average supply voltage to within ±5 percent of normal.

All loads vary their demand for reactive power in spite of the fact that they differ widely in their ranges and rates of variation .In all cases, variations in the demand for reactive power leads to variations in the voltage at the point of supply, and this can interfere with the efficient operation of all power systems and stations connected to that point, giving rise to the possibility of interference between loads that belong to different consumers.

$$\text{voltage regulation } \% = \frac{V_{no\,load} - V_{full\,load}}{V_{full\,load}} \times 100\% \tag{2.5}$$

One way to enhance regulation of voltage could be to reinforce the power system, increase the generating unit numbers and transformer size, and make the system densely interconnected. This would generally be uneconomical and it would introduce problems associated with high levels and switch gear ratings. It is much more practical and economical to control the voltage and/or VARs on the load side.

The need for voltage control is not new and many solutions to this problem are well known. The solutions either partially eliminate causes of voltage variation, or enhance a system's ability by means of compensation. The goal, of course, is to maintain economical, reliable, and quality services to all consumers.

Transmission voltage variations can be reduced through the use of:
1. Switched shunt capacitor banks,
2. Switched shunt reactor banks,
3. Change transformer taps,
4. Synchronous condensers, and
5. Occasional use of series capacitors.

Injection a certain amount of reactive power in a feeder will decrease the flow

of reactive current in it up to the point of injection which will decrease the voltage drop up to that point and consequently improve the feeder voltage [1, 20].

2.1.1.3 Load Balancing

The majority of Alternating Current systems are 3-phase, and they are intended for balanced operation. Any unbalanced operation of 3-phase systems gives rise to some current components in incorrect phase sequences (zero and negative sequence components). Such components cause many undesirable effects, including excessive heating of electrical machinery, increased ripples in rectifiers, saturation of transformers, oscillating torque in AC machines, function failure in many types of equipment and excessive losses in neutral currents.

The goal of load balancing is achieved by phase control of static VAR compensation. There are many methods used for phase balancing, such as:

(a) Balancing an unsymmetrical resistive load.

(b) The compensation of admittance networks (the ideal load compensator may be considered to be any passive 3-phase admittance network which, when associated in parallel with the load, will present a symmetrical and real load to the supply [1, 7].

2.1.2 Voltage Support

The major purpose is to decrease the voltage variation at a specific terminal of transmission lines. Therefore, the compensation of reactive power enhances AC system stability by incrementing the maximum real power that can be transmitted. Moreover, it helps to maintain a flat voltage at every power transmission level. It also controls temporary over-voltages and steady-states, as well as enhancing the performance of high-voltage DC (HVDC) conversion terminals, which can avoid disastrous blackouts and increase transmission efficiency [18].

2.2 Conventional Reactive Power Compensation Types

There are various types of reactive power compensators as given below:

2.2.1 Series Capacitor Compensator

This is a method to improve the system voltage by connecting a capacitor into the transmission line serially. In other words, to improve the system impedance, reactive power is inserted serially into the line. This improves the capability of power transfer of the line. It is mostly used in extra and ultra-high voltage lines.

A series capacitor compensator is utilized to shorten the electrical length of the transmission line and increase the flow of power. Generally, it is switched off and switched on depending on voltage conditions and load. For instance, in a longitudinal system, a series capacitor compensator is switched off (bypassed) during low load times to avoid line over-voltage because of the excessive capacitive impacts on the power system. It is switched on (fully utilized) during times of maximum load to increment power transfer without subjecting the transmission line to overload. Until recently, these solutions have served the demands of the electricity supply industry well.

There are many problems associated with this method of compensation such as:

1. The electrical resonance of a synchronous generator and the capacitor compensated transmission line causing sub-synchronous torsional oscillation. This phenomenon is generally known as sub-synchronous resonance (SSR).

2. The series capacitor must carry the line current and also the anticipated fault current; thus, it must be protected by a spark gap across it to prevent excessive currents from flowing through it[21,22].

2.2.2 Synchronous Condensers

Synchronous condensers, or synchronous compensators (and sometimes synchronous machines), are designed for shunt reactive power compensation. They fall into the class of dynamic shunt compensators. Figure 2.1 shows the basic principle of a rotating synchronous condenser.
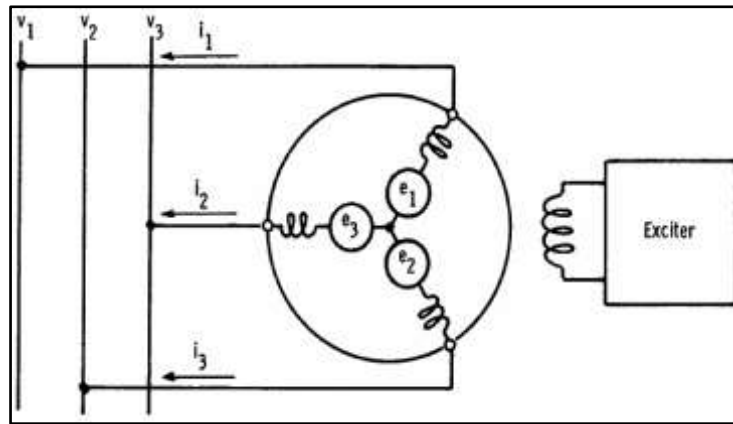
Figure 2.1: synchronous condenser [20].

For purely reactive power flow, the 3-phase induced EMFs of the synchronous condensers are normally excited (in phase with the system voltage). The reactive power can be adjusted by controlling the excitation of synchronous condensers followed by the amplitude of its voltage (E). When a machine is over excited and the amplitude of its voltage (E) increases above the system voltage (V), it acts as a shunt capacitor that produces leading current to be delivered from the AC system. When a machine is under excited and the amplitude of its voltage (E) is reduced to below the system voltage (V), it acts as shunt inductive connection that produces a lagging load to the power network .Under any operating conditions, a small amount of active power flows from the power system to the synchronous condenser to compensate for its electrical losses.

A synchronous machine is used as a dynamic shunt reactive power compensator where it ensures a steady state and dynamic voltage control, lower line losses, and a better voltage profile at the transmission line receiving end.

Currently, synchronous condensers are utilized for major applications including the following [21]:

1. Control of large voltage excursions.
2. Supporting dynamic reactive power at high-voltage DC terminals.

2.2.3 Shunt Capacitor Compensators

These devices are used to control reactive power flow and steady state voltage. They may be:

15

(a) Fixed capacitors (FC):

First use of shunt capacitors occurred in 1914 as power factor correction. The lagging current drawn by the load is compensated for by the leading current that is drawn by the shunt capacitor. They are installed across the supply at the receiving end near the load centers. Their use has increased due to advanced manufacturing techniques, which has resulted in a reduction of their price, improved reliability, and smaller size and weight. The selection of a shunt capacitor depends on many factors, most significant of which is the magnitude of lagging reactive power demanded by the load. In widely fluctuating load cases, reactive power changes over a wide domain. Therefore, fixed capacitor banks may usually lead either to under-compensation or over-compensation. By utilizing switched capacitors, variable VAR compensation is accomplished. A capacitor bank is switched out of, or switched into, the system depending on the total VAR demand. The control smoothness is dependent only on the number of capacitor switching units used. Usually the switching is accomplished by using circuit breakers and relays. However, this method, based on relay and mechanical switches, has the disadvantage of being unreliable and sluggish. Moreover, they require frequent maintenance, and generate high in-rush currents [18].

(b) Thyristor switched capacitors (TSC):

The second type of shunt capacitor is the thyristor switched capacitor (TSC).The VARs released to the host AC system are controlled by switching capacitors into and out of the circuit by using thyristors. Thyristor switches are switched off and on according to the total reactive power provided by the device. The capacitor is switched in when phase voltage is at a minimum, and it is switched out at zero current. This switching is designed so that harmonic currents are not generated. By continuously sensing the load VARs, a number of capacitors are switched into and out of the system individually as required.

1) Principle of Operation of (TSC)

A thyristor switched capacitor is composed of a capacitor bank divided into suitably sized units. The capacitors are switched off and on by utilizing thyristor switches. Every single-phase unit comprises of a capacitor connected serially with anti-parallel thyristor switch and a small inductor as appeared in Figure 2.2a. The purpose of the inductor is to dampen in-rush currents, limit switching transients and

prevent resonance with the network. In 3-phase applications, the basic units are Δ-connected, as shown in Figure 2.2b.
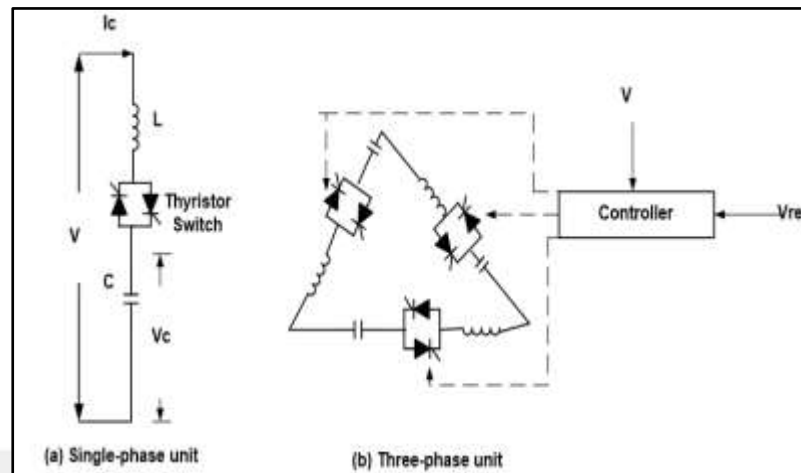
Figure 2.2: Thyristor switched capacitor [3].

The switching of a capacitor can excite transients that may be large or small depending on the capacitors resonant frequency with the external power system. The thyristor firing controls are designed to minimize the switching transients. This is achieved by selecting the switching moment when the voltages over the thyristor switches are at a minimum value, ideally zero.

Figure 2.3 illustrates the operating principle. The switching on moment (t_1) is selected so that bus voltage V is at its highest magnitude and has same polarity as the voltage of the capacitor; this ensures a transient free switching. The switching off moment (t_2) corresponds to a current of zero. The capacitor will then remain charged to a peak voltage, either positive or negative, ready for the next switch-on operation [3, 12].
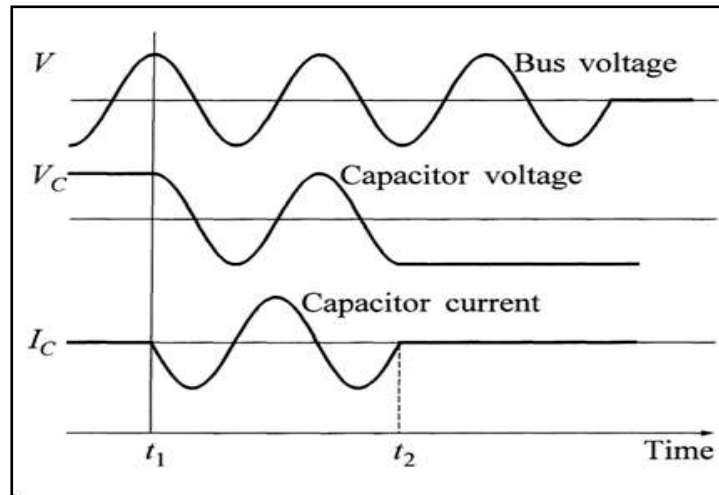
Figure 2.3: Switch operation of a TSC [3].

2.2.4 Shunt Reactors

Shunt reactors are utilized to control reactive power flow, to control steady state voltage, and to decrease or switch surges over voltages [19].

The most common type of shunt reactor is the Thyristor Controlled Reactor.

Thyristor Controlled Reactor (TCR):

This is a system with induction parts only. It consists of a Thyristor Controlled Reactor (TCR) section which is a reactor with thyristor controlled induction. The thyristor controller is a controlling element as two oppositely poled thyristors which conduct the alternate half-cycles of the source voltage waveform frequency. They have been used to reduce response times to a few milliseconds [1, 12].

Principle of Operation of the Thyristor Controlled Reactor (TCR):

The main components of Thyristor Controlled Reactors are a reactor connected serially with an anti-parallel thyristor switch, as seen in Figure 2.4a. A Thyristor Controlled Reactor is controlled in two ways: Integral Angle Control and Phase Angle Control, and depending on the applications, we decide which way is best appropriate. The thyristors conduct alternate half-cycles of source voltage waveform frequency based on the gating angle α, which is measured from a zero intersection of voltage. Gating angles between 0° and 90° are not permitted as they produce asymmetrical current with DC components. Partial conduction is acquired with firing angles between 90° and 180°. Full conduction is acquired with a firing angle of 90°.

18

The current is basically sinusoidal and reactive. The impact of increasing the gating angle is to decrease the current fundamental harmonic component.

If we let σ be the conduction angle, then:

$$\sigma = 2(\pi - \alpha) \tag{2.6}$$

The instantaneous current i is given by:

$$i = \begin{cases} \frac{\sqrt{2}\,V}{X_L}\,(\cos\alpha - \cos\omega t) & \text{for}\quad \alpha < \omega t < \alpha + \sigma \\ 0 & \text{for}\quad \alpha + \sigma < \omega t < \alpha + \pi \end{cases} \tag{2.7}$$

The fundamental current component is given by Fourier analysis for the current waveform:

$$I_1 = \frac{V}{X_L} \cdot \frac{\sigma - \sin\sigma}{\pi} \tag{2.8}$$

Where,

I_1 : is the root mean square (R.M.S) value of current,

V: is the root mean square (R.M.S) value of voltage, and

X_L : is the reactor reactance at the fundamental frequency.

The impact of increasing α (i.e., decreasing σ) is to decrease the fundamental component .This is equivalent to increasing the effective inductance of the reactor.

Equation (2.8) can be written as:

$$I_1 = B_{TCR}\,(\sigma)\,V \tag{2.9}$$

Where,

B_{TCR} : is an adjustable fundamental frequency susceptance controlled by the conduction angle σ as per the equation:

$$B_{TCR}\,(\sigma) = \frac{\sigma - \sin\sigma}{\pi X_L} \tag{2.10}$$
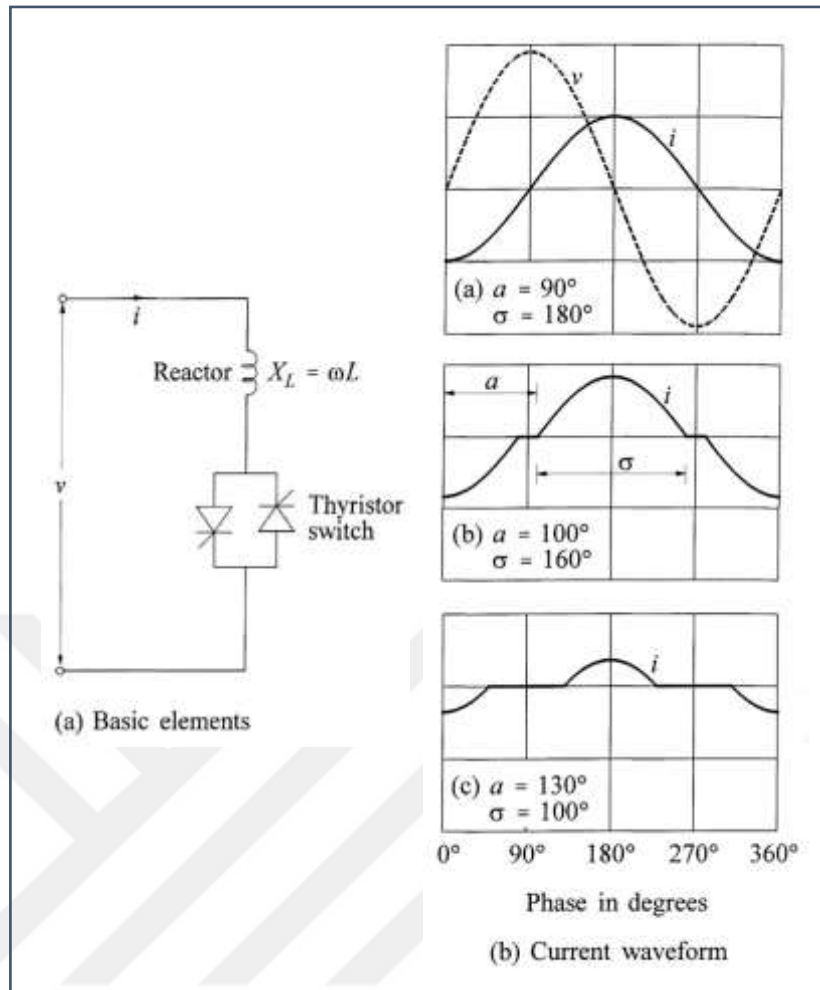
Figure 2.4: Thyristor controlled reactor TCR [24].

Figure 2.5 shows the curve of the control law. The maximum value of the effective susceptance B_{TCR} is $1/X_L$, which is acquired at ($\alpha = 90°$ or $\sigma = 180°$), that meaning a full conduction occurs in the thyristor controller. On the other hand, the minimum value of the effective susceptance B_{TCR} is zero, which is acquired at ($\alpha = 180°$ or $\sigma = 0°$) [1, 3, 12].
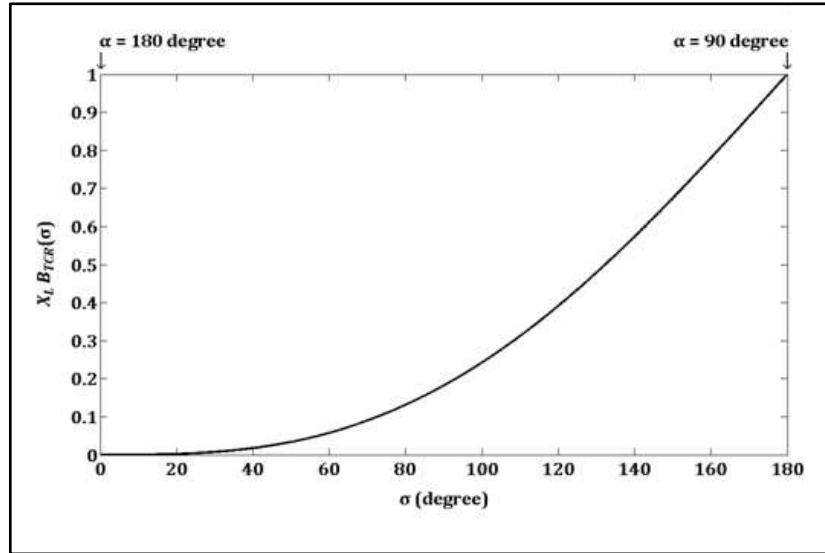
Figure 2.5: The control law of elementary TCR [3].

This susceptance control principle is recognized as phase angle control. For a controllable fraction, the susceptance is switched into the system for each half cycle. The variance in the TCR current as well as the susceptance is continuous and smooth.

A Thyristor Controlled Reactor requires a control system that decides the firing moments (i.e., firing angle α) measured from the last zero intersection of the voltage (firing angles synchronization). In some designs, the control system responds to a signal that indicates the required susceptance directly. In others, the controls respond to wrong signals such as auxiliary stabilizing signals, voltage deviations, etc. The result is a steady state V/I characteristic, which can be described thus:

$$V = V_{ref} + X_{SL} I_1 \tag{2.11}$$

Where,

X_{SL} : is the slope reactance determined by the control system gain [1, 23].

2.2.5 Thyristor Controlled Transformer (TCT)

A Thyristor Controlled Transformer is shown in Figure 2.6.
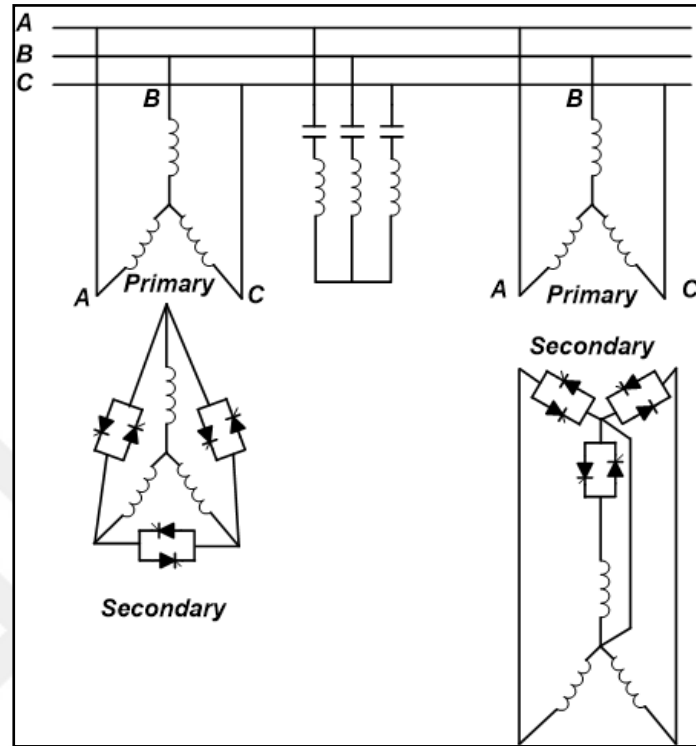
Figure 2.6: Thyristor controlled transformer (TCT).

a - Δ-connected Thyristor Controlled.
b - Y-connected Thyristor Controlled [3].

Rather than utilizing linear reactors and separate step-down transformers which are designed with very high leakage reactance, the secondary windings are simply short-circuited through the thyristor controllers. A gapped core is important to acquire high leakage reactance, and the transformers can appear as three signal-phase transformers. With the configurations in Figure 2.6, there is no secondary bus and a shunt capacitor must be associated at the primary voltage unless separate step-down transformers are provided. The high leakage reactance ensures transformers against short-circuit forces during secondary faults. Due to its large thermal mass and linearity, the TCT can usefully withstand overload in the lagging regime [1, 21].

2.3 Static VAR Compensator

The term "Static VAR" has been adopted to apply to a number (set) of static VAR compensation devices which are used in shunt reactive control. These devices can consist of static reactive elements (no moving parts) connected in a shunted manner (linear or nonlinear capacitor and reactor) designed into a VAR compensating system. Over some rated range of VARs, the reactive power flowing in these devices is controllable, so this feature is considered to be a special property in static VAR compensation. SVCs are automated impedances matching devices that are designed to fetch the system nearer to unity PF.

In modern power supply systems, the thyristor controlled Static VAR Compensator is the most commonly used for load compensating because of its simple control strategy and low cost. Such a Static VAR Compensator may comprise the following components:

1. Fixed capacitor (FC).
2. Thyristor switched capacitor (TSC).
3. Thyristor switched reactor (TSR).
4. Thyristor controlled reactor (TCR).

Under steady state conditions, static VAR compensators introduce harmonic currents into the AC power system to which they are connected. The harmonic currents result from the operation of TCR at different conduction angles due to their operation strategies [4, 7, 19].

2.4 SVC Configurations

The static VAR compensation with any range of controls may be configured by utilizing the mixes of components mentioned previously. Various SVC configurations have been applied successfully in order to meet differing system necessities. The required speed of response, losses, flexibility, costs, and size ranges are the most important considerations when selecting a suitable configuration for any particular application. There are two common SVC configurations [3, 24]:

1. Thyristor Switched Capacitor-Thyristor Controlled Reactor (TSC-TCR).
2. Fixed Capacitor-Thyristor Controlled Reactor (FC-TCR).

2.4.1 TSC-TCR

The TSC-TCR consists of two types of components. The first is the Thyristor Switched Capacitor (TSC) which responsible for generating the reactive power, while the second is the Thyristor Controlled Reactors (TCR), which are responsible for absorbing the reactive power. In the scheme shown in Figure 2.7, the TCR and TSC are connected in Δ and Y configurations, respectively. The TCR provides continuous and smooth variable susceptance, while the TSC provides a stepped response [1,8]. The major motivation in improving TSC-TCRs is to enhance the operational flexibility of the VAR compensators in times of extensive disturbance and decrease of steady-state losses [21].
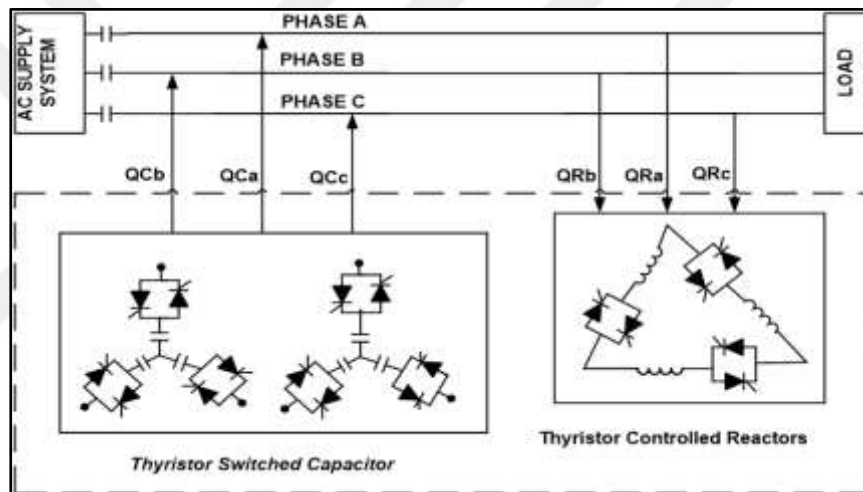
Figure 2.7: Schematic diagram of TSC-TCR [5].

2.4.2 FC-TCR

In the FC-TCR configuration, two types of component are used. The fixed capacitor (FC) is used in a shunted manner with a thyristor controlled reactor (TCR) Figure 2.8. Such a device is able to supply continuous leading and lagging VARs to the power system. FC is considered a reactive power source and TCR receives any reactive power. By controlling the gating angle of the back-back thyristor valves, circulating current through the reactor is adjusted, whereas capacitor supplies leading VARs to the power system. The fixed capacitor banks are typically connected in a Y configuration. An (FC-TCR) acts as a parallel LC circuit which tends to set up a

resonance with the power system impedance in times of extensive disturbances [15, 21].

*In this work, this configuration is used as reactive power compensation.
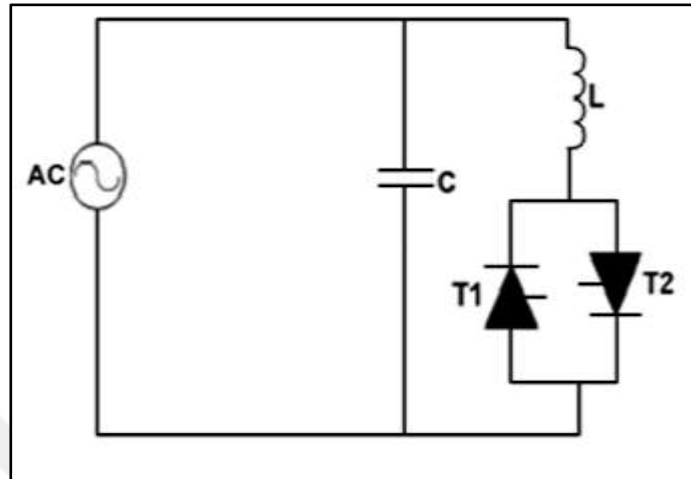
Figure 2.8: Schematic diagram of FC-TCR [15].

2.5 SVC Applications

Since their first application in the late 1970s, their utilization in transmission systems has been expanding steadily. By virtue of its capability to provide rapid and continuous control of voltages and reactive power, SVC can improve the performance of various aspects of transmission systems. The most common applications of SVC are as follows:

a) Enhancement of voltage level;

b) Transient stability enhancement;

c) Damping of power oscillation; and

d) Mitigation of sub-synchronous resonance.

At distribution system levels and at the sub-transmission, SVCs are used for balancing 3-phase systems supplying unbalanced loads. Additionally, they are used to reduce variations in supply voltage caused by repetitive effect loads such as rolling mills, arc furnaces, and the dragline loads of mining plants [3].

In this thesis, the SVC will be used to reduce system losses and enhance voltage levels by controlling the reactive power in a power system.

CHAPTER THREE

FACTS DEVICES, STABILITY OF THE POWER SYSTEM AND HARMONICS

3.1 Flexible AC Transmission Systems (FACTS) Devices

The past decades have seen a rapid development and improvement of advanced digital controllers and solid state power electronics. The present electrical market offers fast working FACTS devices. These new devices perform well at controlling power systems [25]. For high-power levels, devices have been made accessible in converters for high voltage levels and even higher.

Any element of a network may affect the impedance or reactive power of an AC power system. For the application of a FACTS device, classification in terms of static and dynamic requires some explanation. For fast controllability of FACTS devices, the term dynamic is used provided by power electronics. This is one of major factors that distinguish them from traditional devices. When devices have no moving parts, such as mechanical switches to achieve dynamic controllability, they are called static devices. Thus, most FACTS devices can equally be dynamic and static [26].

FACTS devices can be utilized to improve system stability and to control power flow. Especially with deregulation of the electricity market, there is rising interest in utilizing FACTS devices in the control and operation of power systems with new power flow conditions and loadings. Installing FACTS devices in existing power systems becomes important to increase their capacities and controllability. There are two major features that need to be considered in FACTS device use: the first is flexible power systems operation corresponding to FACTS device power flow control ability. The second feature is the development of a steady state and a transient stability of the system.

According to IEEE, FACTS (Flexible Alternating Current Transmission Systems) is defined as follows: "Alternating current transmission systems incorporating power electronic based and other static controllers to enhance controllability and increase power transfer capability" [27].

3.2 FACTS Applications

Many FACTS devices have been presented for different applications worldwide. A number of new kinds of FACTS devices are in the stage of being presented in practice. Their controllability is used in most applications to avoid landscape requiring extensions or cost intensive power systems and for demand such as development or additions of power lines and substations. FACTS devices present better modifications to the usage of existing installations as well as improvements and varying operational conditions. The main FACTS devices applications are [26]:

1. Reactive power compensation;
2. Improvement of power quality;
3. Mitigation of flicker;
4. Stability enhancement;
5. Voltage control;
6. Increase in transmission capacity;
7. Controlling power flow; and
8. The interconnection of distributed generation, renewable, and storages.

3.3 Classification of FACTS Devices

3.3.1 According to The Type of Connection

FACTS devices can be divided, depending on the connection type to the network, into four categories [24]:

i. Shunt controllers;

ii. Series controllers;

iii. Combined shunt-series controllers; and

iv. Combined series-series controllers.

1) Shunt controller:

This controller can be regarded as a variable source, variable impedance, or a combination of these. A shunt controller injects currents into the AC power system at the connection point. If the injected current is in phase quadrature with the line voltage, the shunt controllers consume or supply the reactive power only. For any other phase relationship, the shunt controller adjusts both active and reactive power. The most common shunt controllers are the STATic COMpensator (STATCOM) and the Static VAR Compensator (SVC).

2) Series controller:

Series controllers would be with variable impedances, like reactors, capacitors, etc., or power electronics based variable sources of major frequency, harmonic frequencies and sub synchronous to serve the desired demand by inject voltage in series with the line. Since the injected voltage is in phase quadrature with line current, series controllers consume or supply the reactive power only. While any other phase relationship, the shunt controller adjusts both active and reactive power. The most common series controllers are Static Synchronous Series Compensator (SSSC), Thyristor Controlled Phase Shifting Transformer (TCPST), and Thyristor Controlled Series Compensator (TCSC).

3) Combined shunt-series controller:

This combined controller consists of separate shunt and series controllers that are controlled in a coordinated manner, or it consists of a united power flow controller with a shunt and series elements. In theory, a series component injects a series voltage into the system while the shunt component injects the current. The most common combined shunt-series controller is the Static Phase Shifting Transformer (SPST) and the Unified Power Flow Controller (UPFC).

4) Combined series-series controller:

This Combined controller consists of two or more separate series controllers that are controlled in a coordinated manner in a multi-line transmission system. Alternatively, it may be a united controller, where a series controller provides impartial series reactive compensation for each line but also transferring active power among the lines through the power link. In this category, the Interline Power Flow Controller (IPFC) can be used to adjust both reactive and active power [2].

3.3.2. According to Power Electronic Devices Used in the Control

FACTS controllers can be categorized according to the power electronic devices that are used in their control into two basic categories [24]:

   i. First generation (Variable impedance type).

  ii. Second generation (Voltage Source Converter (VSC) based type).

* There is also Current Source Converters (CSCs) but they are not under our consideration in this investigation.

These two divisions are separate; for example, existing devices of a group in the first category can belong to different groups in the second category. The capacity to interchange active power and generate reactive power is a major difference between the second and first generation devices. In the first generation, FACTS devices work such that the passive elements using tap changer transformers are controlled by thyristors or by impedance. However, in the second generation, FACTS device module and angles controlled voltage sources work without inertia, created in converters, and use electronic stress sources (auto switched voltage sources, three-phase inverters, voltage source control, synchronous voltage sources) that are controllable and rapid proportioned and are static synchronous current and voltage sources [2].

1) Variable impedance type

The variable impedance controller types are:

a. Static VAR Compensator (SVC).

b. Thyristor Controlled Phase Shifting Transformer (TCPST).

c. Thyristor Controlled Series Capacitor or Compensator (TCSC).

2) Voltage Source Converter (VSC) based type

The VSC based FACTS controllers are:

a. Interline Power Flow Controller (IPFC).

b. Static synchronous Compensator (STATCOM).

c. Unified Power Flow Controller (UPFC).

d. Static Synchronous Series Compensator (SSSC).

Table 3.1 shows the classification of common FACTS devices depending on power electronic devices that are used in the control and connection type [24].

Connection type	FACTS controller	
	Voltage Source Converter (VSC)	Variable Impedance
Shunt	STATic COMpensator (STATCOM)	Static VAR Compensator (SVC)
Series	Static Synchronous Series Compensator (SSSC)	Thyristor Controlled Series compensator (TCSC)
Combined shunt - series	Unified Power Flow Controller (UPFC)	Static phase shifting transformer (SPST)
Combined series-series	Interline Power Flow Controller (IPFC)	----------------

3.4. Installation Factors for FACTS Devices

Before installing FACTS devices, there are three factors to be considered:

1. The device type;

2. The required capacity; and

3. The location that optimizes the device functioning.

Among these factors, the third is of great significance because the proper system features and the desired effect depend on the location of controllers [28].

3.5 Typical FACTS Devices

The main five typical FACTS devices are SVC, SSSC, TCSC, UPFC and STATCOM.

3.5.1 Static VAR Compensator (SVC)

SVCs are shunt FACTS devices which are considered variable impedance type devices. SVC contains a TCR with capacitor banks in parallel. From the operational point of view, the SVC device acts as a variable shunt reactance, which either absorbs or generates reactive power to maintain the magnitude of voltage to the alternating current network connection point. It is used significantly to provide voltage regulation support and fast reactive power. Controlling the gating angle of

the thyristor enables the static VAR compensator to have almost instant speed of response and it determines the equivalent shunt admittance presented to an AC power system. SVC configuration is shown in Figure 3.1, which essentially consists of a thyristor controlled reactor and a fixed capacitor.

The essential task of SVC devices is to regulate the voltage at a particular bus by means of reactive power compensation (acquired by varying thyristor gating angles). The SVC device has been utilized for transient voltage control and high performance steady state compared with traditional shunt compensation. The SVC is also utilized to reduce system losses, dampen power swings, and enhance transient stability by optimizing reactive power control [23, 29].
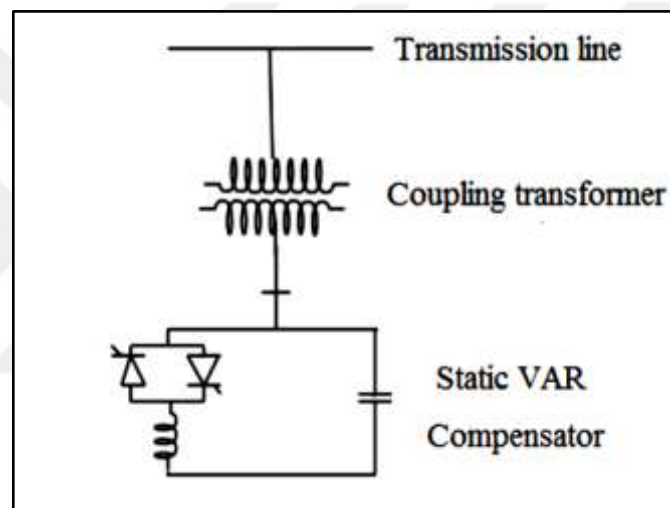
Figure 3.1: SVC connected to a transmission line [30].

3.5.2. Static Synchronous Series Compensator (SSSC)

SSSC is a part of the FACTS family such that it is connected serially with power systems. It contains a solid state voltage source converter that generates controllable AC voltages at a fundamental frequency. As the injected voltage is saved in quadrature with the line current, it can emulate capacitive or inductive reactance so as to impact the power flow in transmission lines. Though the essential function of an SSSC is to control steady state power flow, it also enhances the transient stability of power systems [30].

SSSCs provide an alternative compensation to the traditional series capacitive line. An SSSC device is a synchronous voltage source that generates the required

compensating voltage internally independent of the current of the line and in series with it, as shown in Figure 3.2.
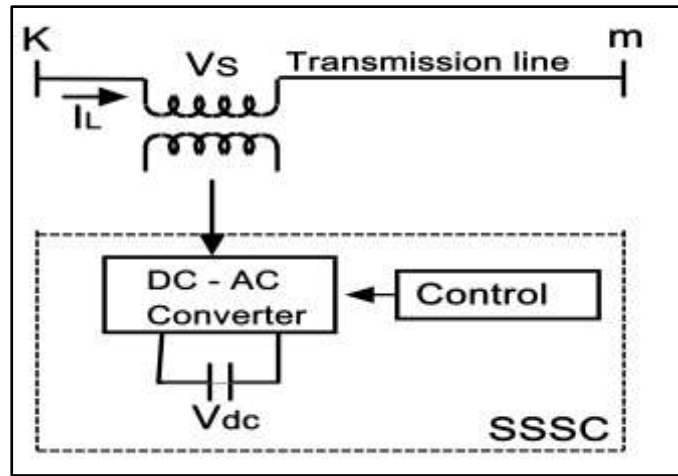
Figure 3.2: Configuration of Static synchronous series compensator [30].

SSSC devices may be deemed ideal generators functionally. The SSSC device can be produced at the desired fundamental frequency set of three alternating voltages with controllable phase angles and amplitudes. Furthermore, an SSSC device can absorb or generate reactive power when joined to an electric power system for purposes such as a compensator synchronous condenser and convert active power with an AC system that it exchanges into a DC voltage compatible with an electrical energy source or storage. Moreover, transferred power turns into a parametric role of the injected voltage. Both powers, active and reactive, can be controlled simply with SSSC by controlling the angular position of the injected voltage according to the current of the line. Unique FACTS controller arrangements, by selecting suitable configurations of SVSs, can control reactive and active power flows in individual lines independently, balance reactive and active flows between lines, and they can be created. From the view of practical applications, stability improvements or steady-state flow control, the SSSC device obviously has a considerably wider range of control than the controlled series capacitor (for the same MVA rating) [31].

3.5.3 Thyristor-Controlled Series Capacitor (TCSC)

This is one of the best known and most important FACTS controllers. It has been used for long time to enhance system stability as well as to increase power transfer. Figure 3.3 shows the main circuit of a TCSC. It consists of three major components: a bypass inductor, a capacitor bank and antiparallel thyristors. The TCSC reactance is adjusted by controlling thyristor firing angles according to a system control algorithm, regularly in response to some component parameter variation. Corresponding to the variation of thyristor conduction angles or firing angles, this procedure can be modeled as a very fast switch between corresponding reactances presented to the system. The TCSC can be controlled to work either in the inductive or capacitive domain to avoid resonance in steady state [30].
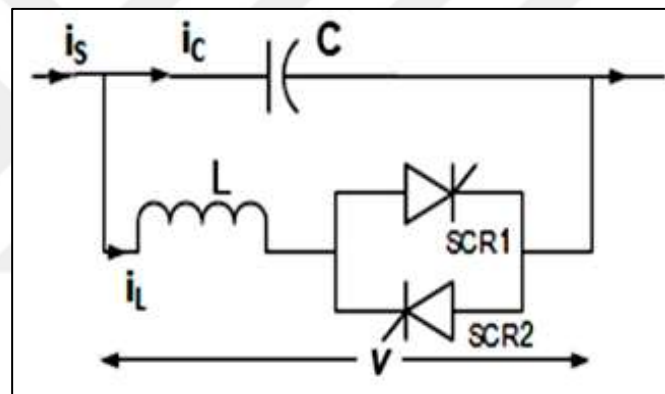
Figure 3.3: Configuration of a TCSC [30].

3.5.4 Unified Power Flow Controller (UPFC)

These contain two VSCs with a DC-link capacitor joint. The two converters are linked to one transmission line by two-coupling transformers; one is linked in series and the other is linked in a shunt. The series linked compensating voltage is of variable phase angle and magnitude; additionally, it is with the prevailing current of line at any phase-angle. Therefore, it exchanges reactive and active powers with the transmission line. Active power is the exchanged bidirectional flow through the shared link from and to the same transmission line under compensation. The configuration of UPFC is shown in Figure 3.4. Both series and shunt-linked VSCs may also deliver independent reactive power compensation at their respective AC

terminals. For special cases, when DC-link capacitors of two-VSCs are not linked together, both series linked VSCs (SSSC) and shunt-linked VSCs (STATCOM) provide reactive power compensation independently at their respective AC terminals and there is no active power exchange between them.
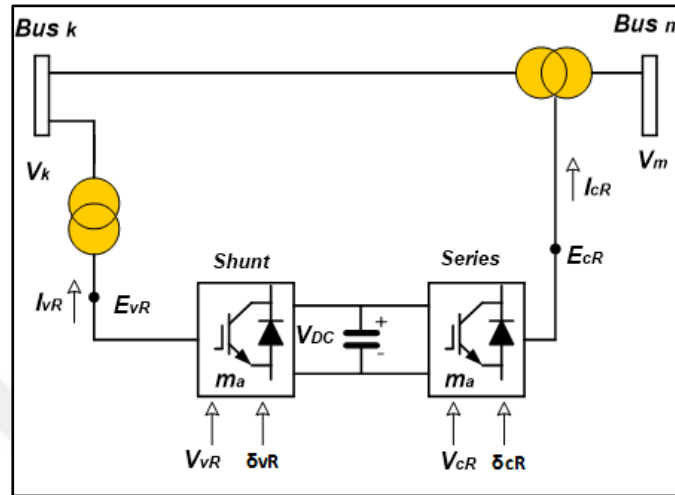
Figure 3.4: Configuration of UPFC [2].

3.5.5 Static Synchronous Compensator (STATCOM)

This static synchronous generator works as a shunt connected SVC whose inductive or capacitive output current can be controlled independently of system voltage. It is a solid state switching converter that is able to absorb or generate independently controllable reactive and active power at its output terminals when it is fed from a device of appropriate rating, such as energy storage or an energy source. A STATCOM incorporates a voltage source inverter (VSI) that produces a set of 3- phase AC output voltages, each of which is in phase with, and coupled to, the corresponding AC system voltage through a relatively small reactance. Normally, this small reactance is provided by the coupling transformer per phase leakage reactance. The DC storage capacitor derives the VSI. The reactive power exchanges between the AC power system and STATCOM is controlled by regulating the produced output voltage magnitude [32].

34
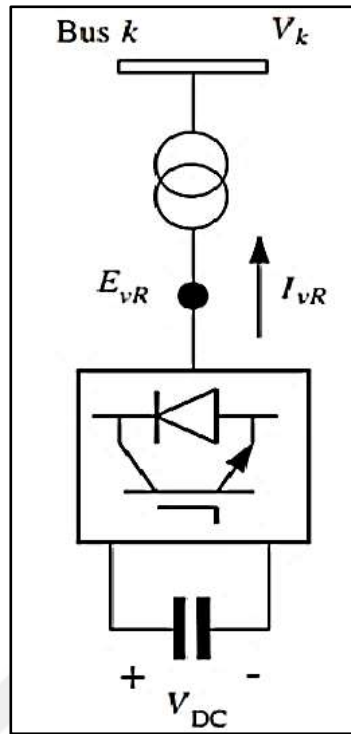
Figure 3.5: Static compensator (STATCOM) system [3].

Static synchronous compensators (STATCOMs) contain a 3-phase PWM inverter/rectifier primarily which can be shunt connected to a power system to compensate the system reactive power requirement dynamically. Similarly to a 3-phase PWM inverter/rectifier, a STATCOM device is a VSC which changes DC-power to AC-power of variable phase angle and amplitude, by varying the phase angle and amplitude of the 3-phase AC-currents at its AC-side. Moreover, the STATCOM can supply a precise and variable quantity of reactive-power to the connected AC power system.

The STATCOM device has been mainly applied to voltage support over the past decade for voltage stability and power quality improvements. Its dynamic response may work faster than thyristor based static compensators or conventional synchronous generators. However, a STATCOM device is limited in its capacity for power system stability margin improvement because of its limited ability to deliver active power. Significant developments have been made in energy storage technologies in recent years, including fuel cells technologies for batteries, flywheel storage for bulk energy storage, and superconducting magnetic storage of energy for power balancing of grid-systems. The use of STATCOM devices with the mentioned storages has become viable such that they can withstand power outages and be used

for steady-state voltage control. These systems have a number of limits due to their slow response. Super capacitors (sometimes known as ultra capacitors) are devices that can store significant quantities of energy and release it quickly. Their major function is to (power boost) any type of application requiring rapid response stores of energy.

A STATCOM is utilized for voltage compensation at the receiving end of a transmission lines, hence replacing shunt capacitor banks. When used for this purpose, STATCOMs offer a number of advantages over shunt capacitor banks, such as increase the stability of transmission line during load variations and much tighter voltage compensation control at the receiving end of the transmission line.

FACTS devices based on VSC, such as STATCOM, are increasingly utilized in power systems due to their capability of providing enhanced performance in comparison to conventional thyristor-based FACTS devices. A STATCOM device consists of one VSC and its associated shunt connected transformer. It is the static equivalent of the rotating synchronous condenser but it absorbs or generates reactive power at a faster rate because no moving elements are involved. The STATCOM fundamentally includes a DC voltage source behind self-commutated inverters using a coupling transformer and IGBT.

Principle of Operation for STATCOM:

A STATic COMpensator (STATCOM), which is part of the FACTS device family, consists fundamentally of a 3-phase PWM inverter/rectifier that can be shunt-connected to a system to compensate the reactive power requirement dynamically. Similar to a 3-phase PWM inverter/rectifier, a STATCOM is a VSC that changes DC power to AC power of variable phase angle and amplitude, by varying the phase angle and amplitude of 3-phase AC-currents at the AC side, Moreover a STATCOM can supply a precise and variable quantity of reactive power to the connected AC power system.
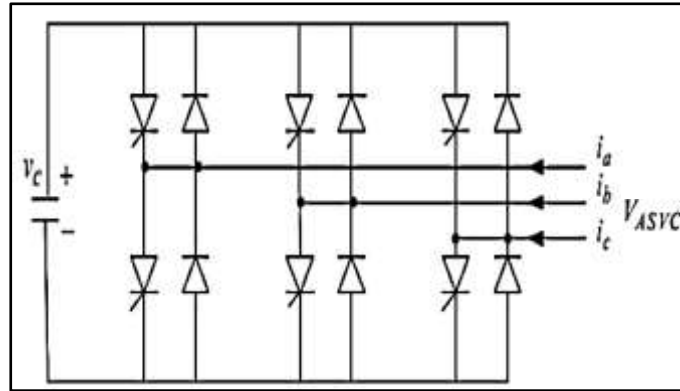
Figure 3.6: Circuit of STATCOM [3].

Figure 3.6 shows the main connection of a STATCOM to the fully controlled valve (GTO) and its control element. The characteristic of the ideal GTO-switch is that under positive valve-voltage and with a positive current of control on its gate, it turns on, and with a negative current of control on its gate valve, it is turned-off. Its resistance is infinity when it is turned off and zero when it conducts. A GTO can achieve a switch-off by gate control in comparison to a thyristor wherever switch off is possible only at current zero crossing. Figure 3.6 shows a STATCOM of voltage type self-commutation full bridge inverter corresponding to the power electronics theory.

The capacitor DC voltage behaves as an ideal DC voltage source to support the inverter. A regular diode is linked in the opposite parallel direction with the GTO, which is a path for a continuous current, providing a route for the feedback-energy from the AC side. The usual function of the inverter is to convert the DC voltage to AC voltage that has a controllable phase angle and magnitude at the same frequency as the AC system [2, 33].

3.6 Stability of Power System

Power system stability is defined as the capability of a power system that enables it to remain in stable operating equilibrium under normal operating conditions and to regain an acceptable state of equilibrium after being subjected to a disturbance [34]. Power system stability can be classified into two categories:

1- Voltage Stability.

2- Rotor Angle Stability.

3.6.1 Voltage Stability

It is the capability of a power system to maintain a steady state voltage at all buses in the system with usual operating conditions. After disturbances such as when the load admittance increases, load power will increase so that both voltage and power are controllable. Furthermore, voltage collapse is defined as being the process by which voltage instability leads to a very low voltage in a significant part of the system [35]. This depends on the ability to maintain equilibrium between the load demand and load supply from the system. The major factor contributing to voltage instability is generally the dropped voltage, which limits power transfer between buses (transmission networks capacity). Any instability that may result takes place in the form of a rise in voltage or a progressive fall of a few buses. The possible result of voltage instability is a load loss in the zone where the voltage falls to unacceptable minimum values or loss of power system integrity.

The progressive drop of bus voltages can be associated with rotor angles whenever it goes out of step. Where the gradual loss of machine synchronism as rotor angles between two couples of the machines approach or exceed 180°, it could result in very low voltages at intermediate points in the network near to the electrical center. Voltage instability is essentially a local phenomenon; however, it has a widespread impact. Voltage collapse is more complex than simple voltage instability and it is usually the result of a sequence of events accompanying voltage instability leading to a low voltage profile in a significant part of the power system [34, 36].

While the disturbance leading to voltage collapse may be attributable to a variety of causes, the underlying problem is an inherent weakness in the power system. The only way to save the system from voltage collapse is to reduce the reactive power load or add additional reactive power prior to reaching the point of voltage collapse [2].

3.6.2 Rotor Angle Stability

Rotor angle stability is the capability of synchronous generators to continue in synchronism under steady state conditions after being exposed to a disturbance. It depends on the capability of each the synchronous generators in the power system to continue equilibrium between the mechanical torque and electromagnetic torque. A

major factor is the change in the synchronous generators' angles of the rotor as they follow the changes in demand for the power from the power system during a disturbance and after a disturbance. Under steady state conditions, the output electrical torque and input mechanical torque remain in balance and the speed of the rotor remains constant. Instability that may result occurs in the form of increasing angular swings of some generators leading to synchronism loss with other generators. The angle of rotor stability problem includes the study of the electromechanical oscillations inherent in power systems. A fundamental factor in this problem is the manner in which the power outputs of synchronous machines vary as their rotor angles change [34, 36].

Stability Conditions

For the purpose of analysis there are three stability conditions namely (Steady-state, Transient stability, and Dynamic stability), described as follows:

(1) Steady-state stability:

This is may be defined as the ability of an electric power system to maintain machine synchronism within the system and the external tie line following a small and slow disturbance (normal load fluctuations) including the action of the AVR and turbine governors.

Steady-state stability limit: This refers to maximum power which can be transferred through the system without loss of stability under small and slow disturbance.

(2) Transient Stability:

After a large sudden disturbance, the synchronous power system can regain and maintain synchronism. Large disturbances include (fault, sudden load change, inadvertent tripping of lines and generator). In the other definition, transient stability is the ability to remain in synchronism during the period following a disturbance and prior to the time that the governors can act. (The first swing of the machine rotors will take approximately 1 second following a disturbance).

Transient stability, Steady-state stability limit: This refers to the maximum power which can be transferred through the system without loss of stability under sudden disturbance.

(3) Dynamic Stability:

This is the ability of a power system to remain in synchronism after an initial swing (transient stability period) until the power system has settled down into the new steady-state equilibrium conditions. When sufficient time has passed after a disturbance, the prime mover governors will react to decrease or increase input energy as required in order to re-establish a balance between existing electrical load and input energy. (This usually occurs about 1 to 1.5 seconds after the disturbance).

Dynamic stability studies cover longer real-time intervals, sometimes 5-10 seconds and occasionally up to 30 seconds depending on the inertias of the system and the characteristics of the governors. During this period, the governors open or close valves as required to increase or decrease input energy to the prime movers [34].

3.7 Harmonics

Fourier series expansion for periodic signals is given by:

$$f(x) = a_0 + \sum_{n=1}^{\infty} a_n \, \cos\left(\frac{2\pi n}{T} \, t\right) + \sum_{n=1}^{\infty} b_n \, \sin\left(\frac{2\pi n}{T} \, t\right). \qquad (3.1)$$

Where,

a_0 : constant coefficients $= \frac{1}{T} \int_0^T f(t) \, dt.$

a_n: constant coefficients $= \frac{2}{T} \int_0^T f(t) \, \cos\left(\frac{2\pi n}{T} \, t\right) dt.$

b_n: constant coefficients $= \frac{2}{T} \int_0^T f(t) \, \sin\left(\frac{2\pi n}{T} \, t\right) dt.$

$f_n \; = \; n/T, \qquad n = 0, 1, 2, \ldots$

- $f_n \; = \; 0 \qquad$ (constant DC component).

- $f_n \; = \frac{1}{T} \quad$ (fundamental frequency).

- $f_n \; = \frac{2}{T}, \frac{3}{T}, \ldots, \frac{k}{T}, \ldots$ (Harmonic frequency).

The series in Equation (3.1) is a linear combination of sine and cosine functions with various frequencies, which are integer multiples of the fundamental frequency and the coefficient a_0 can be considered the portion with zero frequency (i.e. the DC component) in a signal [37].

Harmonic can be defined as a sinusoidal component of a periodic wave (current or voltage) having frequency that is an integral multiple of the main frequency produced by generators (the actual system frequency) [38].A pure

sinusoidal signal have not any harmonic [5]. If the fundamental frequency of a system is 50 Hz, then the third harmonic of the system is 150 Hz, the fifth 250 Hz, and so on. Harmonics occur by means of non-linear loads due to the current not being drawn as a pure sine wave. Electronic equipment draws current in pulses when turning from AC to DC; these pulses are rich in harmonics that distort the current wave. The electronic equipment in the system will act as harmonic current generators. These harmonic currents then flow back into other parts of the electrical power system and distort it. Moreover, the voltage waveform in turn becomes non-sinusoidal. These voltages can then affect other loads and equipment in the system that shares a branch circuit or a transformer with the original harmonic load.

The level of electric power system harmonic currents and voltages has expanded significantly and there has been a large interest in eliminating harmonic signals. Analytical methods are required in order to calculate the harmonics in a power system. A harmonic study is a numerical tool applied to study the propagation and generation of harmonics in an arbitrary topology network [38].

3.7.1 Harmonic Analysis

The primary concern in studying harmonics is studying the effect of harmonics on the AC power system rather than on the component that generates these harmonics. The effects of harmonics on an AC power system are generally measured by calculating the Total Harmonic Distortion (THD) and the Total Demand Distortion (TDD) [39].

1- Total Harmonic Distortion (THD)

This is defined as a measure of the deviation of the current or voltage wave from the sinusoidal shape. It is also defined as the ratio of square root of the sum of the squares of the R.M.S values of the harmonic components to the R.M.S value of the fundamental component; THD for voltage is given by:

$$THD_V = \frac{\sqrt{\Sigma_{h=2}^{\infty} V_h^2}}{V_1} \qquad (3.2)$$

Where,

THD_V : is the total harmonic distortion for voltage,

V_h : is the R.M.S value of the hth harmonic component of the voltage,

V_1 : is the R.M.S value of the fundamental component of the voltage.

THD for current; the most commonly used harmonic index; is given by:

$$THD_I = \frac{\sqrt{\sum_{h=2}^{\infty} I_h^2}}{I_1} \tag{3.3}$$

Where,

THD_I : is the total harmonic distortion for current,

I_h : is the R.M.S value of the hth harmonic component of the line current,

I_1 : is the R.M.S value of the fundamental component of the line current.

This is commonly used as the ratio of R.M.S value of the harmonic component to the R.M.S value of the fundamental component and usually expressed in percent. Total Harmonic Distortion is used as a measure of the effect of harmonics on a power system [5].

2- Total Demand Distortion (TDD)

Harmonics distortion is most significant when calculated at Point of Common Coupling (PCC) which is Point on a public power supply system, electrically nearest to a particular load, at which other loads are, or could be, connected. The PCC is a point located upstream of the considered installation. Therefore, the TDD is based on the load demand current (I_L) as follows [6]:

$$TDD = \frac{\sqrt{\sum_{h=2}^{\infty} I_h^2}}{I_L} \tag{3.4}$$

Where,

I_h : is the R.M.S value of the hth harmonic component of the line current,

I_L : is the rated load current (maximum demand load current).

3.7.2 Harmonics Due to SVC

The disadvantage of unbalanced load compensation is that the harmonic currents generated by each phase of the compensator are unequal. The thyristor-controlled reactive devices are widely used in power systems to meet unbalanced loads. It is used also for voltage regulation, increasing system stability and power transfer. The most important static reactive power compensation devices are the Thyristor Switch Capacitor (TSC) and Thyristor-Controlled Reactor (TCR) due to their fast response, high reliability and low cost maintenance [1, 5].

As the Thyristor-Controlled Reactor (TCR) firing angle α is increased from $0° \ to \ 90 \ °$ (measured from $0°$ crossing current), the waveform of the current

becomes less sinusoidal, meaning that the TCR generates harmonics. For the single-phase device considered so far, if the firing of the thyristors is symmetrical (equal for both thyristors), only odd harmonics are generated. For a 3-phase system, the preferred arrangement is to have the three single-phase TCR elements Δ-connected (6-pulse TCR), as shown in Figure 3.7a. For balanced conditions, all triple harmonics (3, 9, 15…) circulate within the closed delta and are therefore absent from the line currents. Filters are often used to remove harmonic currents.

Elimination of the 5th and 7th harmonics can be achieved by using two 6-pulse TCRs with equal rating, fed from two secondary windings of the step-down transformers, one Y-connected in and the other Δ-connected, as shown in Figure 3.7b. Since the voltages applied to the TCRs have a 30-degree phase difference, the 5th and 7th harmonics are eliminated from the primary-side line current. This is known as a 12-pulse arrangement because there are 12 thyristor firings for every cycle of the three-phase line voltage. With the 12-pulse scheme, the lowest-order characteristic harmonics are the 11th and 13th. These can be filtered with a simple capacitor bank.

The TCR responds in approximately 5 to 10 ms, but delays are introduced by measurement and control circuits. To ensure control loop stability, the response rate may have to be limited. For these reasons, response times are typically around 1 to 5 cycles of the supply frequency [3].
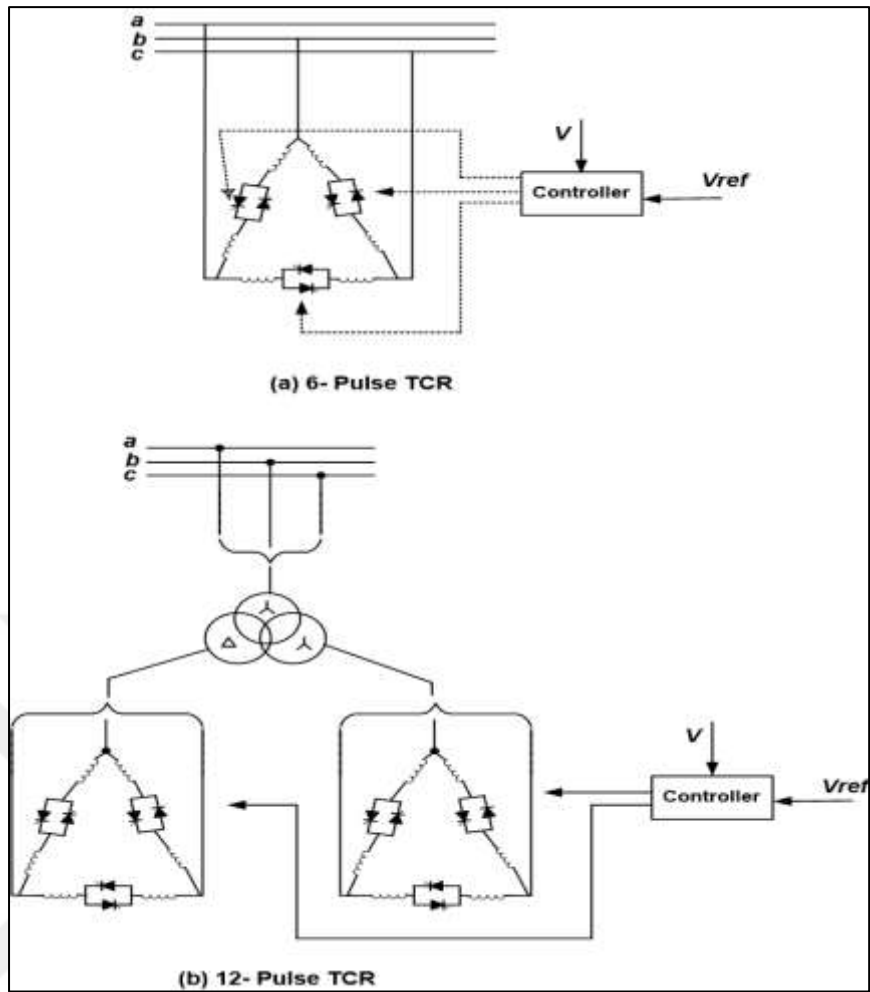
Figure 3.7: Three phase TCR arrangements [3].

CHAPTER FOUR

THEORETICAL ANALYSIS AND SIMULATION RESULTS

4.1 Analysis of Theoretical Model of a Typical Power System

A. Rajapakse and Anawat Puangpairoj [6] presented an algorithm for computing firing angles and harmonics indices. In this chapter a similar algorithm with minor modifications is utilized in our work to evaluate the required VARs for a reactive compensator. SVC control algorithm takes phase wise active and reactive power demands of the load as inputs and determines the unsymmetrical firing angles of the TCR as outputs. A set of equations is derived to calculate the reactive power generated from the compensator to meet unbalanced load reactive power demand. Values of firing angles for thyristors are defined based on the Forward Backward Sweep Method (FBSM) to balance the load and minimize the harmonics generated by the reactive compensator.

4.1.1 Compensation Requirement for Load Balancing

The proposed Static VAR Compensator, FC-TCR type, with the typical power system is considered for the analysis in this work. The model used to represent the typical load requiring compensation appears in Figure 4.1. FC and TCR are connected in Y and Δ configurations, respectively.
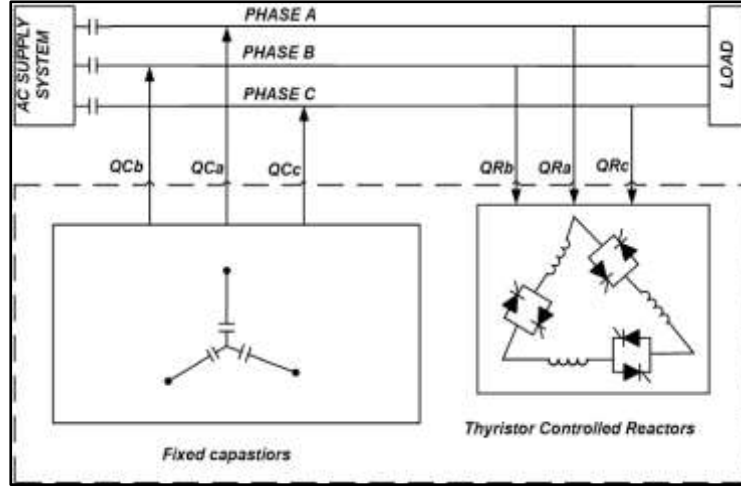
Figure 4.1: Load compensator model (FC-TCR) Type [5].

The FC-TCR compensator basically functions as a variable reactance by controlling the TCR firing angle. A series of such unbalanced steady state loads at different moments of time are utilized in order to establish the basic compensation requirements in load balancing. With this assumption that the compensator requirement is to generate or absorb the unbalanced reactive power between the supply system and load demand, and when it is associated with the load, it can represent balanced reactive power to the supply system.

If we consider a system (as shown in Figure 4.1), bus bar (1) represents the AC source system and bus bar (2) represents the load bus with SVC (FC-TCR) type connected at that bus. We let the phase-wise loads demand at a given instance of time be $P_{La} + jQ_{La}, P_{Lb} + jQ_{Lb}$, and $P_{Lc} + jQ_{Lc}$ .After compensation, we let the phase-wise loads seen by the source be $P_{La} + jQ_{Sa}, P_{Lb} + jQ_{Sb}$, and $P_{Lc} + jQ_{Sc}$, respectively. The phase-wise complex voltages at the load bus after the compensation are given by:

$$[V_L] = [V_S] - [Z][I] \tag{4.1}$$

Where,

$V_L = [V_{La}, V_{Lb}, V_{Lc}]^{\mathrm{T}}$: is the complex voltage vector at the load bus,

$V_S = [V_{Sa}, V_{Sb}, V_{Sc}]^{\mathrm{T}}$: is the complex voltage vector at the source bus,

$[Z] = \mathrm{diagonal}[Z_a, Z_b, Z_c]^{\mathrm{T}}$: is the line impedance matrix between the buses, and

46

$[I] = [I_a, I_b, I_c]^T$: is the line current between the source bus and the load bus after compensation which obtained from [17]:

$$I_a = (P_{La} - jQ_{Sa}) / V_{La}^* \tag{4.2a}$$

$$I_b = (P_{Lb} - jQ_{Sb}) / V_{Lb}^* \tag{4.2b}$$

$$I_c = (P_{Lc} - jQ_{Sc}) / V_{Lc}^* \tag{4.2c}$$

The set of non-linear complex Equations given by (4.1) and (4.2) can be solved for load bus voltages using the Forward Backward Sweep Method (FBSM) as evaluated in this chapter section (4.3)[40].

The Equation which is required for balanced system to meet unbalanced operation is:

$$[Q_S]^{abc} + [Q_C]^{abc} = [Q_R]^{abc} + [Q_L]^{abc} \tag{4.3}$$

Where,

$Q_S = [Q_{Sa}, Q_{Sb}, Q_{Sc}]^T$: is the phase –wise vector of reactive power supplied by the source bus,

$Q_C = [Q_{Ca}, Q_{Cb}, Q_{Cc}]^T$: is the phase –wise vector of reactive power supplied by fixed capacitance (FC),

$Q_R = [Q_{Ra}, Q_{Rb}, Q_{Rc}]^T$: is the phase –wise vector of reactive power absorbed by the TCR, and

$Q_L = [Q_{La}, Q_{Lb}, Q_{Lc}]^T$ is the phase –wise vector of load reactive power demand [17].

In the case of load balancing application ,we want to make the reactive power per phase supplied by the source balanced and equal, that is $Q_{Sa} = Q_{Sb} = Q_{Sc} = Q_S$ Further, we want to have the value of Q_S as close as possible to zero, we also have $Q_{Ca} = Q_{Cb} = Q_{Cc} = Q_C$ reactive power supplied by the fixed capacitor. After setting the values of Q_S and Q_C the unbalanced reactive power $[Q_R]^{abc}$, that absorbs by the TCR, can be obtained by solving Equation (4.3) [6].

The values of $X_{ab}, X_{bc}, and \ X_{ca}$ (Δ-connected TCR compensator reactance) required to absorb the unbalanced reactive power $[Q_R]^{abc}$ computed from Equation (4.3) can be obtained from the below equations, these equations are evaluated from Figure (4.2) in Appendix D [1].

$$Q_{Ra} = [\, V_{\text{La}}^2 - V_{\text{La}}\, V_{\text{Lb}} \cos(\delta_a - \delta_b)\,]\ \text{B}_{\text{ab}}$$

$$+ [V_{\text{La}}^2 - V_{\text{La}}\, V_{\text{Lc}} \cos(\delta_a - \delta_c)]\text{B}_{\text{ca}} \tag{4.4a}$$

$$Q_{Rb} = [\, V_{\text{Lb}}^2 - V_{\text{La}}\, V_{\text{Lb}} \cos(\delta_b - \delta_a)\,]\ \text{B}_{\text{ab}}$$

$$+ [V_{\text{Lb}}^2 - V_{\text{Lb}}\, V_{\text{Lc}} \cos(\delta_b - \delta_c)]\text{B}_{\text{bc}} \tag{4.4b}$$

$$Q_{Rc} = [\, V_{\text{Lc}}^2 - V_{\text{Lc}}\, V_{\text{Lb}} \cos(\delta_c - \delta_b)\,]\ \text{B}_{\text{bc}}$$

$$+ [V_{\text{Lc}}^2 - V_{\text{Lc}}\, V_{\text{La}} \cos(\delta_c - \delta_a)]\text{B}_{\text{ca}} \tag{4.4c}$$

Where,

$B_{ab}, B_{bc}, and\ B_{ca}$: are TCR unsymmetrical admittances.

$$\text{B}_{\text{ab}} = \frac{1}{X_{ab}} \tag{4.5a}$$

$$\text{B}_{\text{bc}} = \frac{1}{X_{bc}} \tag{4.5b}$$

$$\text{B}_{\text{ca}} = \frac{1}{X_{ca}} \tag{4.5c}$$

Where,

$X_{ab}, X_{bc}, and\ X_{ca}$: are TCR unsymmetrical reactances.
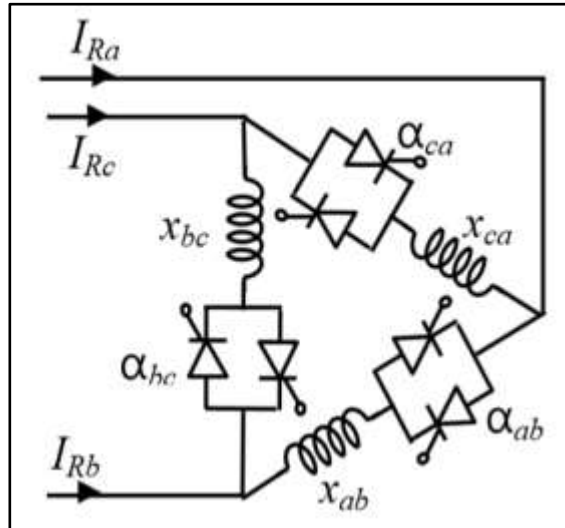
Figure 4.2: Delta connected thyristor controlled reactor [6].

48

4.1.2 Variable Reactances Formulation

The variable reactances $X_{ab}, X_{bc},$ and X_{ca} of the TCR compensator seen by the fundamental component of the current are achieved by delaying the closure of anti-parallel thyristors by an angle α from $(0 \text{ to } \pi/2)$ measured from the zero crossing current. The unsymmetrical firing angles $\alpha_1, \alpha_2, and \alpha_3$ of the anti-parallel thyristors required to obtain the unsymmetrical $\Delta -$ connected TCR reactances (for the fundamental components only) can be acquired by solving the following equations:

$$X_{ab} = X_{ab}^{\circ}/\left[1 - \frac{2\alpha_1}{\pi} - \frac{\sin(2\alpha_1)}{\pi}\right] \tag{4.6a}$$

$$X_{bc} = X_{bc}^{\circ}/\left[1 - \frac{2\alpha_2}{\pi} - \frac{\sin(2\alpha_2)}{\pi}\right] \tag{4.6b}$$

$$X_{ca} = X_{ca}^{\circ}/\left[1 - \frac{2\alpha_3}{\pi} - \frac{\sin(2\alpha_3)}{\pi}\right] \tag{4.6c}$$

Where,

$\alpha_1, \alpha_2, and \alpha_3$: are the TCR unsymmetrical firing angles.

$X_{ab}^{\circ}, X_{bc}^{\circ}$ and X_{ca}°: are the TCR reactances for full conduction of anti-parallel thyristors (corresponding to zero firing angles, when $\alpha_1 = \alpha_2 = \alpha_3 = 0^{\circ}$) [6].

4.1.3 Calculation of the Effects of Harmonics

Because of the unsymmetrical firing delay angles of TCR, the harmonics that injected into the power system are increased. Therefore the firing delay angles for balanced operation must be obtained with minimum harmonic injection. All harmonic indices are defined for single-phase systems (or balanced three-phase systems). In case of three-phase unbalanced systems, individual phases may carry different harmonic currents and there is no single index that can be used to evaluate the overall harmonic distortion situation. The effect of harmonics in the power system at the Point of Common Coupling (PCC) usually measured by the calculation of the Total Harmonic Distortion (THD) factor, which is a measure of the AC sinusoidal current distortion. The performance index (THD) is given by:

$$THD_a = \frac{1}{I_{fa}} \sqrt{\sum_{h=2}^{m} I_{ha}^2} \qquad (4.7a)$$

$$THD_b = \frac{1}{I_{fb}} \sqrt{\sum_{h=2}^{m} I_{hb}^2} \qquad (4.7b)$$

$$THD_c = \frac{1}{I_{fc}} \sqrt{\sum_{h=2}^{m} I_{hc}^2} \qquad (4.7c)$$

Where,

$I_{fa}, I_{fb}, and\ I_{fc}$: are the root mean square (R.M.S) values of the fundamental component of the line current,

$I_{ha}, I_{hb}, and\ I_{hc}$: are the root mean square (R.M.S) values of the $h^{th} - order$ harmonic component of the line current, and

h : is the harmonic order.

The fundamental and harmonic components of the line currents can be obtained as a difference of the corresponding branch currents. The harmonics can be deduced from the Fourier expansion of 2nd and higher frequency components in the Fourier expansion.

The fundamental component of the line current is given by:

$$I_{fa} = \frac{V_{am}}{2\pi\omega L_a} \sqrt{G_{af}^2 + H_{af}^2} \sin(\omega t - \varphi_a - \theta_{fa}) \qquad (4.8a)$$

$$I_{fb} = \frac{V_{bm}}{2\pi\omega L_b} \sqrt{G_{bf}^2 + H_{bf}^2} \sin(\omega t - \varphi_b - \theta_{fb}) \qquad (4.8b)$$

$$I_{fc} = \frac{V_{cm}}{2\pi\omega L_c} \sqrt{G_{cf}^2 + H_{cf}^2} \sin(\omega t - \varphi_c - \theta_{fc}) \qquad (4.8c)$$

Where,

$V_{am}, V_{bm}, and\ V_{cm}$: are the peak values of line voltage,

ω : is the fundamental frequency in radians /second,

$L_a, L_b, and\ L_c$: are the inductances of delta connected reactances (henries),

$\varphi_a, \varphi_b, \varphi_c$: are the phase difference between line voltages, and

$\theta_{fa}, \theta_{fb}, \theta_{fc}$: are the phase difference between fundamental voltage and current.

$$\theta_f = \tan^{-1}(H_f / G_f) \qquad (4.9)$$

$$G_{af} = 3\pi - 4\alpha_1 - 2\sin(2\alpha_1) - 2\alpha_3 - \sin(2\alpha_3) \tag{4.10a}$$

$$G_{bf} = 3\pi - 4\alpha_2 - 2\sin(2\alpha_2) - 2\alpha_1 - \sin(2\alpha_1) \tag{4.10b}$$

$$G_{cf} = 3\pi - 4\alpha_3 - 2\sin(2\alpha_3) - 2\alpha_2 - \sin(2\alpha_2) \tag{4.10c}$$

$$H_{af} = \sqrt{3}[\pi - 2\alpha_3 - \sin(2\alpha_3)] \tag{4.11a}$$

$$H_{bf} = \sqrt{3}[\pi - 2\alpha_1 - \sin(2\alpha_1)] \tag{4.11b}$$

$$H_{cf} = \sqrt{3}[\pi - 2\alpha_2 - \sin(2\alpha_2)] \tag{4.11c}$$

The harmonic components of the line current for h^{th} order harmonic is given by:

$$I_{ha} = \frac{2V_{am}}{\pi\omega L_a}\sqrt{G_{ah}^2 + H_{ah}^2}\ \sin[h(\omega t - \varphi_a) - \theta_{ha}] \tag{4.12a}$$

$$I_{hb} = \frac{2V_{bm}}{\pi\omega L_b}\sqrt{G_{bh}^2 + H_{bh}^2}\ \sin[h(\omega t - \varphi_b) - \theta_{hb}] \tag{4.12b}$$

$$I_{hc} = \frac{2V_{cm}}{\pi\omega L_c}\sqrt{G_{ch}^2 + H_{ch}^2}\ \sin[h(\omega t - \varphi_c) - \theta_{hc}] \tag{4.12c}$$

Where,

$\theta_{ha}, \theta_{hb}, \theta_{hc}$: are the phase difference between harmonic voltage and current,

$$\theta_h = \tan^{-1}(H_h/G_h) \tag{4.13}$$

$$G_{ah} = \frac{\sin[(h+1)\alpha_1]}{h+1} - \frac{\sin[(h-1)\alpha_1]}{h-1} - \frac{2\sin(\alpha_1)\cos(h\alpha_1)}{h} + \frac{1}{2}\left\{\frac{\sin[(h+1)\alpha_3]}{h+1} - \right.$$
$$\left. \frac{\sin[(h-1)\alpha_3]}{h-1} - \frac{2\sin(\alpha_3)\cos(h\alpha_3)}{h}\right\} \tag{4.14a}$$

$$G_{bh} = \frac{\sin[(h+1)\alpha_2]}{h+1} - \frac{\sin[(h-1)\alpha_2]}{h-1} - \frac{2\sin(\alpha_2)\cos(h\alpha_2)}{h} + \frac{1}{2}\left\{\frac{\sin[(h+1)\alpha_1]}{h+1} - \frac{\sin[(h-1)\alpha_1]}{h-1} - \right.$$
$$\left. \frac{2\sin(\alpha_1)\cos(h\alpha_1)}{h}\right\} \tag{4.14b}$$

$$G_{ch} = \frac{\sin[(h+1)\alpha_3]}{h+1} - \frac{\sin[(h-1)\alpha_3]}{h-1} - \frac{2\sin(\alpha_3)\cos(h\alpha_3)}{h} + \frac{1}{2}\left\{\frac{\sin[(h+1)\alpha_2]}{h+1} - \frac{\sin[(h-1)\alpha_2]}{h-1} - \right.$$
$$\left. \frac{2\sin(\alpha_2)\cos(h\alpha_2)}{h}\right\} \tag{4.14c}$$

$$H_{ah} = \pm\sqrt{\frac{3}{2}}\left\{\frac{\sin[(h-1)\alpha_3]}{h-1} - \frac{\sin[(h-1)\alpha_3]}{h+1} - \frac{2\sin(\alpha_3)\cos(h\alpha_3)}{h}\right\} \quad (4.15a)$$

$$H_{bh} = \pm\sqrt{\frac{3}{2}}\left\{\frac{\sin[(h-1)\alpha_1]}{h-1} - \frac{\sin[(h-1)\alpha_1]}{h+1} - \frac{2\sin(\alpha_1)\cos(h\alpha_1)}{h}\right\} \quad (4.15b)$$

$$H_{ch} = \pm\sqrt{\frac{3}{2}}\left\{\frac{\sin[(h-1)\alpha_2]}{h-1} - \frac{\sin[(h-1)\alpha_2]}{h+1} - \frac{2\sin(\alpha_2)\cos(h\alpha_2)}{h}\right\} \quad (4.15c)$$

Where,

h = harmonic order, $(6K \pm 1), K = 1,2,3 \dots$,

$(+Ve)$ sign is for harmonic of order $(6K + 1)$.

$(-Ve)$ sign is for harmonic of order $(6K - 1)$.

For three phase systems, the prefer arrangements of TCR is in Δ-connection, because when the system is balanced, all the triplen harmonics (multiples of third) circulate in the closed Δ − connection path are absent from the line currents as follows:

For triple harmonics (3rd, 9th, ……)[17]:

$$G_{ah} = \frac{\sin[(h+1)\alpha_1]}{h+1} - \frac{\sin[(h-1)\alpha_1]}{h-1} - \frac{2\sin(\alpha_1)\cos(h\alpha_1)}{h} + \frac{\sin[(h+1)\alpha_3]}{h+1} - \frac{\sin[(h-1)\alpha_3]}{h-1} - $$
$$\frac{2\sin(\alpha_3)\cos(h\alpha_3)}{h} \quad (4.16a)$$

$$G_{bh} = \frac{\sin[(h+1)\alpha_2]}{h+1} - \frac{\sin[(h-1)\alpha_2]}{h-1} - \frac{2\sin(\alpha_2)\cos(h\alpha_2)}{h} + \frac{\sin[(h+1)\alpha_1]}{h+1} - \frac{\sin[(h-1)\alpha_1]}{h-1} - $$
$$\frac{2\sin(\alpha_1)\cos(h\alpha_1)}{h} \quad (4.16b)$$

$$G_{ch} = \frac{\sin[(h+1)\alpha_3]}{h+1} - \frac{\sin[(h-1)\alpha_3]}{h-1} - \frac{2\sin(\alpha_3)\cos(h\alpha_3)}{h} + \frac{\sin[(h+1)\alpha_2]}{h+1} - \frac{\sin[(h-1)\alpha_2]}{h-1} - $$
$$\frac{2\sin(\alpha_2)\cos(h\alpha_2)}{h} \quad (4.16c)$$

$$H_{ah} = H_{ah} = H_{ah} = 0$$

4.2 Unbalanced Load Compensation Procedure

For a given set of unbalanced reactive power load demands $[Q_L]^{abc}$, and depending on the Equations from (4.1) to (4.15) in MATLAB , a simulation is built in order to compute the combination of firing angles of the $\Delta-$ connected reactors with the corresponding phase-wise THD values for unity source power factor condition ($Q_S = 0$) in order to achieve a balanced operation.

The summery of the approach included in the program is as the followings:

Step (1): Read the data of the system related to:

(a) The line impedance between load and source buses;

(b) The source bus voltage (bus bar 1);

(c) Unbalanced load demand$[P_L]^{abc}$, $[Q_L]^{abc}$;

(d) The SVC rated capacity, that is,

  o Capacitive range for FC.

  o Inductive range for TCR.

Step (2): At first, we suppose the reactive power load demand is met totally by the SVC only, that is, the unity power factor load is seen by the source (bus 1). Set $Q_{Sa} = Q_{Sb} = Q_{Sc} = $ zero .

Step (3): We compute load bus voltages (bus 2) after compensation by using the Forward Backward Sweep Method (FBSM) which is explained in Section (4.3). We assume the phase-wise load seen by the source (bus1) as $P_{La} + jQ_{Sa}$, $P_{Lb} + jQ_{Sb}$, and $P_{Lc} + jQ_{Sc}$ respectively.

Step (4): Calculate the phase–wise reactive power that absorbed by the TCR ($Q_{Ra}, Q_{Rb},$ and Q_{Rc}) .After setting the values of the reactive power supplied from the source bus (Q_S) and the reactive power supplied by the fixed capacitor (Q_C) , the unbalanced reactive power $[Q_R]^{abc}$ that is absorbed by the TCR can be obtained by solving Equation (4.3).

Step (5): We compute the corresponding values of $X_{ab}, X_{bc},$ and X_{ca} ($\Delta-$ connected TCR compensator reactance) required to absorb the unbalanced reactive power and meet voltage condition at the TCR.

The values of $X_{ab}, X_{bc},$ and X_{ca} can be obtained by solving Equations (4.4) and (4.5).

Step (6): We check Δ – connected reactances design limitation of the TCR $(X^\circ_{ab}, X^\circ_{bc}$ and $X^\circ_{ca})$ .If unsatisfactory, go to step 9.

Step (7): Corresponding to the reactances from steps 5 and 6, the unsymmetrical gating angle of the TCR $(\alpha_1, \alpha_2, $ and $\alpha_3)$ can be computed by solving Equation (4.6).

Step (8): We compute the THD by performing the harmonics analysis of the 3-phase line current.

THD can be obtained by solving Equations (4.7) to (4.15).

Step (9): We assume a balanced increased of source reactive power in small value above the zero $Q_{Sa} = Q_{Sb} = Q_{Sc}$; go to step 3.

Step (10): We print the result to file and stop the program [5, 17].

Figure 4.3 shows a flowchart of the written program [6].
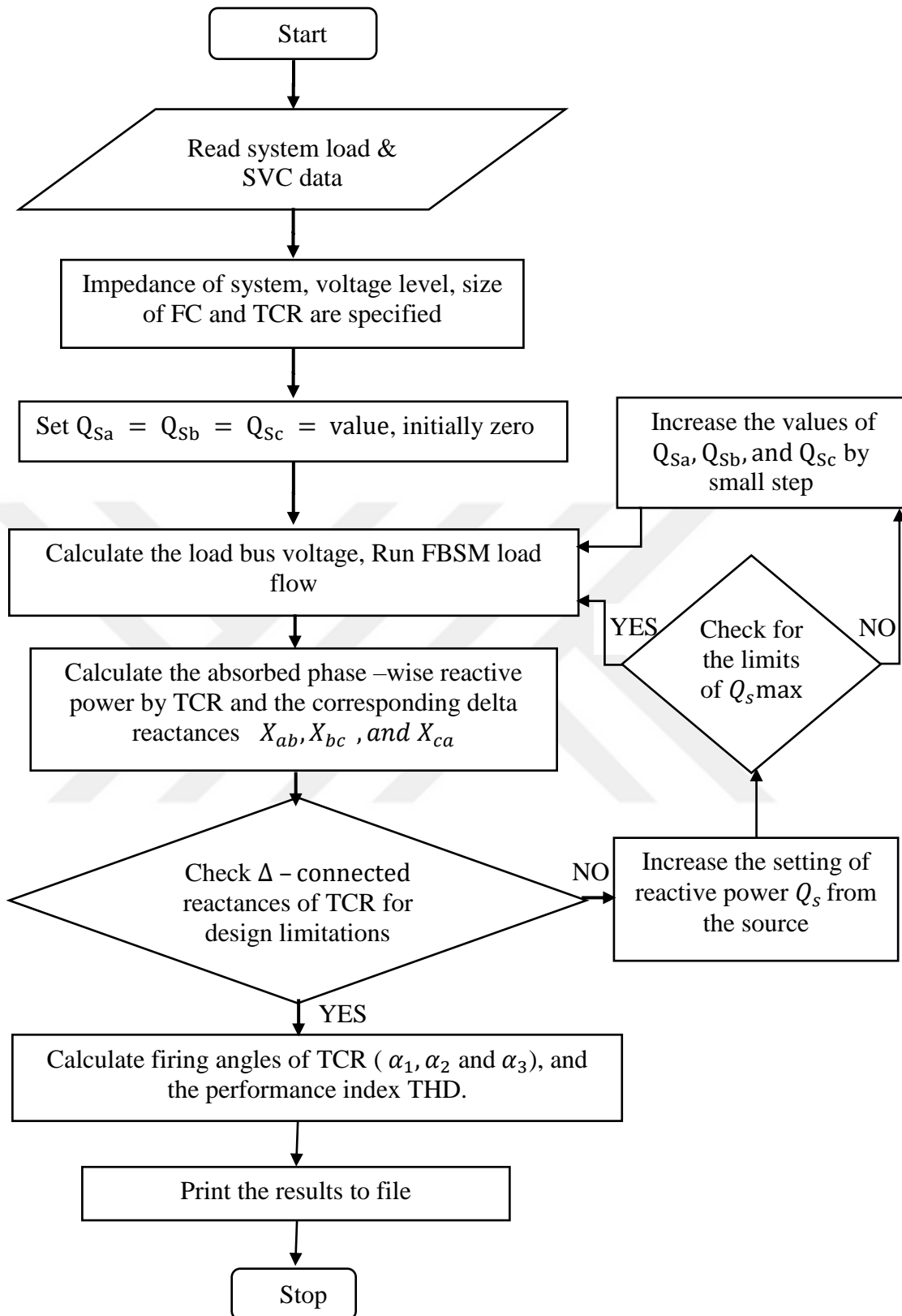
Figure 4.3: Conventional algorithm flowchart of the written program [6].

4.3 Forward- Backward Sweep Method (FBSM)

It is a simple and efficient method for solving power flow issues for radial distribution system. It involves the evaluation of a very simple algebraic expression of all the receiving – end voltages of the network. This method which depends on Backward-Forward Sweep procedure using Kirchhoff's current and voltage laws is distinguished by fast and good convergence characteristics. Diagram of one line of a test system with single feeder (2 buses) is shown in Figure 4.4.
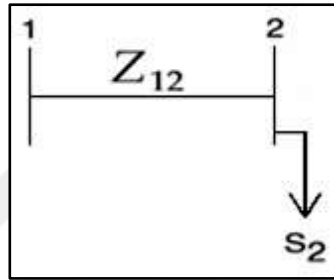
Figure 4.4: Diagram of one line, 2- Bus distribution system [39].

Let consider bus1 of Figure (4.4) is the source bus with specified voltage equal to V_S. Now the forward sweep method begins by assuming the voltage on bus 2 V_2 is equal to V_s, the load current at bus 2 computed by:

$$I_2 = \left(\frac{S_2}{V_2}\right)^*$$ (4.17)

The current flowing in the line section 1-2 is:

$$I_{12} = I_2$$ (4.18)

The computed voltage at source bus 1 given by:

$$V_1 = V_2 + Z_{12} . I_{12}$$ (4.19)

Now, at this point the magnitude of the computed voltage V_1 at source bus Eq. (4.19) is compared with the specified source voltage V_s;

$$Error = \left||V_S| - |V_1|\right|$$ (4.20)

If the error Equation (4.20) is less than a specified tolerance rate, the solution is achieved. But if the error is more than the specified tolerance rate then the backward sweep method begins. A typical tolerance usually used is 0.001 per unit.

The backward sweep method begins by set the voltage at source bus 1 equal to specified source voltage V_s.

$$V_1 = V_S \qquad (4.21)$$

Now the voltage at bus 2 can be computed by using this value of bus 1 Eq. (4.21) and the computed line current from the forward sweep method as follow:

$$V_2 = V_1 - Z_{12} \cdot I_{12} \qquad (4.22)$$

After finding the voltage at bus 2 the first iteration is completed. At this point the forward sweep method is repeated again but only this time starting with the new voltage at bus 2 Eq. (4.22) rather than the initially assumed voltage.

The forward-backward sweep method is repeated until the tolerance error rate is achieved.

The source power factor of the feeder during this work can be calculated from the following:

$$PF_n = \cos\left(tan^{-1}\frac{Q_{Sn}}{P_{Sn}}\right) \qquad (4.23)$$

Where,

Q_{Sn} : represents the reactive power drawn from the source for each phase respectively,

P_{Sn} : is the source active power for each phase respectively.

This method can be work efficiently on different number of buses as improved in [40].

The flow chart of the written program in MATLAB to solve the load flow issue of New Jadrea-Arkheta substations is presented in Figure 4.5. This method was repeated for every single phase of the proposed network because of the unbalance situation.

```
                        ┌─────────────┐
                        │    Start    │
                        └─────────────┘
                               │
                               ▼
                      ╱─────────────────╲
                     ╱     Read the       ╲
                     ╲   system data      ╱
                      ╲─────────────────╱
                               │
                               ▼
        ┌──────────────────────────────────────────────┐
        │  Set S_n = complex (P_n, Q_s) refers to adding│
        │           the SVC to the proposed line        │
        └──────────────────────────────────────────────┘
                               │
                               ▼
        ┌──────────────────────────────────────────────┐
        │   Assume load voltage = specified source      │
        │                    voltage                    │
        └──────────────────────────────────────────────┘
                               │
                               ▼
              ┌──────────────────────────────┐
              │      Set iteration count      │
              └──────────────────────────────┘
                               │                          ┌────────────────────────┐
                               │                          │   Update load voltage   │
                               │              ◄───────────└────────────────────────┘
                               ▼                                       ▲
        ┌──────────────────────────────────┐                          │
        │  Calculate the line current Eq.   │          ┌────────────────────────────┐
        │  (4.18) and source voltage Eq.    │          │  Calculate the new load     │
        │              (4.19)               │          │   voltage Eq. (4.22)        │
        └──────────────────────────────────┘          └────────────────────────────┘
                               │                                       ▲
                               ▼                                       │
                     ╱─────────────────╲          NO      ┌────────────────────────────┐
                    ╱   Is error Eq.     ╲                 │  Set source voltage equals  │
                   ╱   (4.20) less than   ╲───────────────►│  specified source voltage   │
                   ╲   the tolerance rate? ╱                │         Eq. (4.21)          │
                    ╲─────────────────────╱                └────────────────────────────┘
                               │ YES
                               ▼
        ┌──────────────────────────────────────────────┐
        │  Calculate the line losses, MW, MVar, and     │
        │  MVA. Calculate the load on each bus          │
        └──────────────────────────────────────────────┘
                               │
                               ▼
              ┌──────────────────────────────┐
              │       Print the result        │
              └──────────────────────────────┘
                               │
                               ▼
                        ┌─────────────┐
                        │     End     │
                        └─────────────┘
```

Figure 4.5: Flowchart of FBSM method with SVC device.

4.4 Case Study and Results

This work takes into account the spring and summer seasons of 2016 in Iraq. Appendix B shows the load profile of the collected data.

This section presents the results obtained from the analysis of the proposed system with the SVC device described in Chapter 4 Section (4.1) in order to obtain the firing angles (α_1, α_2 and α_3) of the TCR and to achieve balanced system operation .The next step in the calculation part is to calculate the compensator reactive power. Finally, the total harmonic distortion (THD) factor should be obtained.

The following unbalanced power load demand was selected randomly from Appendix B:

$$S_a = 4.637 + j3.478 \text{ MVA}$$
$$S_b = 4.523 + j3.393 \text{ MVA}$$
$$S_c = 4.382 + j3.286 \text{ MVA}$$

By applying the procedure of the flow chart in Figure 4.3, the calculated values of the firing angles of the thyristors at $Q_S = 0.4$ MVAR satisfies the balance condition in Equation (4.3) with SVC rating of 5MVAR for FC and 5MVAR for TCR because the SVC should be rated at a value greater than the load demand at an acceptable level:

$$\alpha_1 = 14.69^\circ.$$
$$\alpha_2 = 12.60^\circ.$$
$$\alpha_3 = 13.53^\circ.$$

The reactive powers of TCR compensator are:

$$Q_{Ra} = 1922 \text{ KVAR}.$$
$$Q_{Rb} = 2007 \text{ KVAR}.$$
$$Q_{Rc} = 2114 \text{ KVAR}.$$

Now checking for the balance condition:

$$Q_{Ra} + Q_{La} - Q_{Sa} = Q_{Ca} = 5 \text{ MVAR}.$$
$$Q_{Rb} + Q_{Lb} - Q_{Sb} = Q_{Cb} = 5 \text{ MVAR}.$$
$$Q_{Rc} + Q_{Lc} - Q_{Sc} = Q_{Cc} = 5 \text{ MVAR}.$$

$THD_{avg.} = 13\%$, which is acceptable value. In case of three-phase unbalanced systems, individual phases may carry different harmonic currents and

there is no single index that can be used to evaluate the overall harmonic distortion situation [6]. According to IEEE Std 519™-2014 harmonic limits are recommended for both voltages and currents. The recommended limits apply only at the point of common coupling and should not be applied to either individual piece of equipment or at locations within a user's facility. In most cases, harmonic voltages and currents at these locations could be found to be significantly greater than the limits recommended at the PCC due to the lack of diversity, cancellation, and other phenomena that tend to reduce the combined effects of multiple harmonic sources to levels below their algebraic summation.

Therefore, by repeating the same procedure for all values of the data in Appendix B, we can obtain different values of firing angles (α_1, α_2, and α_3), by substituting the values of firing angles in Equations (4.14), (4.15) and (4.13) we can obtain different values of harmonic components of current based on Equation (4.12), also by substituting the values of firing angles in Equations (4.10), (4.11) and (4.9) we can obtain different values of fundamental components of current based on Equation (4.8). We can obtain the values of THD by substituting the values of the current harmonic components and the current fundamental components in Equation (4.7). Firing angles of the TCR compensator and the average total harmonic distortion $(\text{THD}_{\text{avg.}})$ factor which satisfies the balance conditions as illustrated in Table (4.1).

Table 4.1: TCR firing angles and total harmonic distortion with $\text{THD}_{\text{avg.}}$

Sample No.	α_1 (deg.)	α_2 (deg.)	α_3 (deg.)	THD1%	THD2%	THD3%	THD(avg.)%
1	5.95	3.86	5.46	13%	3%	3%	6%
2	6.51	3.94	5.44	13%	3%	3%	7%
3	6.35	4.67	5.82	14%	3%	3%	7%
4	5.89	5.59	5.65	13%	3%	4%	7%
5	7.04	6.01	7.12	16%	3%	4%	8%
6	10.45	9.43	7.92	21%	4%	5%	10%
7	9.54	7.63	8.85	20%	4%	5%	10%
8	8.48	7.42	9.08	19%	4%	5%	9%
9	7.94	7.86	8.24	18%	4%	5%	9%
10	6.83	6.34	7.14	16%	3%	4%	8%
11	8.18	5.86	7.67	18%	4%	4%	9%
12	7.51	6.15	7.34	17%	3%	4%	8%
13	8.82	5.93	7.01	18%	4%	4%	9%
14	9.64	8.26	9.46	21%	4%	5%	10%
15	9.64	7.96	10.08	21%	4%	5%	10%
16	11.51	9.59	10.73	23%	5%	6%	11%

17	8.71	9.79	11.28	19%	4%	6%	10%
18	7.83	5.96	6.89	17%	4%	4%	8%
19	8.42	5.75	7.27	18%	4%	4%	9%
20	4.32	2.75	4.11	10%	2%	2%	5%
21	5.49	1.83	3.50	10%	3%	2%	5%
22	5.27	2.88	4.01	10%	3%	2%	5%
23	5.85	3.01	3.78	11%	3%	2%	5%
24	5.97	3.58	4.54	12%	3%	3%	6%
25	8.74	7.46	7.94	19%	4%	5%	9%
26	9.01	7.49	8.60	19%	4%	5%	9%
27	9.27	7.57	8.53	20%	4%	5%	9%
28	10.08	7.83	9.05	21%	4%	5%	10%

Table 4.1 (Continuation): TCR firing angles and reactive power with THD$_{avg}$.

Sample No.	α_1 (deg.)	α_2 (deg.)	α_3 (deg.)	THD1%	THD2%	THD3%	THD(avg.)%
29	10.68	7.63	8.60	22%	4%	5%	10%
30	14.84	12.11	13.63	28%	5%	7%	13%
31	14.26	12.24	13.12	27%	5%	7%	13%
32	14.01	11.88	12.96	27%	5%	7%	13%
33	13.75	10.96	13.69	26%	5%	6%	12%
34	13.81	12.19	13.42	26%	5%	7%	13%
35	14.18	12.49	13.43	27%	5%	7%	13%
36	17.90	17.46	17.68	30%	5%	9%	14%
37	15.80	13.93	15.32	28%	5%	7%	14%
38	14.69	12.60	13.53	28%	5%	7%	13%
39	13.64	12.21	13.17	26%	5%	7%	13%
40	13.25	11.68	13.05	26%	5%	6%	12%
41	13.32	11.66	12.56	26%	5%	6%	12%
42	13.22	11.43	12.53	26%	5%	6%	12%
43	7.79	6.88	5.77	15%	4%	4%	8%
44	8.40	6.47	6.50	17%	4%	4%	8%
45	8.36	6.37	6.29	16%	4%	4%	8%
46	7.47	5.23	5.62	15%	3%	4%	7%
47	18.32	16.58	18.32	30%	5%	8%	14%
48	18.41	17.34	18.09	30%	5%	9%	15%
49	18.49	17.10	18.24	30%	5%	9%	15%
50	18.31	18.14	17.88	30%	5%	9%	15%
51	17.76	18.53	17.99	29%	5%	10%	15%
52	18.75	19.59	17.91	31%	5%	10%	15%
53	17.89	17.13	19.06	28%	5%	8%	14%
54	17.38	21.78	19.13	27%	5%	11%	15%
55	18.89	19.42	17.32	32%	5%	10%	16%
56	18.02	17.70	18.65	29%	5%	9%	14%
57	18.45	18.33	18.02	30%	5%	9%	15%
58	17.05	17.03	18.66	28%	5%	9%	14%
59	20.23	17.72	17.82	33%	5%	9%	16%
60	20.59	19.39	19.92	30%	5%	10%	15%

Figures 4.6 to 4.8 show the effect of adding the SVC device to the proposed case study on the operation efficiency, namely line currents, voltage profiles and KVA losses. The following conclusion can be made:

1. Figures 4.6a, 4.6b and 4.6c show the line current before and after adding the SVC device for phases a, b, and c, respectively. It can be observed that the current flowing through the line is far lower than before the load compensation, as shown in Figure 4.6.

2. Figures 4.7a, 4.7b and 4.7c show the load voltage before and after adding the SVC device for phases a, b, and c, respectively. An improvement in voltage is achieved after adding the SVC device, as shown in Figure 4.7.

3. Figures 4.8a, 4.8b and 4.8c show the losses before and after adding the SVC device for phases a, b, and c, respectively. It can be observed that the KVA losses after adding the SVC device are lower than without the SVC.

Results are presented in per unit (p.u) system so as constants lie in a reasonably narrow numerical range.

$$\text{Quantity}_{\text{in p.u}} = \frac{\text{Actual value of quantity}}{\text{base value of quantity}} \tag{4.24}$$

Hence, per unit system is dimensionless. For each phase we have four parameters (S, V, I, Z) we choose base values for any two (arbitrary) then we find the other base values.

In a power system, usually power and voltage bases are chosen first, so we choose base value of power =6MVA and base value of voltage =18KV.

We get the results of power in per unit by applying the following equation:

$$\text{power}_{\text{in p.u}} = \frac{\text{Actual value of power}}{\text{base value of power}} \tag{4.25}$$

We get the results of voltage in per unit by applying the following equation:

$$\text{voltage}_{\text{in p.u}} = \frac{\text{Actual value of voltage}}{\text{base value of voltage}} \tag{4.26}$$

After choose the base value of power and base value of voltage we can find the base current value by:

$$\text{base current} = \frac{\text{base value of power}}{\text{base value of voltage}} \tag{4.27}$$

We get the results of current in per unit by:

$$\text{current}_{\text{in p.u}} = \frac{\text{Actual value of current}}{\text{base value of current}} \tag{4.28}$$
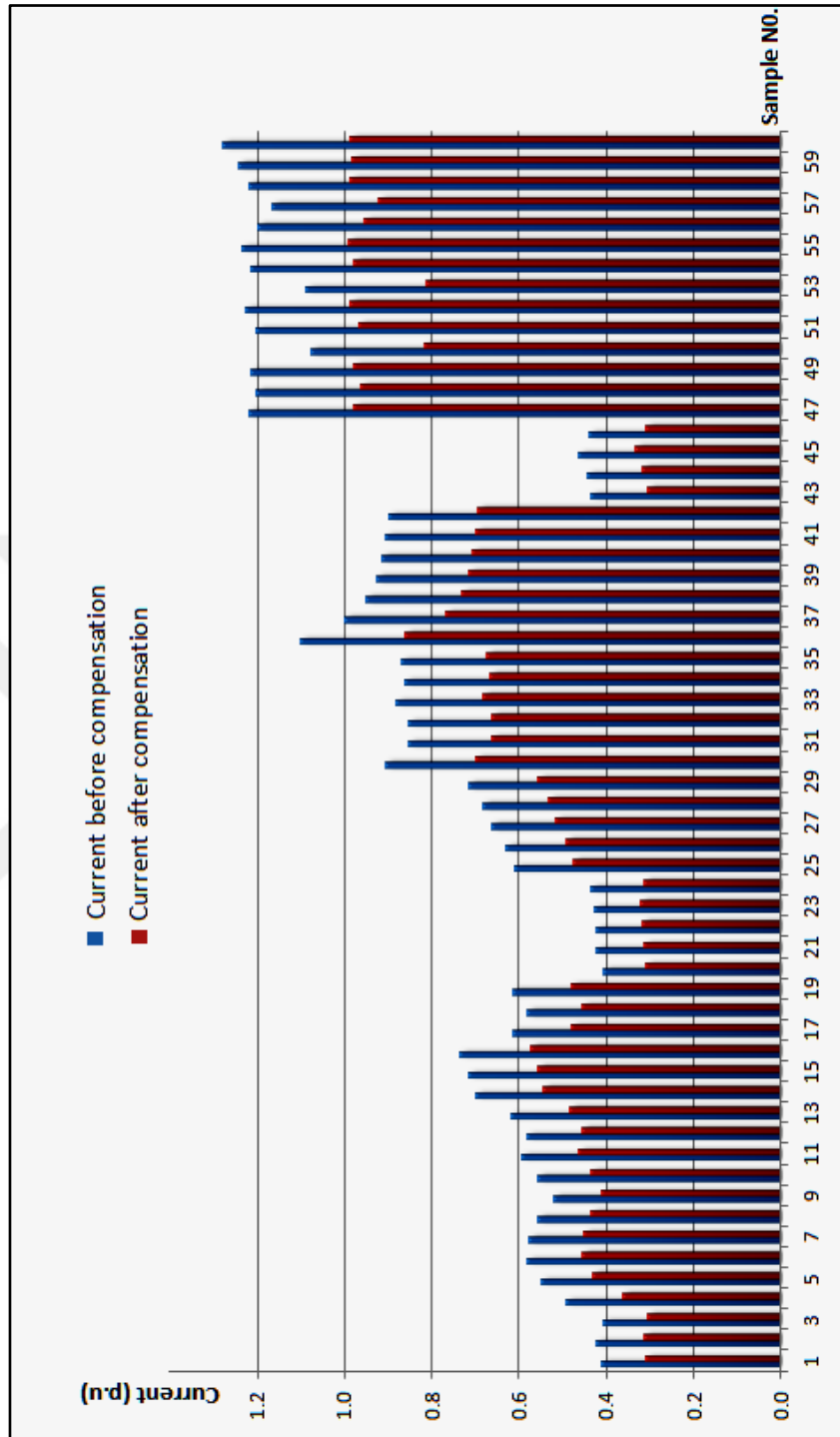
Figure 4.6.a: Line current for phase A before and after compensation.
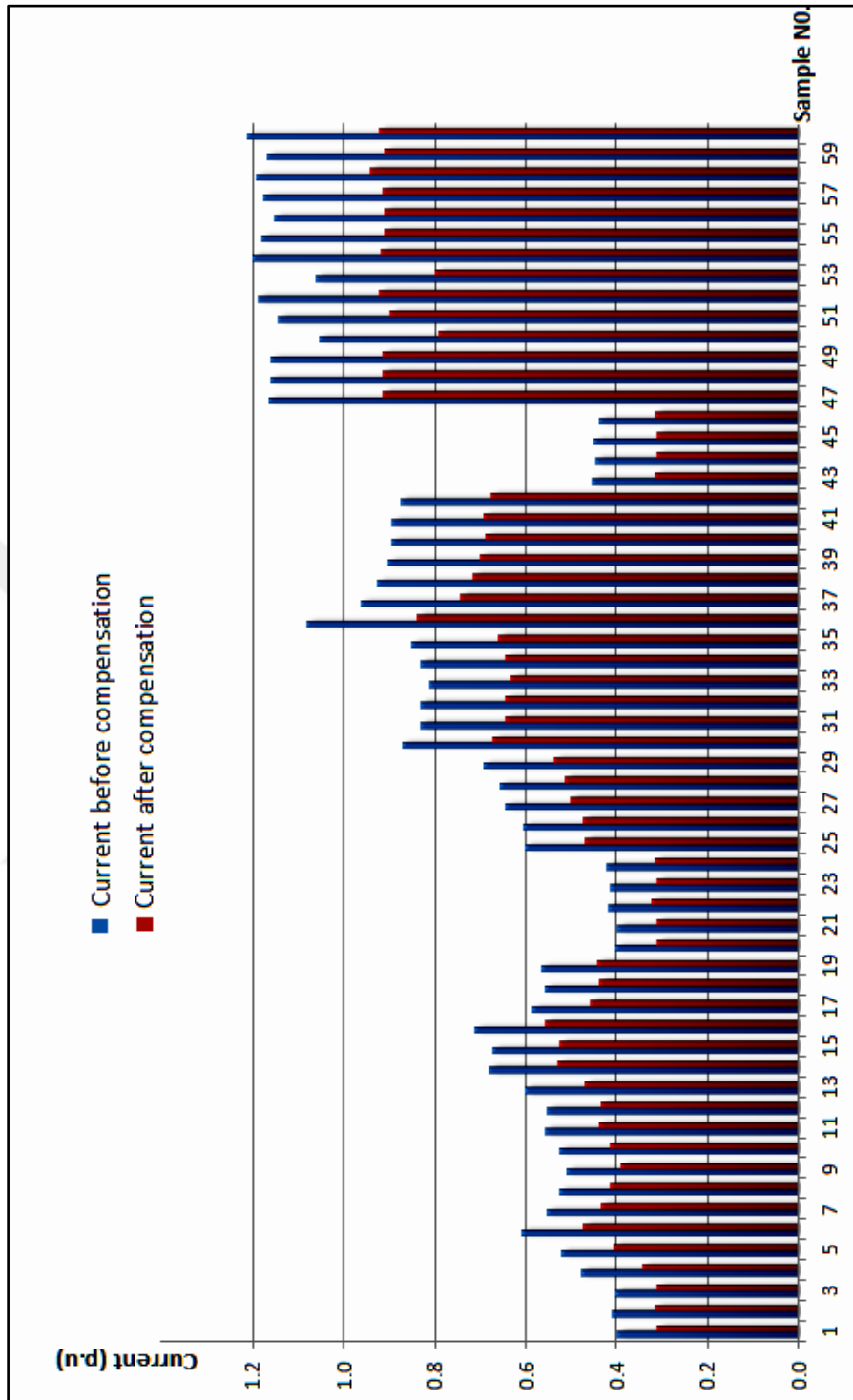
Figure 4.6.b: Line current for phase B before and after compensation.
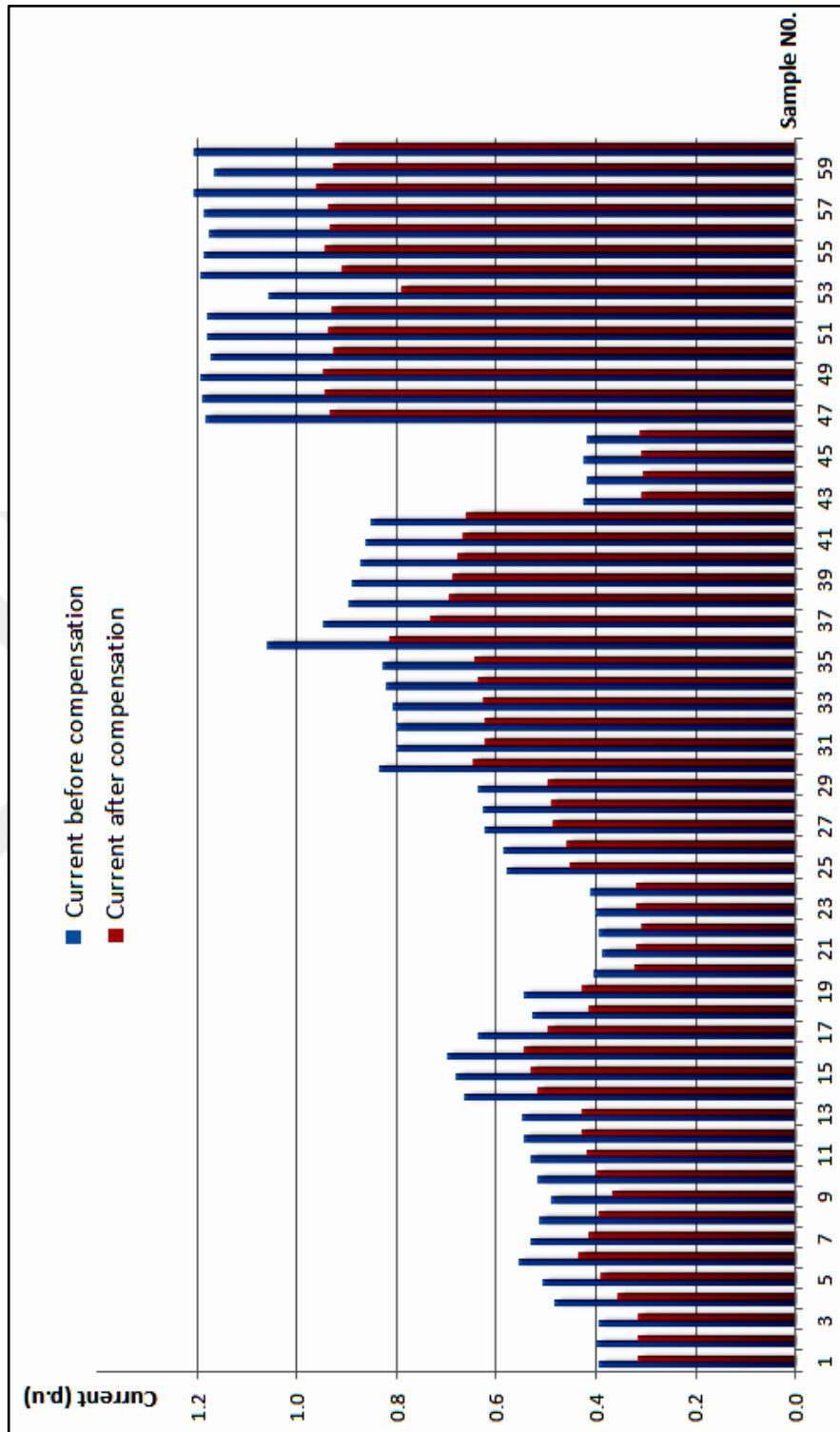
Figure 4.6.c: Line current for phase C before and after compensation.
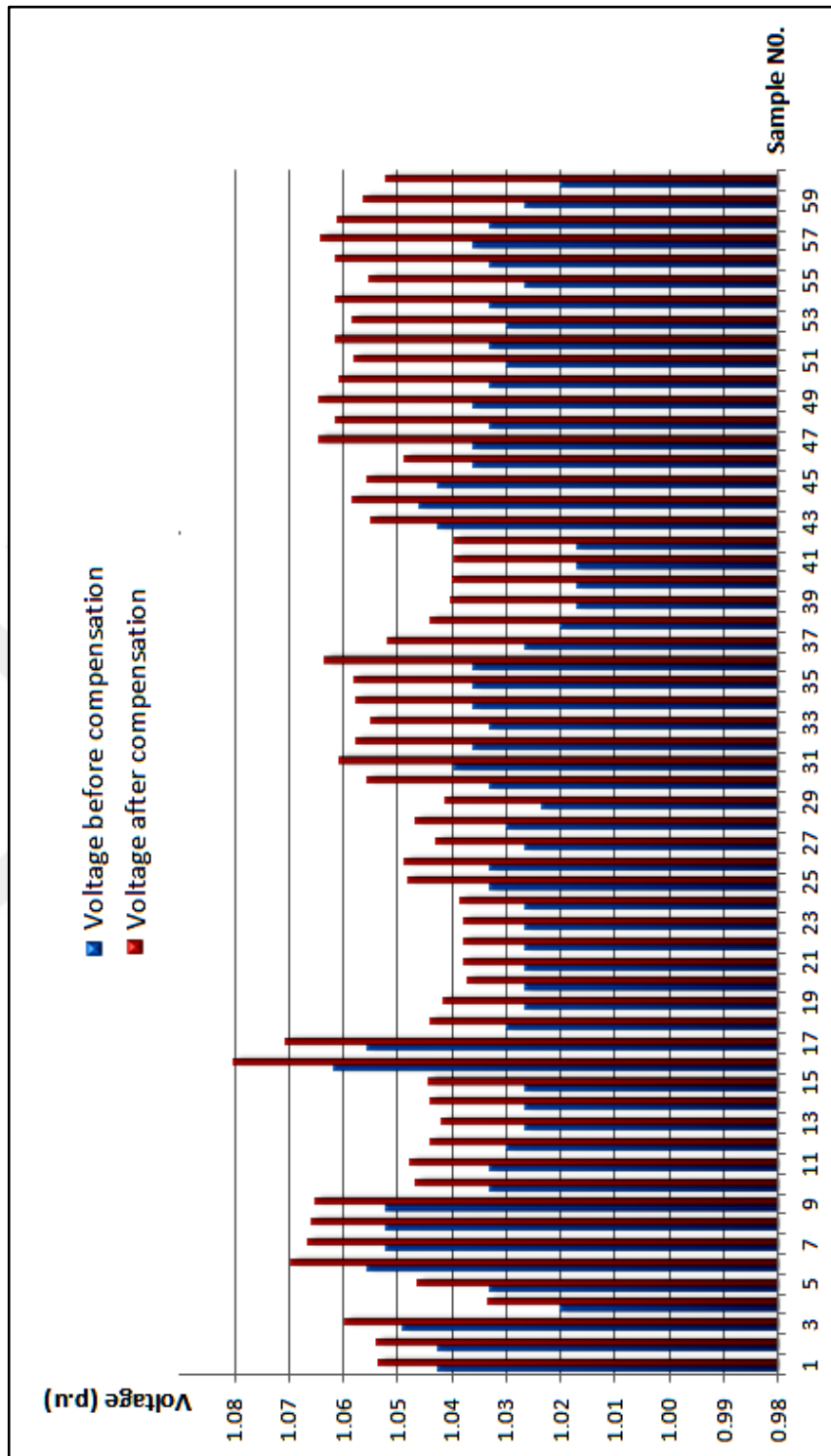
Figure 4.7.a: Load voltage for phase A before and after compensation.
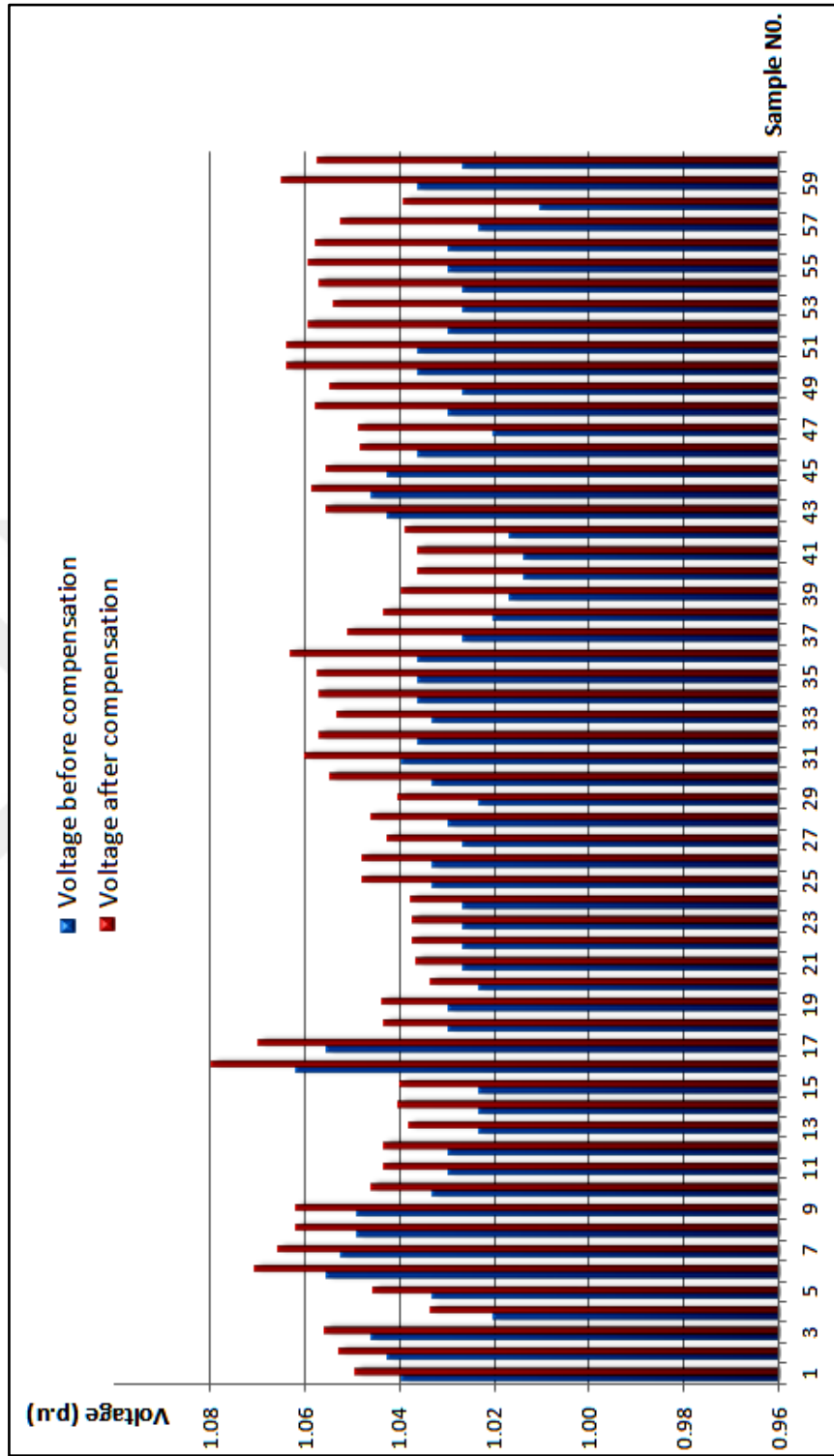
Figure 4.7.b: Load voltage for phase B before and after compensation.
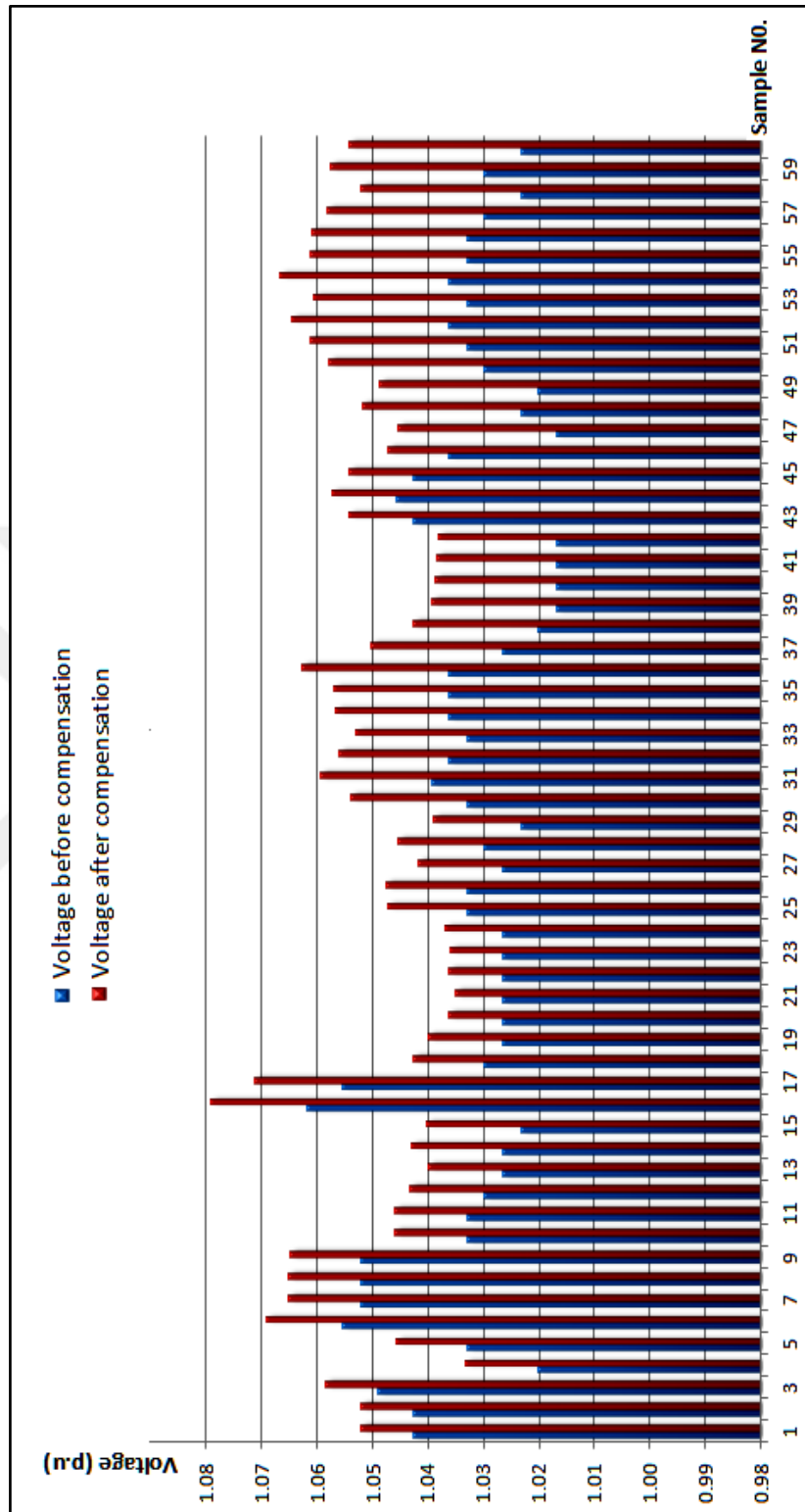
Figure 4.7.c: Load voltage for phase C before and after compensation.
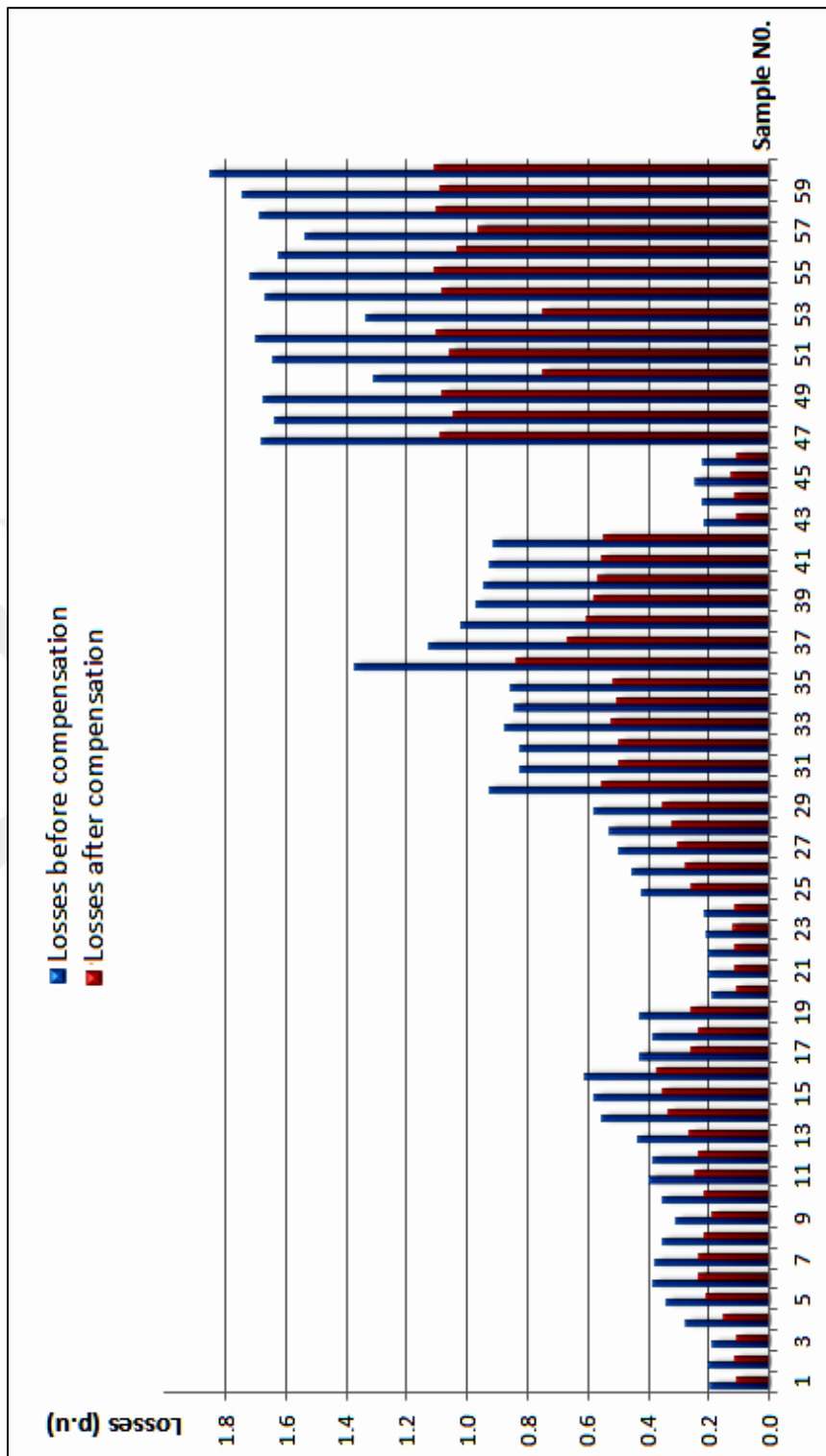
Figure 4.8.a: Losses for phase A before and after compensation.
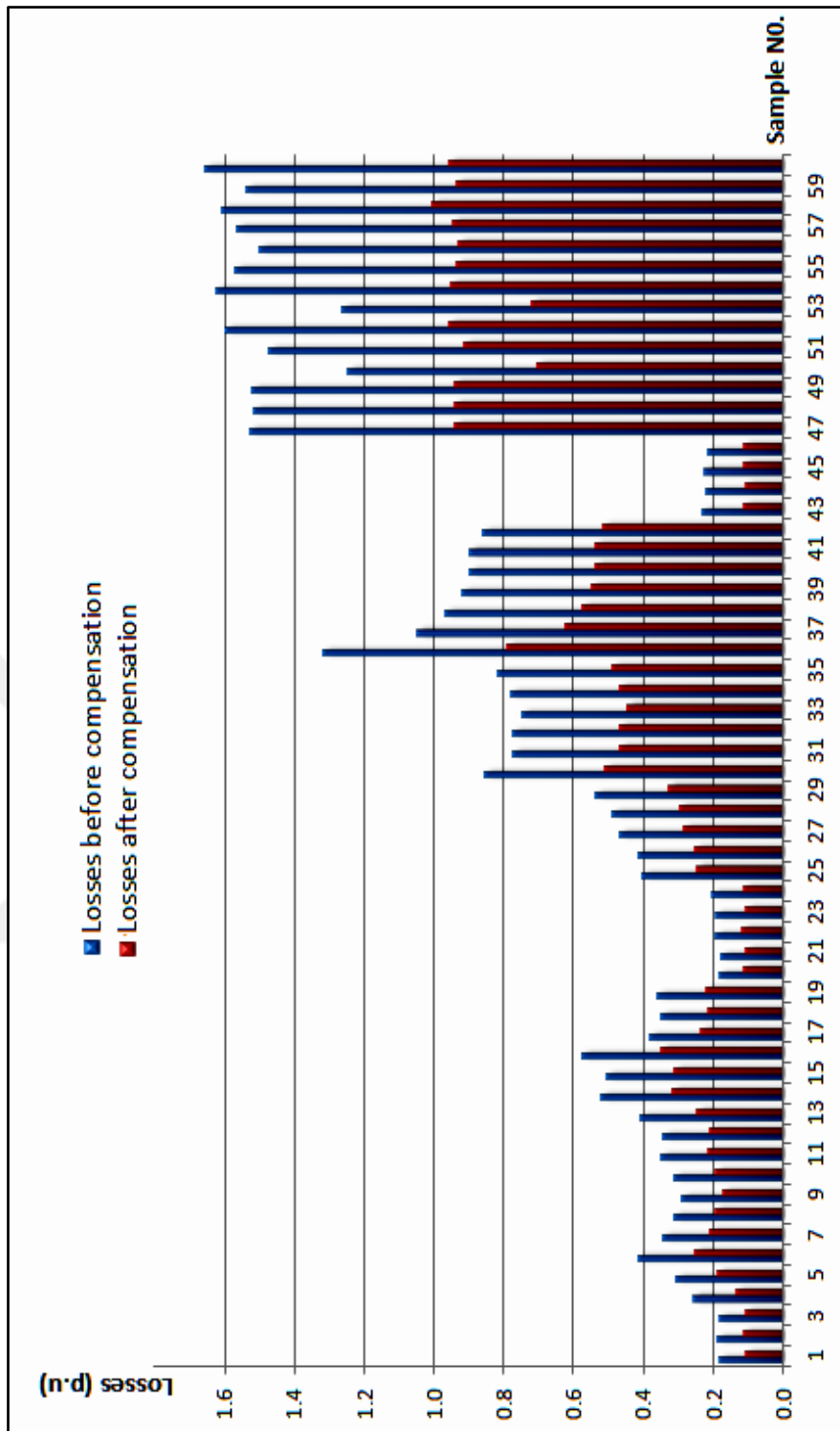
Figure 4.8.b: Losses for phase B before and after compensation.
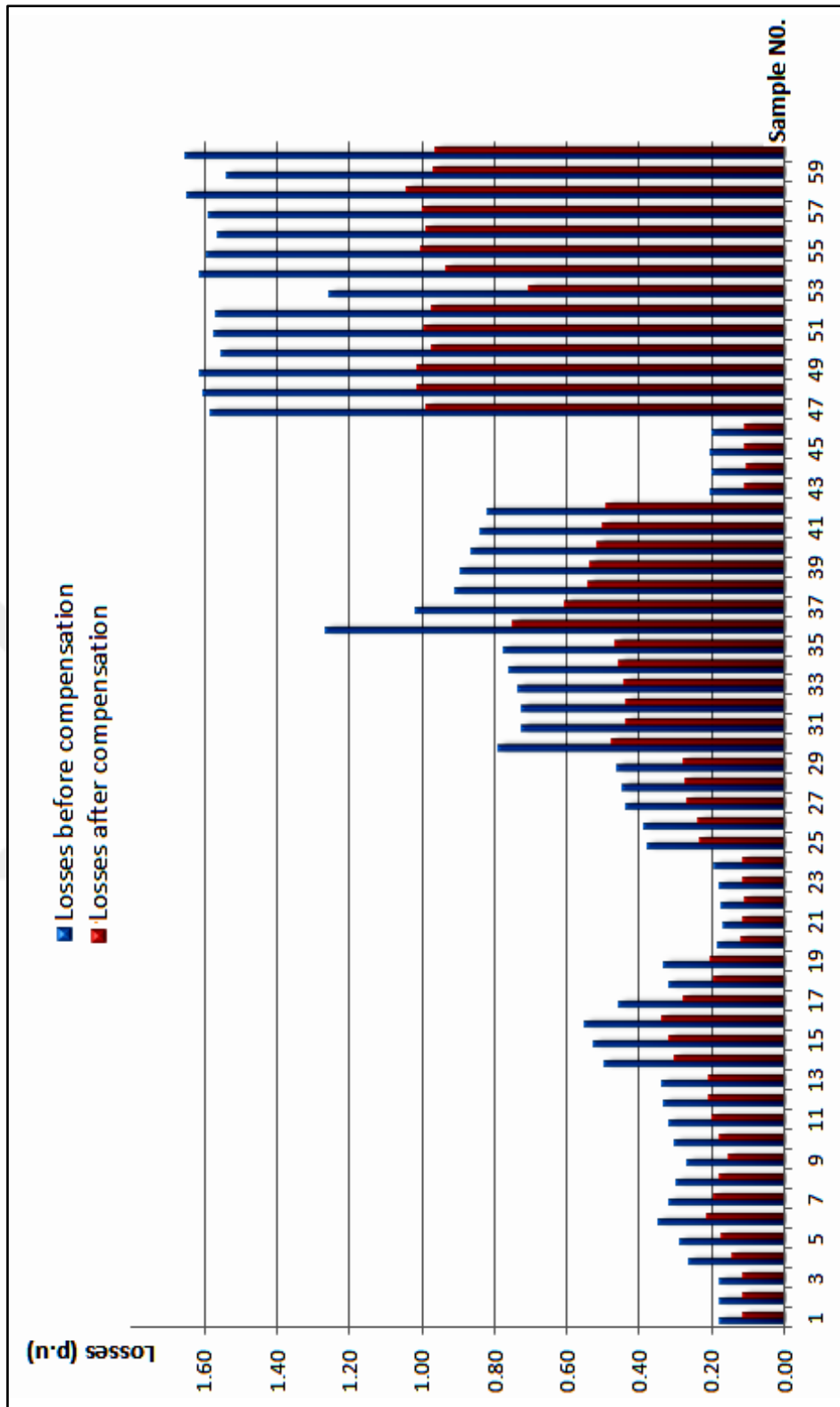
Figure 4.8.c: Losses for phase C before and after compensation.

CHAPTER FIVE

CONCLUSIONS AND FUTURE WORK

5.1 Conclusions

By looking at the results obtained in Section 4.4, it is observed that the usage of SVC gives us a reduction in losses of up to 40%. It also reduces the line current about 20% by removing the reactive component. The voltage drop through the transmission line is also reduced by 3%. The magnitude of the harmonics varies depending on the firing delay angle of the TCR. As it is observed from the Table 4.1 there are different combinations of thyristor firing delay angles that give the same balancing result for the power system but the distortion that they introduce is different. An optimization is possible by selecting the best combination of firing angles. These results mean that the use of a SVC has a significant effect on enhancing the operation efficiency of the proposed system

5.2 Future Work

1- Using the TSC-TCR type to find the optimum firing angle and parameter setting of a SVC instead of a FC-TCR.

The advantages of the TSC-TCR configuration over FC-TCR configuration include:

a) generating fewer harmonics, hence requiring a smaller reactor rating;

b) greater flexibility of control;

c) better functioning under fault conditions of power system operation; and

d) power losses tending to be lower during quiescent operating conditions (with output current near to zero).

2- Studying the effect of adding the SVC device on power system voltage stability.

REFERENCES

[1]   Timothy J. E. Miller, "Reactive power control in Electric Systems", AWiley Interscience Publication,John Wiley & Sons, 2015.

[2]   Mohammed Bahlool Essa, "Optimal Location and Parameters Setting of FACT Devices for Enhancing power system stability", M.Sc. thesis, University of technology, 2016.

[3]   Arshad Abduljabbar Najim , "Static VAR Compensator (SVC) Modeling for the Iraqi National Super High Voltage Grid Sytem", M.Sc. thesis, University of Baghdad, 2011.

[4]   G. R. Udupi and Deepak Balkrishna kulkarni, "ANN-Based SVC Switching at Distribution Level for Minimal-Injected Harmonics ", IEEE Transactions on Power Delivery,Vol. 25, NO. 3, July. 2010.

[5]   D. Thukaram, E Ravi Kumar, H. P. Khinch, "Harmonic Minimization in the Operation of Static VAR Compensators for Unbalanced Reactive Power Compensation" , IEEE International conference on Power System Technology –POWERCON ,Singapore,21-24 Nov., 2004.

[6]   Anawat Puangpairoj and A. Rajapakse," Harmonic Reducing ANN Controller for a SVC Compensating Unbalanced Fluctuating Loads " International Journal of Emerging Electric Power System ,Vol.7, Issue 1, Article 5 , 2006.

[7]   Marouf Pirouti and Ismail K. Said "Neural network-based Load Balancing and Reactive Power Control by Static VAR Compensator"   International Journal of Computer and   Electrical Engineering,Vol.1, No. 1,1793-8198, April 2009.

[8]   G. R. Udupi and Deepak Balkrishna kulkarni, "Optimum Switching of TSC-TCR Using GA Trained ANN for Minimum Harmonic Injection",IEEE Second International Conference on Emerging Trends in Engineering and Technolog,ICETET-09,2009.

[9]   T. Phanindra and V.Lakshmi Devi, "Novel Approach for Minimal Injected Harmonics at Distribution Level-SVC", International Journal of Smart Sensors and Ad Hoc Network (IJSSAN), vol. 1, Issue 1, 2011.

[10]   Noel R.Estoperez and Carl John O. Salaan , "An artificial Neural Network Based Real –time Reactive Power Controller", Proceedings of the World Congress on Engineering and Computer Science,Vol 1, San Francisco, USA,October 19-21 2011.

[11]   Shamsudheen. P.M. and Javid Akhtar, "Power Quality Improvement Using Fuzzy Logic Control Static VAR Compensator in Power System Network", IOSR Journal of Engineering,Volume 2,Issue 8, August 2012.

[12]   Samir P. Desai, C. R. Mehta, Dhruvang R Gayakwad, "Automatic Reactive Power Control Using FC-TCR",International Journal of Advanced Computer Research,Volume 4, Number 2,Issue 15, June 2014.

[13]   Mr. Sanjay Prajapati, Mr. Vishal Gandhi, Mr. Rishikesh Agrawal, Mitul Vekaria, "Mitigating the Harmonic Distortion in Power System using SVC With AI Technique",International Journal for Scientific Research & Development,Vol 3, Issue 03, 2015.

[14]   Ashraf Mohamed Hemeida, Yahia S.Mohamed , Ahmed A.M. El-Gaafary, Al-Attar Ali Mohamed, "Design Static Var Compensator Controller Using Artificial Neural Network Optimized By Modify Grey Wolf Optimization" IEEE,2015.

[15]   Mohammad Hasanuzzaman Shawon, Aleksander Dziadecki , Zbigniew Hanzelka, "Voltage-Current and Harmonic Characteristic Analysis of Different FC-TCR Based SVC", IEEE, University of Science &Technology , Krakow, Poland ,July 2015.

[16]   Sanjay Kumar and Biplab Bhattacharyya, "Loadability enhancement with FACTs devices using gravitational search algorithm", ELSEVIER, Electrical Power and Energy Systems ,470 - 479, 2016.

[17]   P.Sankar Babu and V. Suma Deepthi , "Implementation of Fuzzy Logic Approach on TSC-TCR SVC Switching At Distribution Level for Minimal Injected Harmonics",International Journal of Scientific Engineering and Applied Science (IJSEAS) – Volume-2, Issue-1, January 2016.

[18]   Ricardo Domke, Jose Rodriguez, Luis Moran, and Juan Dixon, "Reactive Power Compensation Technologies :state –of –the –Art Review " IEEE 2005.

[19] Okwe Gerald Ibe and Akwukwaegbu I. O, "Concepts of Reactive Power Control and Voltage Stability Methods in Power System Network" IOSR Journal of Computer Engineering (IOSR-JCE)e-ISSN: 2278-0661, p- ISSN: 2278-8727Vol. 11, Issue 2 (May. - Jun. 2013), PP 15-25.

[20] Laszio Gyugyi, "Reactive Power Generation And Control By Thyristor Circuits" , IEEE Power Electronics Specialist Conference Rector.

[21] Rajiv K. Varma and R. Mohan Mathur "Thyristor - Based FACTS Controllers for Electrical Transmission Systems", John Wiley & Sons , INC. Publications, New York , 2002.

[22] Enrique Acha , cesar Angeles-Camacho , Hugo Ambriz-Perez ,Claudio R. Fuerte-Esquivel   , "FACTS-Modelling-and-Simulation-in-Power-Networks" John Wiley & Sons, Chichester, 2004

[23] Leonard L. Grigsby, "Power Systems", CRC Press, Boca Raton, Third Edition 2007.

[24] K. R. Padiyar , "FACTS Controllers in Power Transmission and Distribution" , New Delhi, New Age, 2007.

[25] Haider A.F. Mohamed, Lokman H. Hassan, and M. Moghavvemi, "Impact of UPFC-based Damping Controller on Dynamic Stability of Iraqi Power Network. " Scientific Research and Essays 6.1 (2011): 136-145.

[26] Zhang, Xiao-Ping, Bikash Pal, and Christian Rehtanz,   "Flexible AC Transmission Systems: Modelling and Control. " Springer Science & Business Media, 2006.

[27] Cai, Lijun, "Robust Coordinated Control of FACTS Devices in Large Power Systems", Diss. University Duisburg-Essen, Department of Electrical Engineering and Information Technology, 2004.

[28] CH Kasi Rama Krishna Reddy, Krishna, and A. Radha, "Power Qualiy Problems and it's Improvement using FACTS Devices. " International Journal of Engineering Trends and Technology (IJETI)– Vol.4, Issue 5 , May 2013.

[29] Ganesh, V., et al. "Improvement of Transient Stability Through SVC" International Journal of Advances in Engineering & Technology (1963): 56-66

[30] Murali, D., Dr M. Rajaram, and N. Reka. "Comparison of FACTS Devices for Power System Stability Enhancement." International Journal of Computer Applications 8.4 (2010): 30-35.

[31] Singh, Amarjeet, and Amit Tiwari. "FACTS Devices for Reactive Power Compensation of Wind Energy Conversion System. ", S-JPSET : ISSN : 2229-7111, Vol. 2, Issue 1 , 2011.

[32] Singh, Bindeshwar, et al. "Introduction of FACTS Controllers, a Critical Review. " International Journal of reviews in computing 8 (2011).

[33] Lab-Volt staff , "Static Synchronous Compensator (STATCOM)" Courseware Sample, Lab-Volt Catalogue, Canada, August 2012.

[34] P. Kundur, "Power System Stability and Control", McGraw-Hill, .New York USA, 1994.

[35]A. Apostolov , et al., "Power System Protection", The Electric Power Engineering Handbook, Virginia Polytechnic Institute, CRC Press LLC, 2001.

[36] J. C. Whitaker, "Power Distribution and Control" ,AC Power Systems Handbook, 2nd Edition, Boca Raton: CRC Press LLC, 1999.

[37] Chiu, Mao-Ching_ Lee, Richard Char-Tung_ Lin, Jung-Shan-Communications engineering _ essentials for computer scientists and electrical engineers-IEEE Press, John Wiley & Sons (Asia) (2007).

[38] Shamam F. Alwash , "Fast Topology Based 3- Phase Load Flow For Distribution System", M.Sc. thesis , University of technology , 2004.

[39] Francisco C. De La Rosa , "Harmonics and Powe Systems". CRC Taylorand Francis group,2006.

[40] William H. Kersting, "Distribution System Modeling and Analysis" , CRC Press LLC, 2002.

APPENDICES

Appendix-A: Program Codes and Explanation

```
clear
clc
 tic
global D
```

Input the value of the line impedance between load and source buses.($Z_A = Z_B = Z_C$)
```
z = complex (1.13295, 2.158);
```

Input the value of three phase unbalanced load ;active power $[P_L]^{abc}$ and reactive power $[Q_L]^{abc}$ (for 60 samples); as shown in APPENDIX-B Table B.1 , Table B.2 respectively.
```
load pa;
load pb;
load pc;

load Qa;
load Qb;
load Qc;
```

Input the value of three phase load bus voltages ; $va\angle daa, vb\angle dbb, vc\angle dcc$; (for 60 samples) as shown in APPENDIX-B Table B.3.
```
load va;
load vb;
load vc;

load daa;
load dbb;
load dcc;

pa = pa*10^6
pb = pb*10^6
pc = pc*10^6
Qa = Qa*10^6
Qb = Qb*10^6
Qc = Qc*10^6
va = va*10^3
vb = vb*10^3
vc = vc*10^3
```

79

QC=5*10^6

load Qs ;
Qs = Qs*10^6

for v=1:60
[Var , dai] = pol2cart(daa(v)*(pi/180),va(v));
[Vbr , dbi] = pol2cart(dbb(v)*(pi/180),vb(v));
[Vcr , dci] = pol2cart(dcc(v)*(pi/180),vc(v));
VA = complex(Var,dai);
VB = complex(Vbr,dbi);
VC = complex(Vcr,dci);
Vaa(v) = VA;
Vbb(v) = VB;
Vcc(v) = VC;
end

for i=1:60

pf1 = cosd(atand(Qa(i)/pa(i)));
pf2 = cosd(atand(Qb(i)/pb(i)));
pf3 = cosd(atand(Qc(i)/pc(i)));
PF1(i) = pf1;
PF2(i) = pf2;
PF3(i) = pf3;

s1 = complex(pa(i),Qa(i));
s2 = complex(pb(i),Qb(i));
s3 = complex(pc(i),Qc(i));

Ila = conj((s1)/(Vaa(i)));
ILa(i) = Ila;

```
Ilb = conj((s2)/(Vbb(i)));
ILb(i) = Ilb;

Ilc = conj((s3)/(Vcc(i)));
ILc(i) = Ilc;
ILA(i)=abs(Ila);
ILB(i)=abs(Ilb);
ILC(i)=abs(Ilc);
```

Calculate the voltage drop at the line before adding the compensator (for 60samples)

```
vda = Ila * z;
VDa(i) = vda;

vdb = Ilb * z;
VDb(i) = vdb;

vdc = Ilc * z;
VDc(i) = vdc;
```

Calculate the source voltage, before adding the compensator (for 60 samples)

```
vsa = vda + Vaa(i);
VSa(i) = vsa;

vsb = vdb + Vbb(i);
VSb(i) = vsb;

vsc = vdc + Vcc(i);
VSc(i) = vsc;
```

Calculate the losses before adding the compensator (for 60 samples) as shown in APPENDIX-C Table C.3.

```
Plosa = (ILA)^2 * real(z);
PLosa(i) = Plosa;

Plosb = (ILB)^2 * real(z);
PLosb(i) = Plosb;

Plosc = (ILC)^2 * real(z);
PLosc(i) = Plosc;
```

Calculate load bus voltages (for 60 samples) after adding the compensator by using the Forward Backward Sweep Method (FBSM)
After compensation we assume the phase-wise load seen by the source as $P_{La} + jQ_{Sa}$, $P_{Lb} + jQ_{Sb}$, and $P_{Lc} + jQ_{Sc}$ respectively.

```
s1n = complex(pa(i),Qs(i));
s2n = complex(pb(i),Qs(i));
s3n = complex(pc(i),Qs(i));

for f=1:10
```

1- Forward:

Now the forward sweep method begins by assuming the load voltage after compensation is equal to specified source voltage (V_s before compensation).

```
vl1=vsa;
vl2=vsb;
vl3=vsc;
```

The load current computed by:
```
ian = conj((s1n)/(vl1));
```
The source voltage computed by:
```
vs1 = vl1+(z*ian);

ibn = conj((s2n)/(vl2));
vs2 = vl2+(z*ibn);

icn = conj((s3n)/(vl3));
vs3 = vl3+(z*icn);
```

The magnitude of the computed voltage at source is compared with the specified source voltage
If the difference is less than specified tolerance the solution is achieved.

```
if  (vsa-vs1) > 0.001 ;
(vsb-vs2) > 0.001;
(vsc-vs3) > 0.001;
```

 If the difference more than specified tolerance the backward sweep method begins
    2- Backward:
The backward sweep method begins by set the voltage at source bus after compensation is equal to specified source voltage (V_s before compensation).
Now the voltage at load bus can be computed by using this value of source bus and the computed line current from the forward sweep method as follow

```
vl1n = vsa-(z*ian);
vl2n = vsb-(z*ibn);
vl3n = vsc-(z*icn);

vl1 = vl1n;
vl2 = vl2n;
vl3 = vl3n;
end
```

end

Va(i) = abs(vl1);
Vb(i) = abs(vl2);
Vc(i) = abs(vl3);

da(i) = angle(vl1)*180/pi;
db(i) = angle(vl2)*180/pi;
dc(i) = angle(vl3)*180/pi;

IAN(i) = abs(ian);
IBN(i) = abs(ibn);
ICN(i) = abs(icn);

VDA1(i) = IAN(i)*z;
VDB1(i) = IBN(i)*z;
VDC1(i) = ICN(i)*z;

dAN(i) = angle(ian)*180/pi;
dBN(i) = angle(ibn)*180/pi;
dCN(i) = angle(icn)*180/pi;

Plosa2 = (abs(IAN(i)))^2 * real(z);
PLosa2(i) = Plosa2;

Plosb2 = (abs(IBN(i)))^2 * real(z);
PLosb2(i) = Plosb2;

Plosc2 = (abs(ICN(i)))^2 * real(z);
PLosc2(i) = Plosc2;

pf11 = cosd(atand(Qs(i)/pa(i)));
pf22 = cosd(atand(Qs(i)/pb(i)));
pf33 = cosd(atand(Qs(i)/pc(i)));
PF11(i) = pf11;
PF22(i) = pf22;
PF33(i) = pf33;

Reactive power absorbed by the TCR can be calculated from the equation:
$$[Q_S]^{abc} + [Q_C]^{abc} = [Q_R]^{abc} + [Q_L]^{abc}$$

Initially assume the load reactive power demand is met completely by the compensator only. That is unity power factor load is seen by the source.

After setting the values of Q_S and Q_C the unbalanced reactive power $[Q_R]^{abc}$ can be obtained from:
QRa=Qs(i)+QC-Qa(i);
QRA(i)=QRa;
QRb=Qs(i)+QC-Qb(i);
QRB(i)= QRb;

QRc=Qs(i)+QC-Qc(i);
QRC(i)= QRc;

The values of delta connected compensator reactances X_{ab}, X_{bc}, and X_{ca} can be obtained as follows:

$[Q_R] = [A].[B]$
Where,
$[B] = [\ 1/X_{ab}\quad 1/X_{bc}\quad 1/X_{ca}\ ]^T$
[A] is a (3x3) matrix with,
$$[A] = \begin{bmatrix} a11 & a12 & a13 \\ a21 & a22 & a23 \\ a31 & a32 & a33 \end{bmatrix}$$

a11 = (Va(i) * Va(i)) - (Va(i) * Vb(i) * cos((da(i) - db(i))*pi/180));
a13 = (Va(i) * Va(i)) - (Va(i) * Vc(i) * cos((da(i) - dc(i))*pi/180));
a21 = (Vb(i) * Vb(i)) - (Vb(i) * Va(i) * cos((db(i) - da(i))*pi/180));
a22 = (Vb(i) * Vb(i)) - (Vb(i) * Vc(i) * cos((db(i) - dc(i))*pi/180));
a32 = (Vc(i) * Vc(i)) - (Vc(i) * Vb(i) * cos((dc(i) - db(i))*pi/180));
a33 = (Vc(i) * Vc(i)) - (Vc(i) * Va(i) * cos((dc(i) - da(i))*pi/180));
a12 = 0;
a23 = 0;
a31 = 0;

A = [a11 a12 a13; a21 a22 a23; a31 a32 a33];
H = inv(A);
Q = [QRa; QRb; QRc];
B = H*Q;
X = 1/B;
Xab(i)=X(1,1);
Xbc(i)=X(2,1);
Xca(i)=X(3,1);

 end

The values of unsymmetrical firing angles $\alpha_1, \alpha_2,$ and α_3 can be obtained as follows:

xab=Xab;
xbc=Xbc;

```
xca=Xca;

Count=0;
for D=xab
Count=Count+1;
z1(Count)= fsolve(@reactancea,0);
end

Count=0;
for D=xbc
Count=Count+1;
z2(Count)= fsolve(@reactanceb,0);
end

Count=0;
for D=xca
Count=Count+1;
z3(Count)= fsolve(@reactancec,0);
end

alpha1=z1;
alpha2=z2;
alpha3=z3;
```

Calculation of fundamental component of current

```
Vab = sqrt(3)*Va;
Vbc = sqrt(3)*Vb;
Vca = sqrt(3)*Vc;

Vma = sqrt(2)*Vab;
Vmb = sqrt(2)*Vbc;
Vmc = sqrt(2)*Vca;

f = 50;
t=0.06;
w = 2*pi*f;
L1 = 0.6939155519;
L2 = 0.6939155519;
L3 = 0.6939155519;
```

Calculation of the fundamental component of the current for phase A

```
phi1=da-30 ;
gamma1=alpha1;
beta1=alpha3;
for k=1:60
Gfa = (3*pi) - (4*gamma1(k)*(pi/180)) - (2*sind (2*gamma1(k)))- (2*beta1(k)*( pi
/180))  - sind(2*beta1(k));
Gf1(k) = Gfa;
```

```
Hfa = sqrt(3) * (pi - (2*beta1(k)*(pi/180)) - sind(2*beta1(k)));
Hf1(k) = Hfa;

thetaf1 = atand(Hfa/Gfa);
thetaf11(k) = thetaf1;

Ifa = (Vma(k)/(2*pi*w*L1)) * sqrt(Gfa^2 + Hfa^2) * sind((w*t) - phi1(k) - thetaf1);
If1(k)=Ifa;

end
```

```
phi2= db-30;
gamma2=alpha2;
beta2=alpha1;

for k=1:60
Gfb = (3*pi) - (4*gamma2(k)*(pi/180)) - (2*sind(2*gamma2(k))) -
(2*beta2(k)*(pi/180)) - sind(2*beta2(k));
Gf1(k) = Gfb;

Hfb = sqrt(3) * (pi - (2*beta2(k)*(pi/180)) - sind(2*beta2(k)));
Hf1(k) = Hfb;

thetaf3 = atand(Hfb/Gfb);
thetaf22(k) = thetaf3;

Ifb = (Vmb(k)/(2*pi*w*L2)) * sqrt(Gfb^2 + Hfb^2) * sind((w*t) - phi2(k) - thetaf3);
If2(k)=Ifb;
end
```

```
phi3=dc-30;
gamma3=alpha3;
beta3=alpha2;

for k=1:60
Gfc = (3*pi) - (4*gamma3(k)*(pi/180)) - (2*sind(2*gamma3(k))) -
(2*beta3(k)*(pi/180)) - sind(2*beta3(k));
Gf1(k) = Gfc;

Hfc = sqrt(3) * (pi - (2*beta3(k)*(pi/180)) - sind(2*beta3(k)));
Hf1(k) = Hfc;

thetaf3 = atand(Hfc/Gfc);
thetaf33(k) = thetaf3;
```

```
Ifc = (Vmc(k)/(2*pi*w*L3)) * sqrt(Gfc^2 + Hfc^2) * sind((w*t) - phi3(k) - thetaf3);
If3(k)=Ifc;
end


IF1 = If1;
IF2 = If2;
IF3 = If3;
```

```
k = [1:5];
h1 = 6*k+1;
h2 = 6*k-1;
```

```
for j=1:60
for g=1:5
GH11  =  ((sind((h1(g)+1)*gamma1(j)))/(h1(g)+1)) - ((sind((h1(g)-1)*gamma1(j)))
/(h1(g)-1))  -  ((2*sind(gamma1(j))*cosd(h1(g)*gamma1(j)))/h1(g))  +  (1/2)  *
(((sind((h1(g)+1)*beta1(j)))/(h1(g)+1))  -  ((sind((h1(g)-1)*beta1(j)))/(h1(g)-1))  -
((2*sind(beta1(j))*cosd(h1(g)*beta1(j)))/h1(g)));
Gh11(j,g) = GH11;

HH11  =(sqrt(3)/2)  *  (((sind((h1(g)-1)*beta1(j)))/(h1(g)+1))  -  ((sind((h1(g)-
1)*beta1(j)))/(h1(g)-1)) - ((2*sind(beta1(j))*cosd(h1(g)*beta1(j)))/h1(g)));
Hh11(j,g) = HH11;


thetah11 = atand(HH11/GH11);
thetaH11(j,g)=thetah11;

IH11 = (2*Vma(j)/(pi*w*L1)) * sqrt(GH11^2 + HH11^2) * sind(h1(g)*((w*t) -
phi1(j)) - thetah11);
Ih11(j,g) = IH11;
end
end
Gh11 = Gh11;
Gh17 = Gh11(:,1);
Gh113 = Gh11(:,2);
Gh119 = Gh11(:,3);
Gh125 = Gh11(:,4);
Gh131 = Gh11(:,5);

Hh11 = Hh11;
Hh17 = Hh11(:,1);
Hh113 = Hh11(:,2);
Hh119 = Hh11(:,3);
Hh125 = Hh11(:,4);
Hh131 = Hh11(:,5);
 thetaH11=thetaH11;

Ih11 = Ih11;
```

```
Ih17 = Ih11(:,1)';
Ih113 = Ih11(:,2)';
Ih119 = Ih11(:,3)';
Ih125 = Ih11(:,4)';
Ih131 = Ih11(:,5)';
```

Calculation of harmonic component for phase A & for h2

```
for j=1:60
for g=1:5
GH12 = ((sind((h2(g)+1) * gamma1(j)))/(h2(g)+1)) - ((sind((h2(g)-1) * gamma1(j)))
/ (h2(g)-1)) - ((2 * sind(gamma1(j)) * cosd(h2(g) * gamma1(j))) /h2(g)) + (1/2) *
(((sind((h2(g)+1) * beta1(j))) /(h2(g)+1)) - ((sind((h2(g)-1) * beta1(j))) / (h2(g)-1)) -
((2 * sind(beta1(j)) * cosd(h2(g)*beta1(j)))/h2(g)));
Gh12(j,g) = GH12;

HH12 =((-1)*(sqrt(3)/2)) * (((sind((h2(g)-1)*beta1(j)))/(h2(g)+1)) - ((sind((h2(g) -
1)*beta1(j)))/(h2(g)-1)) - ((2*sind(beta1(j))*cosd(h2(g)*beta1(j)))/h2(g)));
Hh12(j,g) = HH12;

thetah12 = atand(HH12/GH12);
thetaH12(j,g)=thetah12;

IH12 = (2*Vma(j)/(pi*w*L1)) * sqrt(GH12^2 + HH12^2) * sind(h2(g)*((w*t) -
phi1(j)) - thetah12);
Ih12(j,g) = IH12;
end
end

Gh12 = Gh12;
Gh15 = Gh12(:,1);
Gh111 = Gh12(:,2);
Gh117 = Gh12(:,3);
Gh123 = Gh12(:,4);
Gh129 = Gh12(:,5);

Hh12 = Hh12;
Hh15 = Hh12(:,1);
Hh111 = Hh12(:,2);
Hh117 = Hh12(:,3);
Hh123 = Hh12(:,4);
Hh129 = Hh12(:,5);

thetaH12=thetaH12;
Ih12 = Ih12;
Ih15 = Ih12(:,1)';
Ih111 = Ih12(:,2)';
Ih117 = Ih12(:,3)';
Ih123 = Ih12(:,4)';
```

```
Ih129 = Ih12(:,5)';
```

Calculation of harmonic component for phase B & for h1

```
for j=1:60
for g=1:5
GH21 = ((sind((h1(g)+1) * gamma2(j)))/(h1(g)+1)) - ((sind((h1(g)-1) * gamma2(j)))
/ (h1(g)-1)) - (( 2 * sind(gamma2(j)) * cosd(h1(g) * gamma2(j))) / h1(g)) + (1/2) *
(((sind((h1(g)+1) * beta2(j)))/(h1(g)+1)) - ((sind((h1(g)-1) * beta2(j)))/(h1(g)-1)) -
((2* sind(beta 2(j)) * cosd(h1(g) * beta2(j))) / h1(g)));
Gh21(j,g) = GH21;

HH21   =(sqrt(3)/2)   *   (((sind((h1(g)-1)*beta2(j)))/(h1(g)+1)) - ((sind((h1(g)-
1)*beta2(j))) /(h1(g)-1)) - ((2*sind(beta2(j))*cosd(h1(g)*beta2(j)))/h1(g)));
Hh21(j,g) = HH21;

thetah21 = atand(HH21/GH21);

IH21 = (2*Vmb(j)/(pi*w*L2)) * sqrt(GH21^2 + HH21^2) * sind(h1(g)*((w*t) -
phi2(j)) - thetah21);
Ih21(j,g) = IH21;
end
end
Gh21 = Gh21;
Gh27 = Gh21(:,1);
Gh213 = Gh21(:,2);
Gh219 = Gh21(:,3);
Gh225 = Gh21(:,4);
Gh231 = Gh21(:,5);

Hh21 = Hh21;
Hh27 = Hh21(:,1);
Hh213 = Hh21(:,2);
Hh219 = Hh21(:,3);
Hh225 = Hh21(:,4);
Hh231 = Hh21(:,5);

Ih21 = Ih21;
Ih27 = Ih21(:,1)';
Ih213 = Ih21(:,2)';
Ih219 = Ih21(:,3)';
Ih225 = Ih21(:,4)';
Ih231 = Ih21(:,5)';
```

Calculation of harmonic component for phase B & for h2

```
for j=1:60
for g=1:5
```

```
GH22 = ((sind((h2(g)+1)*gamma2(j)))/(h2(g)+1)) - ((sind((h2(g)-1)*gamma2(j)))  /
(h2 (g)-1)) - ((2 * sind(gamma2(j)) * cosd(h2(g) * gamma2(j)))/h2(g)) + (1/2) *
(((sind((h2(g)+1) * beta2(j)))/(h2(g)+1)) - ((sind((h2(g)-1) * beta2(j)))/(h2(g)-1)) -
((2*sind(beta2(j)) * cosd(h2(g) * beta2(j))) /h2(g)));
Gh22(j,g) = GH22;

HH22 =((-1)*(sqrt(3)/2)) * (((sind((h2(g)-1) * beta2(j))) / (h2(g)+1)) - ((sind((h2(g)-
1)*beta2(j)))/(h2(g)-1)) - ((2*sind(beta2(j))*cosd(h2(g)*beta2(j)))/h2(g)));
Hh22(j,g) = HH22;

thetah22 = atand(HH22/GH22);

IH22 = (2*Vmb(j)/(pi*w*L2)) * sqrt(GH22^2 + HH22^2) * sind(h2(g)*((w*t) -
phi2(j)) - thetah22);
Ih22(j,g) = IH22;
end
end
Gh22 = Gh22;
Gh25 = Gh22(:,1);
Gh211 = Gh22(:,2);
Gh217 = Gh22(:,3);
Gh223 = Gh22(:,4);
Gh229 = Gh22(:,5);

Hh22 = Hh22;
Hh25 = Hh22(:,1);
Hh211 = Hh22(:,2);
Hh217 = Hh22(:,3);
Hh223 = Hh22(:,4);
Hh229 = Hh22(:,5);

Ih22 = Ih22;
Ih25 = Ih22(:,1)';
Ih211 = Ih22(:,2)';
Ih217 = Ih22(:,3)';
Ih223 = Ih22(:,4)';
Ih229 = Ih22(:,5)';
```

Calculation of harmonic component for phase C & for h1

```
for j=1:60
for g=1:5
GH31 = ((sind((h1(g)+1) * gamma3(j)))/(h1(g)+1)) - ((sind((h1(g) -1)*gamma3(j))) /
(h1(g)-1)) - ((2*sind(gamma3(j))*cosd(h1(g) * gamma3(j))) / h1(g)) + (1/2) *
(((sind((h1(g) +1) * beta3(j))) /(h1(g)+1)) - ((sind((h1(g)-1)*beta3(j)))/(h1(g)-1)) -
((2*sind(beta3(j)) *cosd(h1(g)*beta3(j))) /h1(g)));
Gh31(j,g) = GH31;
```

```
HH31 =(sqrt (3)/2) * (((sind((h1(g) - 1) * beta3(j))) / (h1(g) + 1)) - ((sind((h1(g) - 1)
* beta3(j))) / (h1(g) -1)) - ((2*sind (beta3 (j)) *cosd(h1(g)*beta3(j)))/h1(g)));
Hh31(j,g) = HH31;

thetah31 = atand(HH31/GH31);

IH31 = (2*Vmc(j)/(pi*w*L3)) * sqrt(GH31^2 + HH31^2) * sind(h1(g)*((w*t) -
phi3(j)) - thetah31);
Ih31(j,g) = IH31;
end
end

Gh31 = Gh31;
Gh37 = Gh31(:,1);
Gh313 = Gh31(:,2);
Gh319 = Gh31(:,3);
Gh325 = Gh31(:,4);
Gh331 = Gh31(:,5);

Hh31 = Hh31;
Hh37 = Hh31(:,1);
Hh313 = Hh31(:,2);
Hh319 = Hh31(:,3);
Hh325 = Hh31(:,4);
Hh331 = Hh31(:,5);

Ih31 = Ih31;
Ih37 = Ih31(:,1)';
Ih313 = Ih31(:,2)';
Ih319 = Ih31(:,3)';
Ih325 = Ih31(:,4)';
Ih331 = Ih31(:,5)';
```

Calculation of harmonic component for phase C & for h2

```
for j=1:60
for g=1:5
GH32= ((sind((h2(g)+1) * gamma3(j))) / (h2(g)+1)) - ((sind((h2(g)-1) * gamma3(j)))
/ (h2(g)-1)) - ((2 * sind ( gamma3(j)) * cosd (h2(g) * gamma3(j))) / h2(g)) + (1/2) *
(((sind((h2(g)+1)*beta3(j)))/(h2(g)+1))-((sind((h2(g)-1)*beta3(j)))/(h2(g)-1))-((2*
sind (beta3(j)) *cosd(h2(g)*beta3(j))) /h2(g)));
Gh32(j,g) = GH32;

HH32 =((-1)*(sqrt(3)/2)) * (((sind((h2(g)-1) * beta3(j)))/(h2(g)+1)) - ((sind((h2(g) -
1) * beta3(j))) / (h2(g)-1)) - ((2 * sind(beta3(j)) *cosd(h2(g) * beta3(j))) /h2(g)));
Hh32(j,g) = HH32;

thetah32 = atand(HH32/GH32);
```

```
IH32 = (2*Vmc(j)/(pi*w*L3)) * sqrt(GH32^2 + HH32^2) * sind(h2(g)*((w*t) -
phi3(j)) - thetah32);
Ih32(j,g) = IH32;
end
end


Gh32 = Gh32;
Gh35 = Gh32(:,1);
Gh311 = Gh32(:,2); Gh317 = Gh32(:,3);
Gh323 = Gh32(:,4);
Gh329 = Gh32(:,5);

Hh32 = Hh32;
Hh35 = Hh32(:,1);
Hh311 = Hh32(:,2);
Hh317 = Hh32(:,3);
Hh323 = Hh32(:,4);
Hh329 = Hh32(:,5);

Ih32 = Ih32;
Ih35 = Ih32(:,1)';
Ih311 = Ih32(:,2)';
Ih317 = Ih32(:,3)';
Ih323 = Ih32(:,4)';
Ih329 = Ih32(:,5)';
```

THD "Total Harmonic Distortion" Calculation

```
for r=1:60
thd1=sqrt((Ih15(r))^2+(Ih17(r))^2+(Ih111(r))^2+(Ih113(r))^2+(Ih117(r))^2+(Ih119(r
))^2+(Ih123(r))^2+(Ih125(r))^2+(Ih129(r))^2+(Ih131(r))^2)/IF1(r);
THd1(r) = thd1;

thd2=sqrt((Ih25(r))^2+(Ih27(r))^2+(Ih211(r))^2+(Ih213(r))^2+(Ih217(r))^2+(Ih219(r
))^2+(Ih223(r))^2+(Ih225(r))^2+(Ih229(r))^2+(Ih231(r))^2)/IF2(r);
THd2(r) = thd2;


thd3=sqrt((Ih35(r))^2+(Ih37(r))^2+(Ih311(r))^2+(Ih313(r))^2+(Ih317(r))^2+(Ih319(r
))^2+(Ih323(r))^2+(Ih325(r))^2+(Ih329(r))^2+(Ih331(r))^2)/IF3(r);
THd3(r) = thd3;

end
```

Appendix-B: Arkheta-Substation 33KV Side Load Profile of Transformer -1

Table B.1: Unbalance three phase active power data $[P_L]^{abc}$ during 2016.

Sample No.	date	time	Pa (MW)	Pb (MW)	Pc (MW)
1	10-Mar-2016	12:00 PM	1.947	1.947	1.987
2	10-Mar-2016	12:30 PM	1.987	1.988	1.995
3	10-Mar-2016	1:00 PM	1.937	1.968	1.996
4	10-Mar-2016	2:30 PM	2.250	2.114	2.200
5	10-Mar-2016	3:00 PM	2.712	2.561	2.446
6	10-Mar-2016	4:30 PM	2.930	3.061	2.792
7	10-Mar-2016	5:00 PM	2.904	2.768	2.659
8	10-Mar-2016	6:00 PM	2.797	2.629	2.531
9	10-Mar-2016	7:00 PM	2.619	2.493	2.354
10	15-Mar-2016	9:00 AM	2.747	2.590	2.496
11	15-Mar-2016	9:30 AM	2.921	2.738	2.624
12	15-Mar-2016	10:00AM	2.860	2.719	2.678
13	15-Mar-2016	12:00 PM	3.033	2.939	2.683
14	15-Mar-2016	1:00 PM	3.432	3.318	3.256
15	15-Mar-2016	2:00 PM	3.514	3.282	3.333
16	15-Mar-2016	3:00 PM	3.741	3.618	3.551
17	15-Mar-2016	3:30 PM	3.094	2.939	3.206
18	15-Mar-2016	4:00 PM	2.860	2.738	2.600
19	15-Mar-2016	4:30 PM	3.008	2.773	2.668
20	17-Mar-2016	9:00 AM	1.909	1.929	1.994
21	17-Mar-2016	10:00AM	1.958	1.921	1.975
22	17-Mar-2016	10:45AM	1.968	1.991	1.908
23	17-Mar-2016	11:15AM	1.987	1.932	1.978

Table B.1 (Continuation): Unbalance three phase active power data $[P_L]^{abc}$ during 2016.

Sample No.	date	time	Pa (MW)	Pb (MW)	Pc (MW)
24	17-Mar-2016	11:45AM	1.954	1.965	1.975
25	17-Mar-2016	1:00 PM	3.008	2.956	2.851
26	17-Mar-2016	2:00 PM	3.120	2.987	2.886
27	17-Mar-2016	2:30 PM	3.260	3.156	3.051
28	17-Mar-2016	3:45 PM	3.370	3.232	3.090
29	17-Mar-2016	5:00 PM	3.510	3.380	3.120
30	17-Mar-2016	6:15 PM	4.474	4.295	4.132
31	17-Mar-2016	6:45 PM	4.251	4.120	3.983
32	17-Mar-2016	7:45 PM	4.238	4.107	3.976
33	17-Mar-2016	8:30 PM	4.356	4.015	3.988
34	19-Mar-2016	10:30AM	4.277	4.120	4.067
35	19-Mar-2016	11:00AM	4.316	4.211	4.106
36	19-Mar-2016	12:30 PM	5.564	5.408	5.252
37	19-Mar-2016	1:30 PM	4.910	4.729	4.659
38	19-Mar-2016	2:00 PM	4.637	4.523	4.382
39	19-Mar-2016	2:30 PM	4.508	4.396	4.328
40	19-Mar-2016	3:00 PM	4.456	4.327	4.253
41	19-Mar-2016	3:30 PM	4.405	4.328	4.199
42	19-Mar-2016	5:00 PM	4.379	4.250	4.147
43	19-Mar-2016	6:00 PM	1.930	1.990	1.947
44	19-Mar-2016	7:00 PM	2.006	1.963	1.927
45	19-Mar-2016	8:00 PM	2.099	1.972	1.940
46	19-Mar-2016	9:00 PM	1.939	1.978	1.963
47	10-Jul-2016	12:30 PM	6.363	5.829	5.949
48	10-Jul-2016	1:30 PM	6.216	5.884	6.059
49	10-Jul-2016	2:30 PM	6.349	5.857	6.046
50	10-Jul-2016	3:30 PM	5.252	5.092	5.974
51	10-Jul-2016	4:30 PM	6.24	5.817	6.055

Table B.1 (Continuation): Unbalance three phase active power data $[P_L]^{abc}$ during 2016.

Sample No.	date	time	Pa (MW)	Pb (MW)	Pc (MW)
52	10-Jul-2016	5:30 PM	6.394	5.939	6.02
53	15-Jul-2016	12:00 PM	5.231	5.106	5.079
54	15-Jul-2016	1:30 PM	6.323	5.91	5.907
55	15-Jul-2016	2:00 PM	6.379	5.862	6.095
56	15-Jul-2016	2:30 PM	6.186	5.849	6.035
57	15-Jul-2016	3:00 PM	5.974	5.858	6.049
58	15-Jul-2016	4:30 PM	6.392	5.973	6.162
59	15-Jul-2016	5:00 PM	6.326	5.893	5.968
60	15-Jul-2016	6:00 PM	6.343	5.931	5.925

Table B.2: Unbalance three phase reactive power data $[Q_L]^{abc}$ during 2016.

Sample No.	date	time	Qa (MVAR)	Qb (MVAR)	Qc (MVAR)
1	10-Mar-2016	12:00 PM	1.663	1.529	1.449
2	10-Mar-2016	12:30 PM	1.716	1.584	1.460
3	10-Mar-2016	1:00 PM	1.649	1.557	1.461
4	10-Mar-2016	2:30 PM	1.987	1.985	1.950
5	10-Mar-2016	3:00 PM	2.034	1.921	1.935
6	10-Mar-2016	4:30 PM	2.198	2.296	2.094
7	10-Mar-2016	5:00 PM	2.178	2.076	1.994
8	10-Mar-2016	6:00 PM	2.098	1.972	1.998
9	10-Mar-2016	7:00 PM	1.964	1.970	1.966
10	15-Mar-2016	9:00 AM	2.060	1.942	1.972
11	15-Mar-2016	9:30 AM	2.191	2.054	1.968
12	15-Mar-2016	10:00AM	2.145	2.039	2.009
13	15-Mar-2016	12:00 PM	2.274	2.204	2.012
14	15-Mar-2016	1:00 PM	2.574	2.488	2.442
15	15-Mar-2016	2:00 PM	2.636	2.461	2.500
16	15-Mar-2016	3:00 PM	2.806	2.713	2.663
17	15-Mar-2016	3:30 PM	2.321	2.204	2.405
18	15-Mar-2016	4:00 PM	2.145	2.054	1.950
19	15-Mar-2016	4:30 PM	2.256	2.080	2.001
20	17-Mar-2016	9:00 AM	1.612	1.505	1.459

Table B.2 (Continuation): Unbalance three phase reactive power data $[Q_L]^{abc}$ during 2016.

Sample No.	date	time	Qa (MVAR)	Qb (MVAR)	Qc (MVAR)
21	17-Mar-2016	10:00AM	1.677	1.495	1.300
22	17-Mar-2016	10:45AM	1.690	1.589	1.477
23	17-Mar-2016	11:15AM	1.716	1.643	1.438
24	17-Mar-2016	11:45AM	1.805	1.687	1.567
25	17-Mar-2016	1:00 PM	2.256	2.217	2.139
26	17-Mar-2016	2:00 PM	2.340	2.241	2.165
27	17-Mar-2016	2:30 PM	2.445	2.367	2.289
28	17-Mar-2016	3:45 PM	2.527	2.424	2.317
29	17-Mar-2016	5:00 PM	2.633	2.535	2.340
30	17-Mar-2016	6:15 PM	3.356	3.222	3.099
31	17-Mar-2016	6:45 PM	3.188	3.090	2.987
32	17-Mar-2016	7:45 PM	3.178	3.080	2.982
33	17-Mar-2016	8:30 PM	3.267	3.011	2.991
34	19-Mar-2016	10:30AM	3.208	3.090	3.050
35	19-Mar-2016	11:00AM	3.237	3.158	3.079
36	19-Mar-2016	12:30 PM	3.973	3.956	3.939
37	19-Mar-2016	1:30 PM	3.682	3.547	3.494
38	19-Mar-2016	2:00 PM	3.478	3.393	3.286
39	19-Mar-2016	2:30 PM	3.381	3.297	3.246
40	19-Mar-2016	3:00 PM	3.342	3.245	3.190
41	19-Mar-2016	3:30 PM	3.304	3.246	3.149
42	19-Mar-2016	5:00 PM	3.284	3.188	3.111
43	19-Mar-2016	6:00 PM	1.907	1.986	1.795
44	19-Mar-2016	7:00 PM	1.905	1.951	1.769
45	19-Mar-2016	8:00 PM	1.974	1.963	1.787
46	19-Mar-2016	9:00 PM	1.918	1.837	1.685
47	10-Jul-2016	12:30 PM	4.081	4.056	4.072
48	10-Jul-2016	1:30 PM	4.087	4.048	4.057
49	10-Jul-2016	2:30 PM	4.082	4.058	4.076
50	10-Jul-2016	3:30 PM	4.088	4.074	4.065
51	10-Jul-2016	4:30 PM	4.028	4.041	4.076
52	10-Jul-2016	5:30 PM	4.083	4.291	4.143
53	15-Jul-2016	12:00 PM	4.189	4.029	4.093
54	15-Jul-2016	1:30 PM	4.068	4.389	4.479
55	15-Jul-2016	2:00 PM	4.097	4.297	4.099
56	15-Jul-2016	2:30 PM	4.096	4.039	4.065
57	15-Jul-2016	3:00 PM	4.062	4.194	4.098
58	15-Jul-2016	4:30 PM	4.019	4.053	4.096
59	15-Jul-2016	5:00 PM	4.274	4.204	4.012
60	15-Jul-2016	6:00 PM	4.574	4.488	4.441

Table B.3: Unbalance three phase load voltages data during 2016.

N0.	date	time	VPhaseA (p.u)	Daa (deg)	VPhaseB (p.u)	Dbb (deg)	VPhase C (p.u)	Dcc (deg)
1	10-Mar-2016	12:00 PM	1.042	0°	1.039	120°	1.042	240°
2	10-Mar-2016	12:30 PM	1.042	0°	1.040	120°	1.041	240°
3	10-Mar-2016	1:00 PM	1.048	0°	1.046	120°	1.049	240°
4	10-Mar-2016	2:30 PM	1.019	0°	1.020	120°	1.021	240°
5	10-Mar-2016	3:00 PM	1.032	0°	1.034	120°	1.033	240°
6	10-Mar-2016	4:30 PM	1.050	0°	1.055	120°	1.051	240°
7	10-Mar-2016	5:00 PM	1.053	0°	1.051	120°	1.051	240°
8	10-Mar-2016	6:00 PM	1.053	0°	1.049	120°	1.052	240°
9	10-Mar-2016	7:00 PM	1.052	0°	1.049	120°	1.054	240°
10	15-Mar-2016	9:00 AM	1.028	0°	1.033	120°	1.033	240°
11	15-Mar-2016	9:30 AM	1.032	0°	1.030	120°	1.033	240°
12	15-Mar-2016	10:00AM	1.029	0°	1.028	120°	1.030	240°
13	15-Mar-2016	12:00 PM	1.026	0°	1.023	120°	1.025	240°
14	15-Mar-2016	1:00 PM	1.026	0°	1.023	120°	1.026	240°
15	15-Mar-2016	2:00 PM	1.026	0°	1.023	120°	1.023	240°
16	15-Mar-2016	3:00 PM	1.031	0°	1.030	120°	1.027	240°
17	15-Mar-2016	3:30 PM	1.053	0°	1.050	120°	1.055	240°
18	15-Mar-2016	4:00 PM	1.028	0°	1.029	120°	1.029	240°
19	15-Mar-2016	4:30 PM	1.026	0°	1.030	120°	1.026	240°
20	17-Mar-2016	9:00 AM	1.026	0°	1.023	120°	1.026	240°
21	17-Mar-2016	10:00AM	1.025	0°	1.026	120°	1.026	240°
22	17-Mar-2016	10:45AM	1.026	0°	1.025	120°	1.025	240°
23	17-Mar-2016	11:15AM	1.027	0°	1.026	120°	1.026	240°
24	17-Mar-2016	11:45AM	1.026	0°	1.028	120°	1.026	240°
25	17-Mar-2016	1:00 PM	1.033	0°	1.033	120°	1.033	240°
26	17-Mar-2016	2:00 PM	1.033	0°	1.033	120°	1.036	240°
27	17-Mar-2016	2:30 PM	1.027	0°	1.026	120°	1.026	240°
28	17-Mar-2016	3:45 PM	1.030	0°	1.029	120°	1.030	240
29	17-Mar-2016	5:00 PM	1.022	0°	1.023	120°	1.023	240°
30	17-Mar-2016	6:15 PM	1.033	0°	1.032	120°	1.033	240°
31	17-Mar-2016	6:45 PM	1.039	0°	1.040	120°	1.039	240°
32	17-Mar-2016	7:45 PM	1.037	0°	1.036	120°	1.035	240°
33	17-Mar-2016	8:30 PM	1.033	0°	1.032	120°	1.033	240°
34	19-Mar-2016	10:30AM	1.036	0°	1.037	120°	1.036	240°
35	19-Mar-2016	11:00AM	1.037	0°	1.036	120°	1.036	240°
36	19-Mar-2016	12:30 PM	1.036	0°	1.037	120°	1.036	240°
37	19-Mar-2016	1:30 PM	1.026	0°	1.026	120°	1.027	240°

Table B.3 (Continuation): Unbalance three phase load voltages data during 2016.

N0.	date	time	VPhaseA (p.u)	Daa (deg)	VPhaseB (p.u)	Dbb (deg)	VPhase C (p.u)	Dcc (deg)
38	19-Mar-2016	2:00 PM	1.020	0°	1.021	120°	1.020	240°
39	19-Mar-2016	2:30 PM	1.018	0°	1.017	120°	1.017	240°
40	19-Mar-2016	3:00 PM	1.017	0°	1.014	120°	1.017	240°
41	19-Mar-2016	3:30 PM	1.017	0°	1.014	120°	1.016	240°
42	19-Mar-2016	5:00 PM	1.017	0°	1.017	120°	1.018	240°
43	19-Mar-2016	6:00 PM	1.040	0°	1.042	120°	1.041	240°
44	19-Mar-2016	7:00 PM	1.050	0°	1.046	120°	1.044	240°
45	19-Mar-2016	8:00 PM	1.042	0°	1.044	120°	1.041	240°
46	19-Mar-2016	9:00 PM	1.036	0°	1.039	120°	1.036	240°
47	10-Jul-2016	12:30 PM	1.036	0°	1.020	120°	1.017	240°
48	10-Jul-2016	1:30 PM	1.033	0°	1.030	120°	1.023	240°
49	10-Jul-2016	2:30 PM	1.036	0°	1.026	120°	1.020	240°
50	10-Jul-2016	3:30 PM	1.033	0°	1.036	120°	1.030	240°
51	10-Jul-2016	4:30 PM	1.030	0°	1.036	120°	1.033	240°
52	10-Jul-2016	5:30 PM	1.033	0°	1.030	120°	1.036	240°
53	15-Jul-2016	12:00 PM	1.030	0°	1.026	120°	1.033	240°
54	15-Jul-2016	1:30 PM	1.033	0°	1.026	120°	1.036	240°
55	15-Jul-2016	2:00 PM	1.026	0°	1.030	120°	1.033	240°
56	15-Jul-2016	2:30 PM	1.034	0°	1.030	120°	1.033	240°
57	15-Jul-2016	3:00 PM	1.036	0°	1.023	120°	1.030	240°
58	15-Jul-2016	4:30 PM	1.033	0°	1.010	120°	1.023	240°
59	15-Jul-2016	5:00 PM	1.026	0°	1.036	120°	1.030	240°
60	15-Jul-2016	6:00 PM	1.020	0°	1.026	120°	1.023	240°

Appendix-C: The Results Before and After Adding the Compensator

Results before and after adding the compensator of Power Factor, Load Voltage, Load Current, and the Losses are Shown in the Following Tables.

Table C.1: Power factor for three-phase before adding the SVC.

Sample No.	date	time	PF Phase A	PF Phase B	PF Phase C
1	10-Mar-2016	12:00 PM	0.760	0.786	0.807
2	10-Mar-2016	12:30 PM	0.756	0.782	0.806
3	10-Mar-2016	1:00 PM	0.761	0.784	0.806
4	10-Mar-2016	2:30 PM	0.749	0.729	0.748
5	10-Mar-2016	3:00 PM	0.800	0.799	0.784
6	10-Mar-2016	4:30 PM	0.799	0.799	0.800
7	10-Mar-2016	5:00 PM	0.800	0.800	0.800
8	10-Mar-2016	6:00 PM	0.799	0.799	0.784
9	10-Mar-2016	7:00 PM	0.800	0.784	0.767
10	15-Mar-2016	9:00 AM	0.800	0.800	0.784
11	15-Mar-2016	9:30 AM	0.799	0.799	0.800
12	15-Mar-2016	10:00AM	0.800	0.800	0.799
13	15-Mar-2016	12:00 PM	0.800	0.800	0.800
14	15-Mar-2016	1:00 PM	0.800	0.800	0.800
15	15-Mar-2016	2:00 PM	0.799	0.800	0.799
16	15-Mar-2016	3:00 PM	0.799	0.800	0.800
17	15-Mar-2016	3:30 PM	0.799	0.800	0.799
18	15-Mar-2016	4:00 PM	0.800	0.799	0.800
19	15-Mar-2016	4:30 PM	0.800	0.799	0.800
20	17-Mar-2016	9:00 AM	0.764	0.788	0.807
21	17-Mar-2016	10:00AM	0.759	0.789	0.835
22	17-Mar-2016	10:45AM	0.758	0.781	0.790
23	17-Mar-2016	11:15AM	0.756	0.761	0.800
24	17-Mar-2016	11:45AM	0.734	0.758	0.783
25	17-Mar-2016	1:00 PM	0.800	0.800	0.799
26	17-Mar-2016	2:00 PM	0.800	0.799	0.799
27	17-Mar-2016	2:30 PM	0.800	0.800	0.799

Table C.1 (Continuation): Power factor for three-phase before adding the SVC.

Sample No.	date	time	PF Phase A	PF Phase B	PF Phase C
28	17-Mar-2016	3:45 PM	0.800	0.800	0.800
29	17-Mar-2016	5:00 PM	0.799	0.800	0.800
30	17-Mar-2016	6:15 PM	0.799	0.799	0.800
31	17-Mar-2016	6:45 PM	0.800	0.800	0.800
32	17-Mar-2016	7:45 PM	0.800	0.800	0.800
33	17-Mar-2016	8:30 PM	0.800	0.800	0.800
34	19-Mar-2016	10:30AM	0.799	0.800	0.800
35	19-Mar-2016	11:00AM	0.800	0.800	0.800
36	19-Mar-2016	12:30 PM	0.813	0.807	0.800
37	19-Mar-2016	1:30 PM	0.800	0.799	0.800
38	19-Mar-2016	2:00 PM	0.799	0.799	0.800
39	19-Mar-2016	2:30 PM	0.800	0.800	0.800
40	19-Mar-2016	3:00 PM	0.800	0.800	0.799
41	19-Mar-2016	3:30 PM	0.799	0.800	0.800
42	19-Mar-2016	5:00 PM	0.800	0.799	0.799
43	19-Mar-2016	6:00 PM	0.711	0.707	0.735
44	19-Mar-2016	7:00 PM	0.725	0.709	0.736
45	19-Mar-2016	8:00 PM	0.728	0.708	0.735
46	19-Mar-2016	9:00 PM	0.710	0.732	0.758
47	10-Jul-2016	12:30 PM	0.824	0.821	0.825
48	10-Jul-2016	1:30 PM	0.836	0.824	0.831
49	10-Jul-2016	2:30 PM	0.841	0.822	0.829
50	10-Jul-2016	3:30 PM	0.789	0.781	0.827
51	10-Jul-2016	4:30 PM	0.804	0.812	0.803
52	10-Jul-2016	5:30 PM	0.843	0.811	0.824
53	15-Jul-2016	12:00 PM	0.781	0.785	0.779
54	15-Jul-2016	1:30 PM	0.841	0.803	0.797
55	15-Jul-2016	2:00 PM	0.801	0.807	0.830
56	15-Jul-2016	2:30 PM	0.824	0.823	0.829
57	15-Jul-2016	3:00 PM	0.827	0.813	0.828
58	15-Jul-2016	4:30 PM	0.817	0.827	0.803
59	15-Jul-2016	5:00 PM	0.829	0.814	0.800
60	15-Jul-2016	6:00 PM	0.811	0.797	0.800

Table C.2: load current for three-phase before adding the SVC.

Sample No.	date	time	Current (p.u) Phase A	current (p.u) Phase B	current (p.u) Phase C
1	10-Mar-2016	12:00 PM	0.41	0.40	0.39
2	10-Mar-2016	12:30 PM	0.42	0.41	0.40
3	10-Mar-2016	1:00 PM	0.40	0.40	0.39
4	10-Mar-2016	2:30 PM	0.49	0.47	0.48
5	10-Mar-2016	3:00 PM	0.55	0.52	0.50
6	10-Mar-2016	4:30 PM	0.58	0.60	0.55
7	10-Mar-2016	5:00 PM	0.57	0.55	0.53
8	10-Mar-2016	6:00 PM	0.55	0.52	0.51
9	10-Mar-2016	7:00 PM	0.52	0.50	0.49
10	15-Mar-2016	9:00 AM	0.56	0.52	0.51
11	15-Mar-2016	9:30 AM	0.59	0.55	0.53
12	15-Mar-2016	10:00AM	0.58	0.55	0.54
13	15-Mar-2016	12:00 PM	0.62	0.60	0.55
14	15-Mar-2016	1:00 PM	0.70	0.68	0.66
15	15-Mar-2016	2:00 PM	0.71	0.67	0.68
16	15-Mar-2016	3:00 PM	0.76	0.73	0.72
17	15-Mar-2016	3:30 PM	0.61	0.58	0.63
18	15-Mar-2016	4:00 PM	0.58	0.55	0.53
19	15-Mar-2016	4:30 PM	0.61	0.56	0.54
20	17-Mar-2016	9:00 AM	0.41	0.40	0.40
21	17-Mar-2016	10:00AM	0.42	0.40	0.38
22	17-Mar-2016	10:45AM	0.42	0.41	0.39
23	17-Mar-2016	11:15AM	0.43	0.41	0.40
24	17-Mar-2016	11:45AM	0.43	0.42	0.41
25	17-Mar-2016	1:00 PM	0.61	0.60	0.58
26	17-Mar-2016	2:00 PM	0.63	0.60	0.58
27	17-Mar-2016	2:30 PM	0.66	0.64	0.62
28	17-Mar-2016	3:45 PM	0.68	0.65	0.63
29	17-Mar-2016	5:00 PM	0.72	0.69	0.64
30	17-Mar-2016	6:15 PM	0.90	0.87	0.83
31	17-Mar-2016	6:45 PM	0.85	0.82	0.80
32	17-Mar-2016	7:45 PM	0.85	0.83	0.80
33	17-Mar-2016	8:30 PM	0.88	0.81	0.80
34	19-Mar-2016	10:30AM	0.86	0.83	0.82
35	19-Mar-2016	11:00AM	0.87	0.85	0.83
36	19-Mar-2016	12:30 PM	1.10	1.08	1.06
37	19-Mar-2016	1:30 PM	1.00	0.96	0.95

Table C.2 (Continuation): load current for three-phase before adding the SVC.

Sample No.	date	time	Current (p.u) Phase A	current (p.u) Phase B	current (p.u) Phase C
38	19-Mar-2016	2:00 PM	0.95	0.92	0.90
39	19-Mar-2016	2:30 PM	0.92	0.90	0.89
40	19-Mar-2016	3:00 PM	0.91	0.89	0.87
41	19-Mar-2016	3:30 PM	0.90	0.89	0.86
42	19-Mar-2016	5:00 PM	0.90	0.87	0.85
43	19-Mar-2016	6:00 PM	0.44	0.45	0.42
44	19-Mar-2016	7:00 PM	0.44	0.44	0.42
45	19-Mar-2016	8:00 PM	0.46	0.44	0.42
46	19-Mar-2016	9:00 PM	0.44	0.43	0.42
47	10-Jul-2016	12:30 PM	1.22	1.16	1.18
48	10-Jul-2016	1:30 PM	1.20	1.16	1.19
49	10-Jul-2016	2:30 PM	1.21	1.16	1.19
50	10-Jul-2016	3:30 PM	1.07	1.05	1.17
51	10-Jul-2016	4:30 PM	1.20	1.14	1.18
52	10-Jul-2016	5:30 PM	1.22	1.19	1.18
53	15-Jul-2016	12:00 PM	1.08	1.06	1.05
54	15-Jul-2016	1:30 PM	1.21	1.20	1.19
55	15-Jul-2016	2:00 PM	1.23	1.18	1.19
56	15-Jul-2016	2:30 PM	1.20	1.15	1.17
57	15-Jul-2016	3:00 PM	1.16	1.17	1.18
58	15-Jul-2016	4:30 PM	1.22	1.19	1.21
59	15-Jul-2016	5:00 PM	1.24	1.16	1.16
60	15-Jul-2016	6:00 PM	1.28	1.21	1.21

Table C.3: Losses for three-phase before adding the SVC.

Sample No.	date	time	Losses (p.u) Phase A	Losses (p.u) Phase B	Losses (p.u) Phase C
1	10-Mar-2016	12:00 PM	0.190	0.179	0.175
2	10-Mar-2016	12:30 PM	0.200	0.188	0.177
3	10-Mar-2016	1:00 PM	0.185	0.181	0.175
4	10-Mar-2016	2:30 PM	0.273	0.255	0.261
5	10-Mar-2016	3:00 PM	0.339	0.302	0.287
6	10-Mar-2016	4:30 PM	0.383	0.414	0.348
7	10-Mar-2016	5:00 PM	0.375	0.341	0.314
8	10-Mar-2016	6:00 PM	0.347	0.309	0.296
9	10-Mar-2016	7:00 PM	0.305	0.289	0.267
10	15-Mar-2016	9:00 AM	0.351	0.309	0.299
11	15-Mar-2016	9:30 AM	0.393	0.348	0.317
12	15-Mar-2016	10:00AM	0.380	0.344	0.333
13	15-Mar-2016	12:00 PM	0.430	0.406	0.337
14	15-Mar-2016	1:00 PM	0.550	0.517	0.495
15	15-Mar-2016	2:00 PM	0.577	0.506	0.522
16	15-Mar-2016	3:00 PM	0.647	0.607	0.588
17	15-Mar-2016	3:30 PM	0.425	0.386	0.454
18	15-Mar-2016	4:00 PM	0.381	0.349	0.314
19	15-Mar-2016	4:30 PM	0.423	0.357	0.332
20	17-Mar-2016	9:00 AM	0.187	0.180	0.183
21	17-Mar-2016	10:00AM	0.199	0.177	0.167
22	17-Mar-2016	10:45AM	0.201	0.194	0.175
23	17-Mar-2016	11:15AM	0.206	0.192	0.179
24	17-Mar-2016	11:45AM	0.212	0.200	0.190
25	17-Mar-2016	1:00 PM	0.417	0.403	0.375
26	17-Mar-2016	2:00 PM	0.448	0.411	0.382
27	17-Mar-2016	2:30 PM	0.496	0.466	0.435
28	17-Mar-2016	3:45 PM	0.526	0.485	0.443
29	17-Mar-2016	5:00 PM	0.580	0.536	0.458
30	17-Mar-2016	6:15 PM	0.922	0.851	0.787
31	17-Mar-2016	6:45 PM	0.823	0.771	0.722
32	17-Mar-2016	7:45 PM	0.822	0.773	0.725
33	17-Mar-2016	8:30 PM	0.875	0.744	0.732
34	19-Mar-2016	10:30AM	0.838	0.778	0.758
35	19-Mar-2016	11:00AM	0.852	0.813	0.772
36	19-Mar-2016	12:30 PM	1.370	1.315	1.263
37	19-Mar-2016	1:30 PM	1.127	1.044	1.013

Table C.3 (Continuation): Losses for three-phase before adding the SVC.

Sample No.	date	time	Losses (p.u) Phase A	Losses (p.u) Phase B	Losses (p.u) Phase C
38	19-Mar-2016	2:00 PM	1.016	0.967	0.908
39	19-Mar-2016	2:30 PM	0.966	0.919	0.890
40	19-Mar-2016	3:00 PM	0.945	0.897	0.860
41	19-Mar-2016	3:30 PM	0.923	0.896	0.839
42	19-Mar-2016	5:00 PM	0.911	0.859	0.817
43	19-Mar-2016	6:00 PM	0.214	0.229	0.204
44	19-Mar-2016	7:00 PM	0.218	0.221	0.197
45	19-Mar-2016	8:00 PM	0.241	0.223	0.202
46	19-Mar-2016	9:00 PM	0.218	0.212	0.196
47	10-Jul-2016	12:30 PM	1.675	1.525	1.582
48	10-Jul-2016	1:30 PM	1.633	1.515	1.598
49	10-Jul-2016	2:30 PM	1.670	1.516	1.608
50	10-Jul-2016	3:30 PM	1.307	1.247	1.551
51	10-Jul-2016	4:30 PM	1.638	1.471	1.572
52	10-Jul-2016	5:30 PM	1.698	1.594	1.566
53	15-Jul-2016	12:00 PM	1.334	1.263	1.255
54	15-Jul-2016	1:30 PM	1.668	1.618	1.611
55	15-Jul-2016	2:00 PM	1.716	1.569	1.592
56	15-Jul-2016	2:30 PM	1.624	1.500	1.562
57	15-Jul-2016	3:00 PM	1.530	1.560	1.585
58	15-Jul-2016	4:30 PM	1.682	1.606	1.645
59	15-Jul-2016	5:00 PM	1.740	1.536	1.536
60	15-Jul-2016	6:00 PM	1.850	1.652	1.648

Table C.4: load voltages for three-phase after adding the SVC.

Sample No.	date	time	Voltage(p.u) Phase A	voltage(p.u) Phase B	voltage(p.u) Phase C
1	10-Mar-2016	12:00 PM	1.059	1.056	1.058
2	10-Mar-2016	12:30 PM	1.060	1.057	1.058
3	10-Mar-2016	1:00 PM	1.065	1.062	1.065
4	10-Mar-2016	2:30 PM	1.040	1.040	1.040
5	10-Mar-2016	3:00 PM	1.055	1.054	1.054
6	10-Mar-2016	4:30 PM	1.073	1.080	1.073
7	10-Mar-2016	5:00 PM	1.076	1.073	1.073
8	10-Mar-2016	6:00 PM	1.075	1.070	1.073
9	10-Mar-2016	7:00 PM	1.073	1.070	1.073
10	15-Mar-2016	9:00 AM	1.051	1.054	1.054
11	15-Mar-2016	9:30 AM	1.057	1.052	1.054
12	15-Mar-2016	10:00AM	1.053	1.051	1.052
13	15-Mar-2016	12:00 PM	1.051	1.048	1.047
14	15-Mar-2016	1:00 PM	1.055	1.051	1.053
15	15-Mar-2016	2:00 PM	1.055	1.051	1.051
16	15-Mar-2016	3:00 PM	1.062	1.059	1.056
17	15-Mar-2016	3:30 PM	1.078	1.073	1.081
18	15-Mar-2016	4:00 PM	1.051	1.051	1.051
19	15-Mar-2016	4:30 PM	1.051	1.052	1.048
20	17-Mar-2016	9:00 AM	1.043	1.040	1.042
21	17-Mar-2016	10:00AM	1.043	1.042	1.041
22	17-Mar-2016	10:45AM	1.044	1.042	1.041
23	17-Mar-2016	11:15AM	1.045	1.043	1.042
24	17-Mar-2016	11:45AM	1.045	1.045	1.043
25	17-Mar-2016	1:00 PM	1.058	1.057	1.056
26	17-Mar-2016	2:00 PM	1.059	1.057	1.060
27	17-Mar-2016	2:30 PM	1.054	1.052	1.051
28	17-Mar-2016	3:45 PM	1.058	1.056	1.055
29	17-Mar-2016	5:00 PM	1.051	1.051	1.049
30	17-Mar-2016	6:15 PM	1.070	1.068	1.067
31	17-Mar-2016	6:45 PM	1.074	1.074	1.072
32	17-Mar-2016	7:45 PM	1.072	1.070	1.068
33	17-Mar-2016	8:30 PM	1.069	1.065	1.066
34	19-Mar-2016	10:30AM	1.071	1.070	1.070
35	19-Mar-2016	11:00AM	1.072	1.070	1.070
36	19-Mar-2016	12:30 PM	1.081	1.081	1.079
37	19-Mar-2016	1:30 PM	1.066	1.065	1.065

Table C.4 (Continuation): load voltages for three-phase after adding the SVC.

Sample No.	date	time	Voltage(p.u) Phase A	voltage(p.u) Phase B	voltage(p.u) Phase C
38	19-Mar-2016	2:00 PM	1.059	1.058	1.056
39	19-Mar-2016	2:30 PM	1.055	1.054	1.053
40	19-Mar-2016	3:00 PM	1.054	1.050	1.053
41	19-Mar-2016	3:30 PM	1.054	1.050	1.052
42	19-Mar-2016	5:00 PM	1.054	1.052	1.053
43	19-Mar-2016	6:00 PM	1.058	1.062	1.059
44	19-Mar-2016	7:00 PM	1.069	1.065	1.062
45	19-Mar-2016	8:00 PM	1.062	1.064	1.059
46	19-Mar-2016	9:00 PM	1.054	1.057	1.054
47	10-Jul-2016	12:30 PM	1.084	1.067	1.064
48	10-Jul-2016	1:30 PM	1.081	1.076	1.071
49	10-Jul-2016	2:30 PM	1.084	1.073	1.068
50	10-Jul-2016	3:30 PM	1.077	1.080	1.076
51	10-Jul-2016	4:30 PM	1.077	1.082	1.080
52	10-Jul-2016	5:30 PM	1.081	1.078	1.083
53	15-Jul-2016	12:00 PM	1.074	1.070	1.077
54	15-Jul-2016	1:30 PM	1.081	1.076	1.085
55	15-Jul-2016	2:00 PM	1.075	1.077	1.080
56	15-Jul-2016	2:30 PM	1.080	1.076	1.080
57	15-Jul-2016	3:00 PM	1.083	1.071	1.077
58	15-Jul-2016	4:30 PM	1.081	1.058	1.071
59	15-Jul-2016	5:00 PM	1.076	1.083	1.076
60	15-Jul-2016	6:00 PM	1.072	1.076	1.073

Table C.5: Load current for three-phase after adding the SVC.

Sample No.	date	time	Current (p.u) Phase A	Current (p.u) Phase B	Current (p.u) Phase C
1	10-Mar-2016	12:00 PM	0.313	0.314	0.319
2	10-Mar-2016	12:30 PM	0.319	0.320	0.321
3	10-Mar-2016	1:00 PM	0.309	0.315	0.318
4	10-Mar-2016	2:30 PM	0.366	0.345	0.358
5	10-Mar-2016	3:00 PM	0.433	0.410	0.392
6	10-Mar-2016	4:30 PM	0.459	0.477	0.438
7	10-Mar-2016	5:00 PM	0.454	0.434	0.418
8	10-Mar-2016	6:00 PM	0.438	0.414	0.398
9	10-Mar-2016	7:00 PM	0.411	0.393	0.371
10	15-Mar-2016	9:00 AM	0.440	0.414	0.400
11	15-Mar-2016	9:30 AM	0.465	0.438	0.420
12	15-Mar-2016	10:00AM	0.457	0.436	0.429
13	15-Mar-2016	12:00 PM	0.485	0.472	0.432
14	15-Mar-2016	1:00 PM	0.546	0.530	0.519
15	15-Mar-2016	2:00 PM	0.559	0.524	0.532
16	15-Mar-2016	3:00 PM	0.590	0.573	0.564
17	15-Mar-2016	3:30 PM	0.482	0.461	0.498
18	15-Mar-2016	4:00 PM	0.458	0.439	0.417
19	15-Mar-2016	4:30 PM	0.481	0.444	0.429
20	17-Mar-2016	9:00 AM	0.312	0.316	0.325
21	17-Mar-2016	10:00AM	0.319	0.314	0.323
22	17-Mar-2016	10:45AM	0.321	0.325	0.312
23	17-Mar-2016	11:15AM	0.323	0.315	0.323
24	17-Mar-2016	11:45AM	0.318	0.320	0.322
25	17-Mar-2016	1:00 PM	0.478	0.470	0.454
26	17-Mar-2016	2:00 PM	0.495	0.475	0.458
27	17-Mar-2016	2:30 PM	0.520	0.504	0.488
28	17-Mar-2016	3:45 PM	0.535	0.514	0.492
29	17-Mar-2016	5:00 PM	0.560	0.540	0.500
30	17-Mar-2016	6:15 PM	0.700	0.673	0.649
31	17-Mar-2016	6:45 PM	0.663	0.642	0.622
32	17-Mar-2016	7:45 PM	0.662	0.643	0.623
33	17-Mar-2016	8:30 PM	0.682	0.631	0.627
34	19-Mar-2016	10:30AM	0.668	0.645	0.637
35	19-Mar-2016	11:00AM	0.674	0.659	0.643
36	19-Mar-2016	12:30 PM	0.860	0.836	0.813

Table C.5 (Continuation): Load current for three-phase after adding the SVC.

Sample No.	date	time	Current (p.u) Phase A	Current (p.u) Phase B	Current (p.u) Phase C
37	19-Mar-2016	1:30 PM	0.770	0.742	0.732
38	19-Mar-2016	2:00 PM	0.733	0.715	0.694
39	19-Mar-2016	2:30 PM	0.715	0.698	0.688
40	19-Mar-2016	3:00 PM	0.707	0.690	0.676
41	19-Mar-2016	3:30 PM	0.700	0.690	0.668
42	19-Mar-2016	5:00 PM	0.695	0.676	0.660
43	19-Mar-2016	6:00 PM	0.310	0.319	0.313
44	19-Mar-2016	7:00 PM	0.319	0.314	0.309
45	19-Mar-2016	8:00 PM	0.335	0.315	0.312
46	19-Mar-2016	9:00 PM	0.313	0.318	0.317
47	10-Jul-2016	12:30 PM	0.980	0.913	0.934
48	10-Jul-2016	1:30 PM	0.961	0.914	0.945
49	10-Jul-2016	2:30 PM	0.978	0.912	0.946
50	10-Jul-2016	3:30 PM	0.815	0.788	0.927
51	10-Jul-2016	4:30 PM	0.968	0.898	0.937
52	10-Jul-2016	5:30 PM	0.988	0.921	0.928
53	15-Jul-2016	12:00 PM	0.814	0.797	0.789
54	15-Jul-2016	1:30 PM	0.977	0.918	0.909
55	15-Jul-2016	2:00 PM	0.991	0.909	0.942
56	15-Jul-2016	2:30 PM	0.956	0.908	0.934
57	15-Jul-2016	3:00 PM	0.922	0.914	0.938
58	15-Jul-2016	4:30 PM	0.988	0.943	0.961
59	15-Jul-2016	5:00 PM	0.982	0.909	0.927
60	15-Jul-2016	6:00 PM	0.988	0.921	0.923

Table C.6: losses for three-phase after adding the SVC.

Sample No.	date	time	Losses (p.u) Phase A	losses (p.u) Phase B	losses (p.u) Phase C
1	10-Mar-2016	12:00 PM	0.111	0.112	0.115
2	10-Mar-2016	12:30 PM	0.115	0.116	0.116
3	10-Mar-2016	1:00 PM	0.108	0.113	0.115
4	10-Mar-2016	2:30 PM	0.152	0.135	0.145
5	10-Mar-2016	3:00 PM	0.213	0.190	0.174
6	10-Mar-2016	4:30 PM	0.239	0.257	0.218
7	10-Mar-2016	5:00 PM	0.234	0.214	0.198
8	10-Mar-2016	6:00 PM	0.217	0.194	0.179
9	10-Mar-2016	7:00 PM	0.192	0.175	0.156
10	15-Mar-2016	9:00 AM	0.220	0.195	0.181
11	15-Mar-2016	9:30 AM	0.245	0.218	0.199
12	15-Mar-2016	10:00AM	0.237	0.215	0.209
13	15-Mar-2016	12:00 PM	0.267	0.252	0.211
14	15-Mar-2016	1:00 PM	0.338	0.318	0.305
15	15-Mar-2016	2:00 PM	0.353	0.312	0.321
16	15-Mar-2016	3:00 PM	0.395	0.372	0.360
17	15-Mar-2016	3:30 PM	0.264	0.240	0.281
18	15-Mar-2016	4:00 PM	0.237	0.218	0.197
19	15-Mar-2016	4:30 PM	0.262	0.223	0.208
20	17-Mar-2016	9:00 AM	0.110	0.113	0.120
21	17-Mar-2016	10:00AM	0.116	0.112	0.118
22	17-Mar-2016	10:45AM	0.116	0.120	0.110
23	17-Mar-2016	11:15AM	0.118	0.113	0.118
24	17-Mar-2016	11:45AM	0.115	0.116	0.117
25	17-Mar-2016	1:00 PM	0.259	0.251	0.234
26	17-Mar-2016	2:00 PM	0.278	0.256	0.238
27	17-Mar-2016	2:30 PM	0.306	0.288	0.270
28	17-Mar-2016	3:45 PM	0.324	0.300	0.275
29	17-Mar-2016	5:00 PM	0.355	0.330	0.283
30	17-Mar-2016	6:15 PM	0.554	0.514	0.476
31	17-Mar-2016	6:45 PM	0.498	0.467	0.439
32	17-Mar-2016	7:45 PM	0.497	0.468	0.440
33	17-Mar-2016	8:30 PM	0.527	0.451	0.445
34	19-Mar-2016	10:30AM	0.506	0.471	0.459
35	19-Mar-2016	11:00AM	0.514	0.492	0.468
36	19-Mar-2016	12:30 PM	0.839	0.793	0.749
37	19-Mar-2016	1:30 PM	0.672	0.624	0.606

Table C.6 (Continuation): losses for three-phase after adding the SVC.

Sample No.	date	time	Losses (p.u) Phase A	losses (p.u) Phase B	losses (p.u) Phase C
38	19-Mar-2016	2:00 PM	0.608	0.580	0.546
39	19-Mar-2016	2:30 PM	0.579	0.552	0.536
40	19-Mar-2016	3:00 PM	0.567	0.539	0.518
41	19-Mar-2016	3:30 PM	0.555	0.539	0.506
42	19-Mar-2016	5:00 PM	0.548	0.518	0.493
43	19-Mar-2016	6:00 PM	0.109	0.115	0.111
44	19-Mar-2016	7:00 PM	0.115	0.111	0.108
45	19-Mar-2016	8:00 PM	0.127	0.113	0.110
46	19-Mar-2016	9:00 PM	0.111	0.115	0.114
47	10-Jul-2016	12:30 PM	1.088	0.944	0.988
48	10-Jul-2016	1:30 PM	1.046	0.946	1.012
49	10-Jul-2016	2:30 PM	1.084	0.942	1.014
50	10-Jul-2016	3:30 PM	0.753	0.704	0.974
51	10-Jul-2016	4:30 PM	1.061	0.914	0.994
52	10-Jul-2016	5:30 PM	1.105	0.960	0.976
53	15-Jul-2016	12:00 PM	0.750	0.721	0.705
54	15-Jul-2016	1:30 PM	1.082	0.955	0.937
55	15-Jul-2016	2:00 PM	1.112	0.936	1.006
56	15-Jul-2016	2:30 PM	1.036	0.935	0.988
57	15-Jul-2016	3:00 PM	0.963	0.946	0.997
58	15-Jul-2016	4:30 PM	1.105	1.007	1.045
59	15-Jul-2016	5:00 PM	1.092	0.936	0.973
60	15-Jul-2016	6:00 PM	1.106	0.960	0.964

Table C.7: power factor for three-phase after adding the SVC.

Sample No.	date	time	PF Phase A	PF Phase B	PF Phase C
1	10-Mar-2016	12:00 PM	0.979	0.979	0.980
2	10-Mar-2016	12:30 PM	0.980	0.980	0.980
3	10-Mar-2016	1:00 PM	0.979	0.980	0.980
4	10-Mar-2016	2:30 PM	0.984	0.982	0.983
5	10-Mar-2016	3:00 PM	0.989	0.988	0.986
6	10-Mar-2016	4:30 PM	0.990	0.991	0.989
7	10-Mar-2016	5:00 PM	0.990	0.989	0.988
8	10-Mar-2016	6:00 PM	0.989	0.988	0.987
9	10-Mar-2016	7:00 PM	0.988	0.987	0.985
10	15-Mar-2016	9:00 AM	0.989	0.988	0.987
11	15-Mar-2016	9:30 AM	0.990	0.989	0.988
12	15-Mar-2016	10:00AM	0.990	0.989	0.989
13	15-Mar-2016	12:00 PM	0.991	0.990	0.989
14	15-Mar-2016	1:00 PM	0.993	0.992	0.992
15	15-Mar-2016	2:00 PM	0.993	0.992	0.992
16	15-Mar-2016	3:00 PM	0.994	0.993	0.993
17	15-Mar-2016	3:30 PM	0.991	0.990	0.992
18	15-Mar-2016	4:00 PM	0.990	0.989	0.988
19	15-Mar-2016	4:30 PM	0.991	0.989	0.988
20	17-Mar-2016	9:00 AM	0.978	0.979	0.980
21	17-Mar-2016	10:00AM	0.979	0.979	0.980
22	17-Mar-2016	10:45AM	0.980	0.980	0.978
23	17-Mar-2016	11:15AM	0.980	0.979	0.980
24	17-Mar-2016	11:45AM	0.979	0.979	0.980
25	17-Mar-2016	1:00 PM	0.991	0.991	0.990
26	17-Mar-2016	2:00 PM	0.991	0.991	0.990
27	17-Mar-2016	2:30 PM	0.992	0.992	0.991
28	17-Mar-2016	3:45 PM	0.993	0.992	0.991
29	17-Mar-2016	5:00 PM	0.993	0.993	0.991
30	17-Mar-2016	6:15 PM	0.996	0.995	0.995
31	17-Mar-2016	6:45 PM	0.995	0.995	0.995
32	17-Mar-2016	7:45 PM	0.995	0.995	0.995
33	17-Mar-2016	8:30 PM	0.995	0.995	0.995
34	19-Mar-2016	10:30AM	0.995	0.995	0.995
35	19-Mar-2016	11:00AM	0.995	0.995	0.995
36	19-Mar-2016	12:30 PM	0.997	0.997	0.997
37	19-Mar-2016	1:30 PM	0.996	0.996	0.996

Table C.7 (Continuation): power factor for three-phase after adding the SVC.

Sample No.	date	time	PF Phase A	PF Phase B	PF Phase C
38	19-Mar-2016	2:00 PM	0.996	0.996	0.995
39	19-Mar-2016	2:30 PM	0.996	0.995	0.995
40	19-Mar-2016	3:00 PM	0.996	0.995	0.995
41	19-Mar-2016	3:30 PM	0.995	0.995	0.995
42	19-Mar-2016	5:00 PM	0.995	0.995	0.995
43	19-Mar-2016	6:00 PM	0.979	0.980	0.979
44	19-Mar-2016	7:00 PM	0.980	0.979	0.979
45	19-Mar-2016	8:00 PM	0.982	0.980	0.979
46	19-Mar-2016	9:00 PM	0.979	0.980	0.979
47	10-Jul-2016	12:30 PM	0.998	0.997	0.997
48	10-Jul-2016	1:30 PM	0.997	0.997	0.997
49	10-Jul-2016	2:30 PM	0.998	0.997	0.997
50	10-Jul-2016	3:30 PM	0.997	0.996	0.997
51	10-Jul-2016	4:30 PM	0.998	0.997	0.997
52	10-Jul-2016	5:30 PM	0.998	0.997	0.997
53	15-Jul-2016	12:00 PM	0.997	0.996	0.996
54	15-Jul-2016	1:30 PM	0.998	0.997	0.997
55	15-Jul-2016	2:00 PM	0.998	0.997	0.997
56	15-Jul-2016	2:30 PM	0.997	0.997	0.997
57	15-Jul-2016	3:00 PM	0.997	0.997	0.997
58	15-Jul-2016	4:30 PM	0.998	0.997	0.997
59	15-Jul-2016	5:00 PM	0.998	0.997	0.997
60	15-Jul-2016	6:00 PM	0.998	0.997	0.997

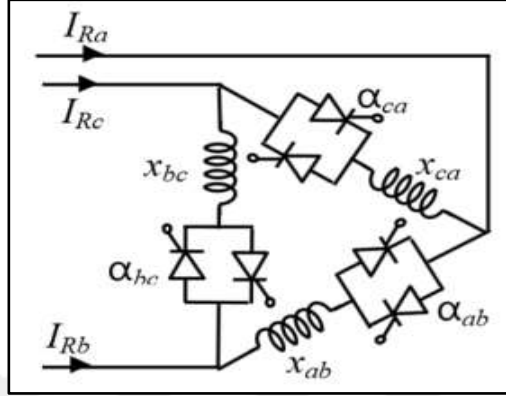## Appendix-D: Calculation of Reactive Power in TCR

Figure (D.1): Delta connected TCR.

The unbalanced Reactive power absored by TCR can be evaluated From Figure (D.1) as follows:

$$Q_{Ra} = Q_{Ra1} + Q_{Ra2}$$

To find Q_{Ra1}:

$$S_{Ra1} = V_a . I_a^*$$

$$P_{Ra1} + j\, Q_{Ra1} = j\, V_a \angle \delta_a . (V_a \angle - \delta_a - V_b \angle - \delta_b). B_{ab}$$

$$= j\, (V_a^2 - V_a . V_b \angle \delta_a - \delta_b). B_{ab}$$

$$= j(V_a^2 - V_a . V_b . \cos(\delta_a - \delta_b) - jV_a . sinc(\delta_a - \delta_b). B_{ab}$$

$$Q_{Ra} = Im\ part\ of\ S_{Ra1}$$

$$Q_{Ra1} = (V_a^2 - V_a . V_b . \cos(\delta_a - \delta_b)). B_{ab}$$

In the same procedure:

$$Q_{Ra2} = (V_a^2 - V_a V_c . \cos(\delta_a - \delta_c)) B_{ca}$$

$$\boxed{Q_{Ra} = [V_a^2 - V_a . V_b . \cos(\delta_a - \delta_b)]\, B_{ab} + [V_a^2 - V_a V_c . \cos(\delta_a - \delta_c)] B_{ca}}$$

By flowing the same steps, we can found that :

$$Q_{Rb} = [V_b^2 - V_a.V_b \cdot \cos(\delta_b - \delta_a)] \, B_{ab} + [V_b^2 - V_b \, V_c \cdot \cos(\delta_b - \delta_c)]B_{bc}$$

$$Q_{Rc} = [V_c^2 - V_cV_b \cdot \cos(\delta_c - \delta_b)]B_{bc} + [V_c^2 \text{-} V_cV_a \cdot \cos(\delta_c - \delta_a)] \, B_{ca}$$

CURRICULUM VITAE

PERSONAL INFORMATION

Name, Surname	:	Ietiqal Mahmood ALWAN
Date and Place of Birth	:	30.5.1974, Baghdad, Iraq
Marital Status	:	married
Phone	:	+905349772589
E-mail	:	eatiqal_mahmood@yahoo.com

EDUCATION

Undergraduate : University of Technology, Electrical Engineering Department, 1997